國立雲林科技大學
九十二學年度研究所博士班招生考試試題

所別：工程科技研究所
科目：工程數學 (甲)

1. (20%) Solve the given differential equations and compare the two solutions.

   a) $\frac{d^2y}{dx^2}+2\frac{dy}{dx}+y=0$ subject to $y(0)=c_1$, $y'(0)=c_2$

   b) $\frac{dy}{dx}+y=(c_2+c_1)e^{-t}$ subject to $y(0)=c_1$

   where c_1 and c_2 are constants.

2. (15%) Find the Fourier transforms of the given two functions, $f(t)$ and $g(t)$, shown in Fig. 1. Find the relationship between these two Fourier transforms.

Fig. 1

3. (15%) Find the Laplace transform of $f(t)$ for $f(t)=\begin{cases} t & 0\le t<2 \\ 0 & t\ge 2 \end{cases}$ in two different ways specified by

   a) using the definition of the Laplace transform $\mathcal{L}\{f(t)\}=\int_0^\infty f(t)e^{-st}dt$,

   b) evaluating the Laplace transform of $tu(t-2)$, where $u(\cdot)$ denotes the unit step function, and then using $\mathcal{L}\{f(t)\}=\mathcal{L}\{tu(t)\}-\mathcal{L}\{tu(t-2)\}$ to find the Laplace transform of $f(t)$.

國立雲林科技大學
九十二學年度研究所博士班招生考試試題

所別：工程科技研究所
科目：工程數學（甲）

4. Evaluate the following line integral along two different paths.

$$\int_C (3x^2y^2 - 6y^3)dx + (2x^3y - 18xy^2)dy$$

(a) C1：straight line from (0,0) to (1,1)　（25%）

(b) C2：$x = t, y = t^2$ from (0,0) to (1,1)

5. 設一直桿受熱後，漸冷卻，其溫度分布遵循下列方程式

$$\alpha^2 \frac{\partial^2 T}{\partial x^2} = \frac{\partial T}{\partial t} + \beta(T - T_0)$$　（25%）

其中α, β爲已知常數與 x, t 無關，T_0爲室溫。若桿兩端（x=0, x=L）溫度恆維持於 T_0，開始時桿的溫度分布爲一已知函數 f(x)，令

$$T(x,t) = T_0 + U(x,t)e^{-\beta t}$$

(a)將解 U（x, t）之方程式與條件式求出

(b)求桿的溫度分布 T(x, t)

國立雲林科技大學
九十二學年度研究所博士班招生考試試題

所別：工程科技研究所
科目：工程數學 (丙)

說明：本試卷共六大題，總分共計１００分。

1. If $\mathbf{A} = \begin{bmatrix} 15 & 6 & -12 \\ 4 & 10 & -2 \\ -4 & 8 & -7 \end{bmatrix}$,

(a) find the eigenvalues of **A** and their corresponding eigenvectors, (10%)

(b) find the diagonal matrix **D** of **A**. (10%)

2. Solve the following differential equations:

(a) $y'''-3y''+3y'-y=0, \qquad y(0)=2, y'(0)=2, y''(0)=10$ (10%)

(b) $x^3y'''+x^2y''-2xy'+2y=x^3\ln x$ (10%)

3. Find the steady-state oscillation corresponding to $y''+cy'+y=r(t)$, where $c>0$ and

$r(t)=\frac{t}{12}(\pi^2-t^2)$ *if* $-\pi<t<\pi$ $\qquad r(t+2\pi)=r(t)$ (10%)

4. If $V=E_0e^{-x}\sin\frac{\pi y}{4}$, where E_0 is a constant. Please determine $\vec{E}=-\vec{\nabla}V$ at the point (0,1,0). (20%)

5. (a) Write down and briefly explain "Divergence theorem". (10%)

(b) Write down and briefly explain "Stokes's theorem". (10%)

6. Given a vector function $\vec{F}=\vec{a_x}(3y-c_1z)+\vec{a_y}(c_2x-2z)-\vec{a_z}(c_3y+z)$, if $\vec{F}$ is irrotational, please determine the constants c_1, c_2, and c_3. (10%)

國立雲林科技大學
九十二學年度研究所博士班招生考試試題

所別：工程科技研究所
科目：工程數學 (乙)

1. (a) Solve the differential equation

$$\begin{aligned} \dot{x} - x &= \delta(t-2), \quad 0 < t < \infty \\ x(0) &= 3 \end{aligned}$$

without using the Laplace transform approach. (10%)

(b) Using the Laplace transform approach to verify the solution obtained in part(a). (5%)

2. (a) Let the Laplace transform of $f(t)$ be $\frac{1}{s(1+0.2s)}$. Find the Laplace transform of $f(2t)$. (10%)

(b) Let the Laplace transform of $f(t)$ be $\ln\left(\frac{s+1}{s-1}\right)$. Find $f(t)$. (10%)

3. Solve the system

$$\begin{aligned} x'' - 2x' + 3y' + 2y &= 4 \\ 2y' - x' + 3y &= 0 \end{aligned}$$

when $x(0) = x'(0) = y(0) = 0$. (15%)

4. Let $f(x) = \begin{cases} -1 & \text{for } -4 \le x < 0 \\ 1 & \text{for } 0 \le x \le 4 \end{cases}$

(a) Write the Fourier series of $f(x)$ on $[-4, 4]$. (10%)

(b) Does the Fourier series converge to $f(x)$ at each point of the interval $[-4, 4]$? (5%)

5. Let $f(x) = x^2/2$ for $-\pi \le x \le \pi$.

(a) Find the Fourier series of $f(x)$. (10%)

(b) Use the Fourier series obtained in part (a) to sum the series $\sum_{n=1}^{\infty}(-1)^n/n^2$. (10%)

6. (a) Show that the Fourier transform of $f(t) = \frac{1}{2}[H(t+3) - H(t-3)]$ is $F(\omega) = \frac{\sin(3\omega)}{\omega}$, where $H(t)$ is the Heaviside function defined by $H(t) = \begin{cases} 0 & \text{if } t < 0 \\ 1 & \text{if } t \ge 0 \end{cases}$. (5%)

(b) The *power content* of a signal $g(t)$ is defined to be $\int_{-\infty}^{\infty} |g(t)|^2\, dt$, assuming that this integral converges. Determine the power content of $g(t) = \frac{\sin(3t)}{t}$. (**Hint:** Use the Parseval's theorem: $\int_{-\infty}^{\infty} |g(t)|^2\, dt = \frac{1}{2\pi}\int_{-\infty}^{\infty} |G(\omega)|^2\, d\omega$, where $G(\omega)$ is the Fourier transform of $g(t)$). (10%)

國立雲林科技大學
九十二學年度研究所博士班招生考試試題

所別：工程科技研究所
科目：營建文獻評論

請在後面三個附件文獻當中，選讀其中一個附件之文獻，並依選讀文獻針對下列問題作答。

選讀附件 1 者，請依下列四點進行文獻評論：

(1). 本篇文獻之目的與主要貢獻為何（20 分）。

(2). 本篇文獻所採用之方法與特色為何（30 分）。

(3). 本篇文獻之缺點與限制為何（30 分）。

(4). 試解釋建議之三階段線性模式中，為何第一階段行為與 FRP 補強貼片之用量無關，而第二階段行為則與 FRP 補強貼片之用量高度相關（20 分）。

選讀附件 2 者，請依下列三點進行文獻評論：

(1). 本篇文獻之目的與主要貢獻為何（20 分）。

(2). 本篇文獻所採用之方法與特色為何（50 分）。

(3). 本篇文獻之缺點與限制為何（30 分）。

選讀附件 3 者，請依下列問題進行文獻評論：

(1). 本篇文獻的主要貢獻為何（20 分）。

(2). 依據本篇文獻的研究步驟，敘述本研究之特色與進行之流程，並彙製研究流程圖（25 分）。又本篇文獻採用的研究方法之主要理由為何（25 分）。

(3).本篇文獻之缺點與限制為何（30 分）？

國立雲林科技大學
九十二學年度研究所博士班招生考試試題
所別：工程科技研究所
科目：營建文獻評論

＜ 附件 1 ＞

ACI STRUCTURAL JOURNAL TECHNICAL PAPER
Title no. 100-S23

Confinement Model for Axially Loaded Short Rectangular Columns Strengthened with Fiber-Reinforced Polymer Wrapping

by Omar Chaallal, Munzer Hassan, and Mohsen Shahawy

This paper presents a confinement model describing the behavior of rectangular concrete columns retrofitted with externally bonded fiber-reinforced polymer (FRP) material and subjected to axial stress. The derivation of the proposed model is based on the findings of an extensive experimental investigation involving the testing of 90 rectangular specimens representing three cross-sectional aspect ratios, two concrete strengths, and five different numbers of FRP layers. The proposed model is trilinear both in the axial and the lateral directions and captures the key parameter observed, namely the ratio of the stiffness of the FRP jacket in the lateral direction to the axial stiffness of the column. The proposed model was found to fairly accurately describe results reported in other research studies.

Keywords: ductility; reinforced concrete; strain; strength; stress; test.

INTRODUCTION

In recent years, the use of externally bonded fiber-reinforced polymers (FRP) has become increasingly popular for civil infrastructure applications, including wrapping of concrete columns. Significant research has been devoted to circular columns retrofitted with FRP and numerous models were proposed.[1-5] FRP wrapping of existing circular columns has proven to be an effective retrofitting technique.[6] In contrast, very limited data have been reported on rectangular columns retrofitted with FRP wrap, even though rectangular columns in need of retrofit are very common. In a recent publication,[7] the authors presented results of an extensive laboratory investigation on 90 rectangular specimens. The parameters of the study included the concrete strength, the aspect ratio of the column's cross section, and the lateral stiffness of the external confinement provided by the FRP wrap. The objective of the present paper is to describe a stress-strain model in the axial and the lateral directions for rectangular concrete columns retrofitted with externally applied FRP jackets and subjected to axially applied compressive loading.

RESEARCH SIGNIFICANCE

The use of an externally bonded FRP composite for strengthening and repair can be a cost-effective alternative for restoring or upgrading the performance of existing concrete columns. The existing confinement models were developed for circular columns, however, and therefore fail to capture the behavior of rectangular columns. This study presents a stress-strain response model in the axial and lateral (transverse) directions for axially loaded rectangular short columns confined with an externally bonded carbon fiber-reinforced polymer (CFRP) jacket. The model enables to quantify the enhancement in strength and in ductility of FRP confined concrete columns. This can be very useful to the practicing engineers who must predict with reasonable accuracy the enhanced compressive strength and ductility of concrete columns retrofitted with externally bonded FRP wrap.

BACKGROUND

Confinement of concrete has been studied since the turn of the past century. Various constitutive models have been developed for constant active confining pressure as well as passive confinement with steel hoops, spirals, or tubes. Researchers in the early '90s attempted to apply the same models to fiber composites. The investigations, however, have shown that the behavior of concrete encased in fiber composites is not fully captured by such models.[8-9] This led to the development of new models for the confinement of circular columns by FRP jackets.[1-5] Only very recently have investigations on rectangular short columns wrapped with the FRP confinement been reported. These studies, however, were either exploratory or too specific to be generalized. Therefore, to the authors' best knowledge, no complete model for rectangular columns is available.

Demers et al.[10] compared the behavior of circular specimens with square specimens confined with varying amounts of FRP materials. They showed that circular specimens behave quite differently from square specimens. Square specimens engage high confining pressures at their corners but little pressure on their flat sides. Therefore, the cross section is not entirely effectively confined, resulting in a lower increase in strength, compared to circular specimens. Rounding off the corners of square members can reduce this shape-related effect. For instance, Rochette and Labossière[11] reported that increasing the corner radius from 1 in. (25 mm) to 1.5 in. (38 mm) of a 6 in. × 6 in. (152 mm × 152 mm) square element resulted in an enhancement of 6 to 16% in the axial force capacity.

Picher, Rochette, and Labossière[12] examined the effect of the orientation of the confining fibers on the behavior of concrete cylinders, as well as of square and rectangular prisms, wrapped with CFRP material. It was found that the wrapping could efficiently be applied to prismatic sections, provided the corners are rounded off. It was also found that an increase of the angle of wrapping orientation did not affect the ductility and resulted in a decrease of the axial strength.

Hosotani, Kawashima, and Hoshikima[13] studied confinement of concrete cylinders and square prisms by carbon fiber

ACI Structural Journal, V. 100, No. 2, March-April 2003.
MS No. 02-023 received January 1, 2002, and reviewed under Institute publication policies. Pertinent discussion will be published in the January-February 2004 *ACI Structural Journal* if received by September 1, 2003.

ACI member **Omar Chaallal** *is Professor of Construction Engineering, University of Quebec, Ecole de Technologie Supérieure, Montreal, Quebec, Canada. He is a member of ACI Committee 440, Fiber Reinforced Polymer Reinforcement. His research interests include experimental and analytical research on the use of FRP composites for strengthening and repair of concrete structures.*

Munzer Hassan *is a research fellow in the Department of Construction Engineering, University of Quebec, Ecole de Technologie Supérieure. His research interests include experimental and analytical research on the use of FRP composites for strengthening and repair of concrete structures.*

ACI member **Moheen Shahawy** *is President of SDR Engineering, Inc. He is a member of ACI Committee 440, Fiber Reinforced Polymer Reinforcement. His research interests include experimental and analytical research on the use of FRP composites for strengthening and repair of concrete structures and bridges.*

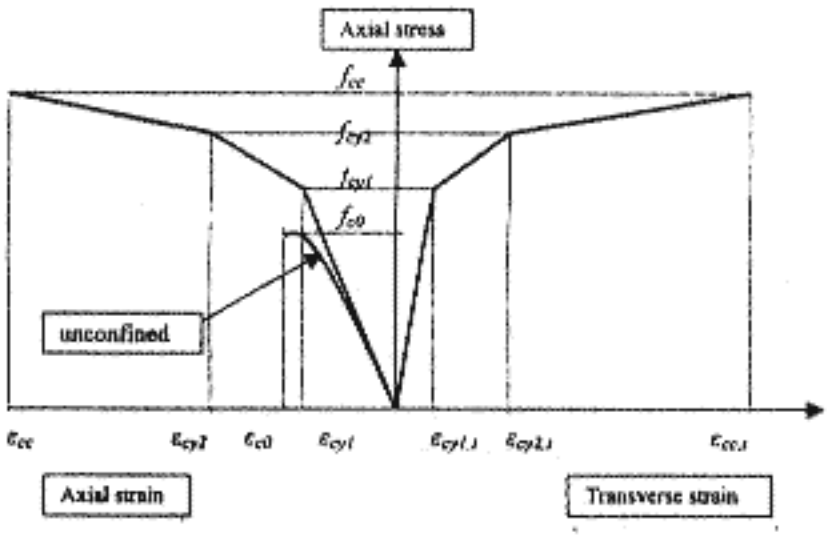

Fig. 1—Definition of proposed stress-strain model in axial and lateral directions.

sheets (CFS) for seismic strengthening. The parameters considered in the tests were the shape of the specimen and the content and the type (normal and high elastic modulus) of CFS. The volumetric ratio of CFS was defined as $\rho_{cf} = 4Nt_{cf}/d$, where t_{cf} is the thickness of a layer of CFS, N is the number of layers, and d is the diameter of circular cylinder or the width of square specimen. One significant outcome of the study was that as the CFS ratio was increased in the range of 0.05 to 0.15% by volume, no increase was achieved in the peak axial stress of the concrete f_{cc} and in the corresponding axial strain ε_{cc}, irrespective of the shape of the specimens. It was also found that at a CFS ratio greater than approximately 1% the concrete's axial stress increased continuously until failure of the CFS.

Harries et al.[14] presented results of an experimental investigation on eight 72 in. (1830 mm) long circular and square reinforced concrete columns confined with external FRP jackets under axial compression. It was found that externally applied FRP jackets can provide a confinement equivalent to that provided by closely spaced, well-detailed conventional transverse steel reinforcement.

Wang and Restrepo[15] proposed analytical expressions based on Mander's model[16] to calculate the capacity of axially loaded reinforced concrete rectangular columns confined with internal steel hoops in addition to an externally applied composite jacket. The equations take into account the confinement effect due to both the steel and the FRP jacket. The predicted values of the ultimate strength of the confined concrete compared favorably to the results from experimental tests, carried out by the same authors, on reinforced concrete columns confined by a FRP jacket.

EXPERIMENTAL WORK

The model proposed in this paper is based on results of an experimental investigation carried out by the authors. Details of the experimental investigation including the parameters of the study, the specimens, the material, and the procedure were fully described elsewhere.[7] The study investigated six series, a total of 90 specimens, of uniaxial compression tests on rectangular and square short columns. The length (12 in. [305 mm]) and the cross-sectional area (28.3 in.^{2} [18,258 mm^2]) were kept constant for all specimens. To improve the behavior of the specimens and to avoid premature failure of the CFRP material due to shearing at sharp corners, the corners of all the specimens were rounded off to a radius equal to 1 in. (25.4 mm). The behavior of the specimens was investigated in the axial and transverse directions. The parameters considered in the study were: (a) the concrete strength—two concrete strengths were tested in the study: f'_c = 3000 psi (20.7 MPa) and f'_c = 6000 psi (41.4 MPa); (b) the aspect ratio of the cross section—three aspect ratios (a/b where a and b are respectively the shorter and the longer sides of the cross section) were studied, a/b = 1, a/b = 0.654, and a/b = 0.5; and (c) the number of CFRP layers: zero, one, two, three, and four layers of CFRP wrap were investigated.

The findings of that research study can be summarized as follows. The CFRP wrapping enhances the compressive strength and ductility of the square and rectangular columns, but to a lesser degree than for cylinders. The increase in strength and ductility is more significant when concrete has a lower strength, representative of poor or degraded concrete, than a normal- to high-strength concrete. Further research is needed on the effect of the aspect ratio before any conclusion can be reached. The key parameter that governs the compressive strength of the confined concrete was found to be the effective confinement coefficient or the stiffness ratio. It is defined as the ratio of the stiffness of the FRP jacket in the lateral direction to the stiffness of the concrete column in the axial direction.

PRESENTATION OF PROPOSED MODEL FOR RECTANGULAR COLUMNS

Figure 1 presents the general form of the stress-strain model in both the axial and the transverse directions for rectangular columns confined with FRP wrap. The response is trilinear and consists of three successive regions. In the first region, the behavior is linear elastic and similar to that of the unconfined concrete. The expansion of the concrete core in this range is insignificant and the FRP wrapping is not effective. The second region called the transition region initiates with the occurrence of the first microcracking and the building up of an increasing lateral confining pressure exerted by the FRP wrap. Hereafter, the upper and lower limits of this region are called the yield points. The third region is characterized by extensive cracking of concrete. Its slope is fully dependent on the stiffness of the FRP wrapping, which is fully mobilized to contain the cracked concrete. The axial stress-strain diagram for the unconfined concrete is also presented in Fig. 1.

Two parameters related to the unconfined concrete stress-strain diagram are useful to define the proposed model. These are the strength of the unconfined concrete f_{c0} and the ultimate axial strain of the unconfined concrete ε_{c0}. To define the axial stress-strain model, three points need to be determined: the so-called yield points (f_{cy1}, ε_{cy1} and f_{cy2}, ε_{cy2}) and the ultimate point (f_{cc}, ε_{cc}), where f_{cy1} and ε_{cy1} are respectively the first yield stress and the corresponding strain of the

confined concrete; f_{cy2} and ε_{cy2} are respectively the second yield stress and the corresponding strain of the confined concrete; and f_{cc} and ε_{cc} are respectively the ultimate strength and the corresponding strain of the confined concrete. Similarly, the transverse stress-strain diagram is also defined by three points: the two transverse yield points (f_{cy1}, $\varepsilon_{cy1,t}$ and f_{cy2}, $\varepsilon_{cy2,t}$) and the ultimate transverse point (f_{cc}, $\varepsilon_{cc,t}$), where $\varepsilon_{cy1,t}$ and $\varepsilon_{cy2,t}$ are the first and second yield transverse strains of the confined concrete corresponding to f_{cy1} and f_{cy2} respectively; and $\varepsilon_{cc,t}$ is the ultimate transverse strain of the confined concrete corresponding to f_{cc}. These parameters are defined as follows.

Ultimate compressive strength of concrete

Chaallal, Shahawy, and Hassan[7] observed that the gain in strength of the confined concrete depends not only on the number of CFRP layers, but also on the concrete properties. In fact, they found that the confinement effectiveness depends mainly on two principal factors, namely the deformability of the concrete, which is inversely proportional to its stiffness, and the stiffness of the confining jacket in the lateral direction. The ratio of the stiffness of the CFRP jacket in the lateral direction $E_{frp} \times A_{frp}$ to the axial stiffness of the unconfined column $E_{c0} \times A_{c0}$ was calculated for a 1 in. column length and plotted versus the gain in compressive strength in Fig. 2. The modulus of elasticity of the unconfined concrete was derived from the stress-strain diagram and was found to be close to the value computed from the ACI Code equation. From the figure, it can be observed that the gain in compressive strength of CFRP confined concrete depends on the stiffness ratio rather than on the concrete strength. The ultimate compressive strength of the confined concrete can be expressed by Eq. (1) with a correlation coefficient of 0.96

$$f_{cc} = f_{c0} + 4.12 \times 10^5 k \quad (1)$$

where f_{cc} is the ultimate compressive strength of the confined concrete in psi, f_{c0} is the compressive strength of the unconfined concrete in psi, and k is the stiffness ratio or the confinement coefficient given by

$$k = \frac{E_{frp} \times A_{frp}}{E_{c0} \times A_{c0}} \quad (2)$$

where E_{frp} is the modulus of elasticity of the FRP jacket, A_{frp} is the area of composite fibers per inch of column length in the lateral direction (A_{frp} = thickness × 1 in.), E_{c0} is the modulus of elasticity of the unconfined concrete, and A_{c0} is the cross-sectional area of the unconfined column.

As can be seen from Eq. (1), the exclusion of the aspect ratio does not significantly affect the accuracy of f_{cc}, at least in the range of the aspect ratios (0.5:1.0) considered in this study. In addition, it must be noted that the stiffness ratio k on which Eq. (1) was based ranged between 0 and 0.8, thereby encompassing a relatively wide range of practical cases.

Ultimate axial strain of confined concrete

The ultimate axial strain of the unconfined concrete ε_{c0} is quasiconstant and equal to 0.002 for 3 ksi concrete and 0.0024 for 6 ksi concrete. The increase in axial strain due to the confining CFRP wrap was plotted versus the stiffness ratio in Fig. 3. From the figure it can be seen that the increase in

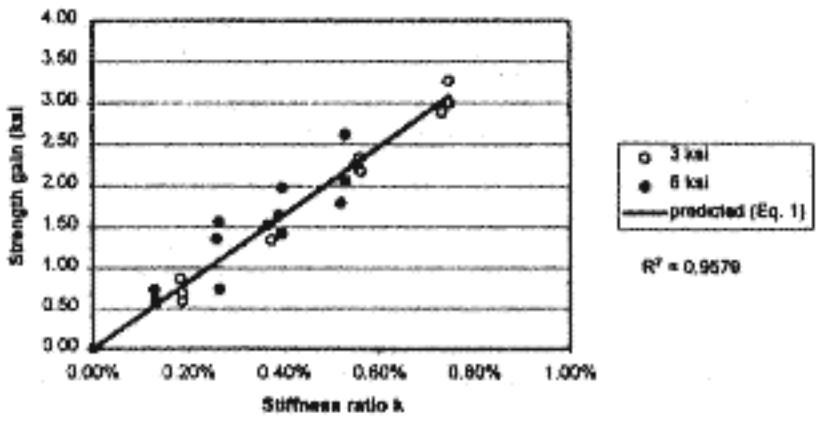

Fig. 2—Compressive strength gain versus CFRP jacket to concrete column stiffness ratio $k = (E_{frp} \times A_{frp})/(E_{c0} \times A_{c0})$.

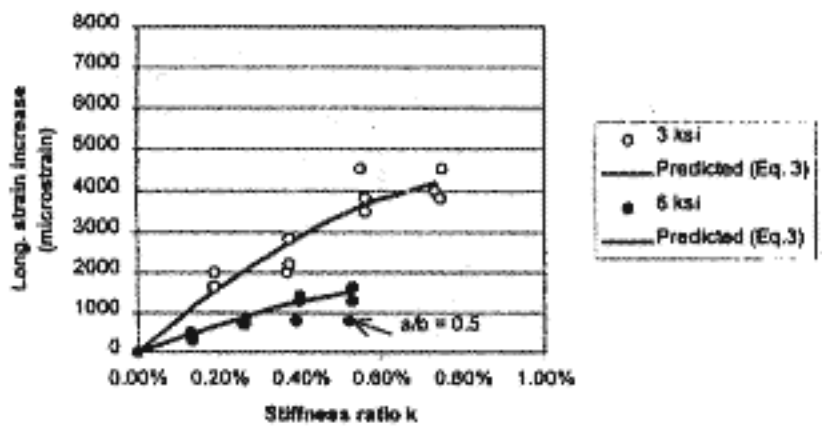

Fig. 3—Axial strain increase versus CFRP jacket to concrete column stiffness ratio.

axial strain depends on both the concrete strength and the stiffness ratio k. The ultimate axial strain of the unconfined concrete ε_{cc} can be expressed by

$$\varepsilon_{cc} = \varepsilon_{c0} + 10^3[3k - 150k^2]/f_{c0} \quad (3)$$

where f_{c0} is expressed in psi. Equation (3) is valid for the 3 ksi and the 6 ksi concretes and for the three aspect ratios considered in this study. It is fairly accurate except for the 6 ksi concrete series of specimens having an aspect ratio $a/b = 0.5$, where the axial strains are overestimated by the equation for three and four CFRP layers. The 3 ksi concrete specimens having the same aspect ratio $a/b = 0.5$ showed a good correlation between the measured and the predicted axial strain values.

Stress-strain response in the axial direction

As mentioned previously, the response of FRP wrapped rectangular concrete columns can be simulated by a trilinear curve with no descending branch. The ultimate compressive strength f_{cc} and the ultimate axial strain ε_{cc}, given respectively by Eq. (1) and (3), define the coordinates of the ultimate point of the stress-strain response model. The branch of the transition zone is defined by the so-called yield points.

The second yield point was found to depend on the stiffness ratio and also on the unconfined concrete strength (refer to Fig. 4). This behavior was also observed in circular columns[8] and was modeled by a bilinear response with a transition zone in the form of a parabolic curve. Other studies[9,12] have shown a similar response for fiber-wrapped circular and rectangular columns with glass, Kevlar, and carbon fibers. From the results, the difference between the stress corresponding to the second yield point f_{cy2} and the compressive concrete strength of the unconfined concrete f_{c0}

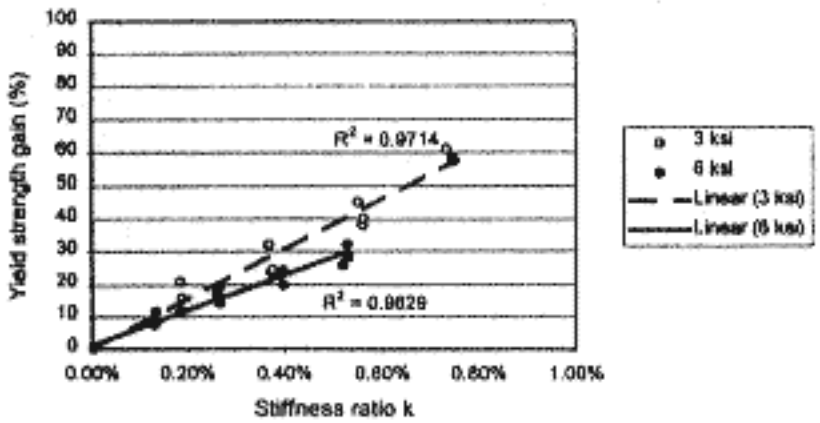

Fig. 4—Second yield strength gain versus CFRP jacket to concrete column stiffness ratio k.

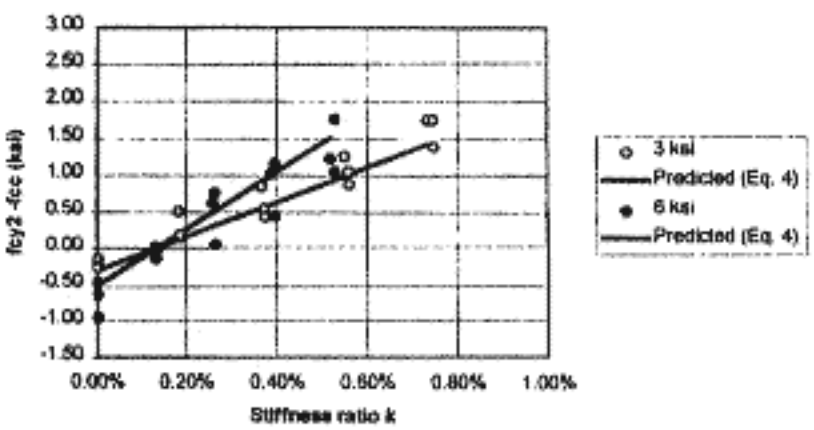

Fig. 5—Difference between second yield strength and f_{c0} versus CFRP jacket to concrete column stiffness ratio.

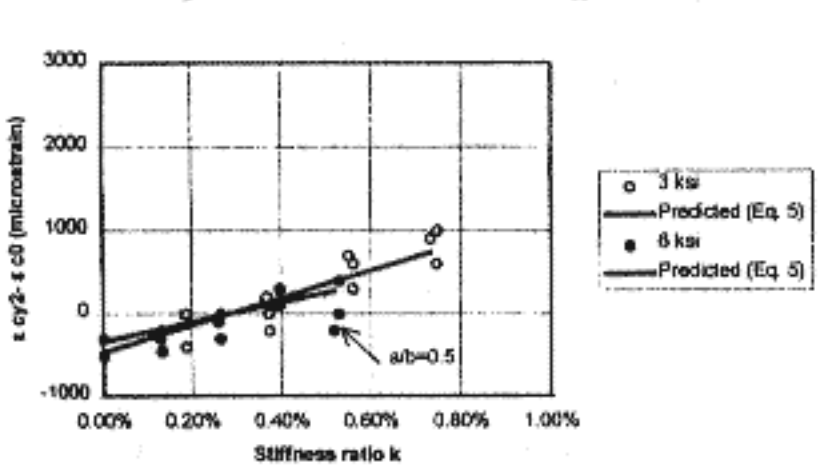

Fig. 6—Difference between second yield axial strain and ε_{c0} versus CFRP jacket to concrete column stiffness ratio.

was calculated and plotted in Fig. 5 versus the stiffness ratio. The correlation between the two variables is clear and the second yield stress f_{cy2} can be expressed by the following equation

$$f_{cy2} = f_{c0} + (1820k - 2.4)f_{c0}^{0.6} \quad (4)$$

where f_{c0} is expressed in psi and all the terms are as previously defined.

Using a similar approach, the difference between the second yield axial strain ε_{cy2} and the ultimate axial strain of the unconfined concrete ε_{c0} was plotted in Fig. 6 versus the stiffness ratio, and the second yield axial strain is given by

$$\varepsilon_{cy2} = \varepsilon_{c0} + 10^{-3} \times (4200k - 11.9)/f_{c0}^{0.4} \quad (5)$$

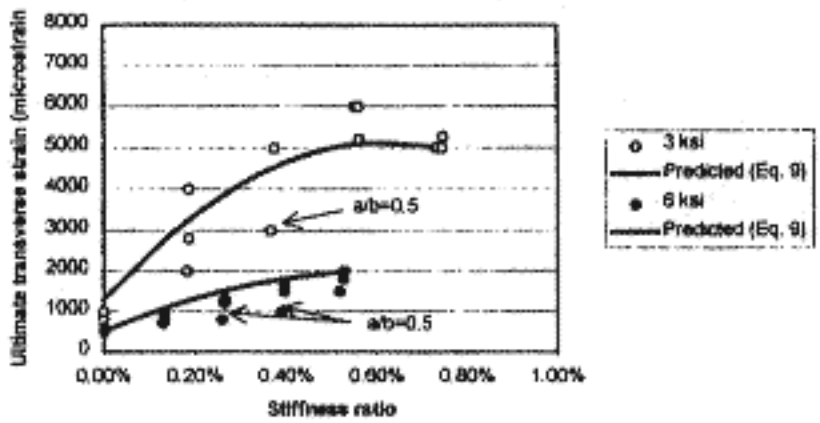

Fig. 7—Maximum transverse strains versus CFRP jacket to concrete column stiffness ratio.

The slope of the first branch of the trilinear stress-strain response in the axial direction is, as expected, independent of the jacket stiffness and can reasonably be expressed by the ACI-318 formula for normalweight concrete. That is

$$E_1 = 57,000f_{c0}^{0.5} \quad (6)$$

where E_1 is the slope of the first branch of the stress-axial strain response, in psi, and f_{c0} is the ultimate compressive strength of the unconfined concrete, in psi.

The first yield stress f_{cy1} was found to be approximately 70% of the second yield stress f_{cy2}. Hence, the first yield point coordinates can be defined as

$$f_{cy1} = 0.7f_{cy2} \quad (7)$$

$$\varepsilon_{cy1} = \frac{f_{cy1}}{E_1} \quad (8)$$

Stress-strain response in transverse direction

Figure 7 shows the transverse strains for the 3 and 6 ksi specimens against the stiffness ratio. Except for the series of specimens that have an aspect ratio of $a/b = 0.5$, the ultimate transverse strain of the confined concrete $\varepsilon_{cc,t}$ can be expressed with a relatively good correlation by

$$\varepsilon_{cc,t} = [4.2 + 4000k - 320,000k^2]/f_{c0} \quad (9)$$

where f_{c0} is expressed in psi.

Figure 8 presents the second yield transverse strain $\varepsilon_{cy2,t}$ for the confined concrete versus the stiffness ratio. It can be observed that $\varepsilon_{cy2,t}$ depends, to a certain extent, on the unconfined concrete strength and can be expressed by

$$\varepsilon_{cy2,t} = 10^{-3} \times [2 - 35k + 45,000k^2]/f_{c0}^{0.2} \quad (10)$$

The first yield transverse strain of the confined concrete, $\varepsilon_{cy1,t}$, can be obtained from Eq. (11) because the behavior is considered linear elastic in the first branch of the stress-strain model.

$$\varepsilon_{cy1,t} = \mu\varepsilon_{cy1} \quad (11)$$

Table 1—Comparison between Wang test results and predicted values by model

Description of test	Number of layers	GFRP modulus, GPa	GFRP thickness, mm	Test results		Ratio f_{cc}/f_{c0}	
				f_{c0}, MPa	f_{cc}, MPa	Measured	Predicted and Δ%
Ten (207 x 207 x 600 mm) prisms wrapped with CFRP. Corner radius = 20 mm	1	23	1.27	37	39.2	1.06	1.05 (–1)
	2	23	2.54	37	40.4	1.09	1.09 (0)
	4	23	5.08	37	42.7	1.15	1.18 (+3)

Note: 1 in. = 25.4 mm, 1 MPa = 0.145 ksi, 1 GPa = 145 ksi, Δ% = (predicted f_{cc}/f_{c0}-measured f_{cc}/f_{c0})/(predicted f_{cc}/f_{c0}) × 100.

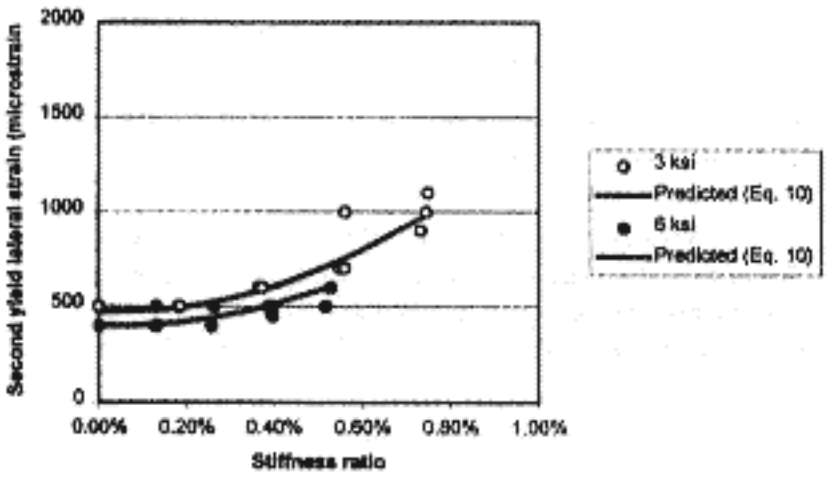

Fig. 8—Second transverse yield strains versus CFRP jacket to concrete column stiffness ratio.

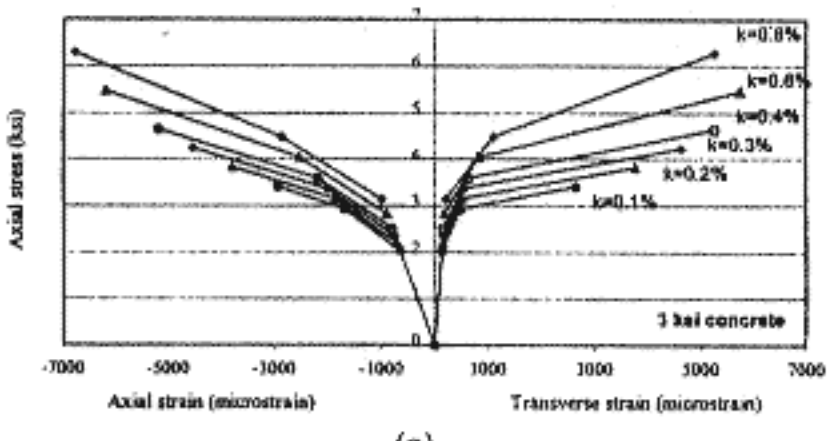

(a)

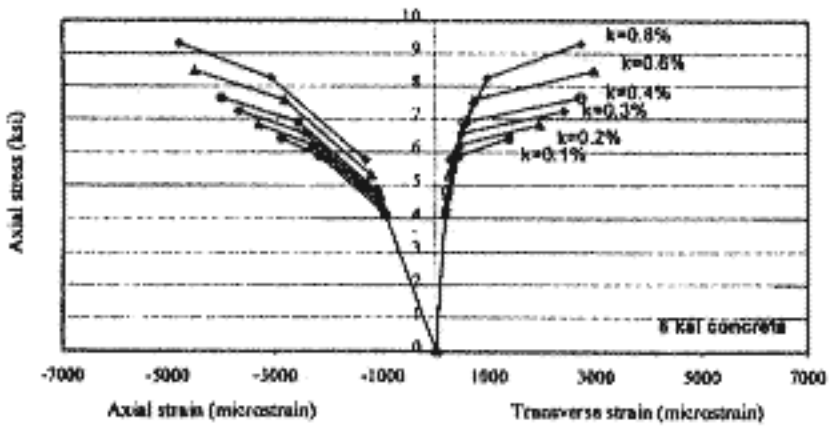

(b)

Fig. 9—Theoretical stress-strain response for confined concrete with different k ratios: (a) 3 ksi concrete; and (b) 6 ksi concrete.

where μ is the Poisson's ratio of concrete and ε_{cyl} is the first axial yield strain of the confined concrete. The stresses corresponding to the yield and ultimate transverse strains are the same as those corresponding to the axial strains and expressed in Eq. (1), (4), and (7).

Thus, using the developed Eq. (1) to (11), the stress-strain response in the axial direction, as well as in the transverse direction (refer to Fig. 1), can be defined. Figure 9 presents the theoretical stress-strain response for 3 and 6 ksi concrete columns wrapped to a stiffness ratio ranging from $k = 0.1\%$ to $k = 0.8\%$.

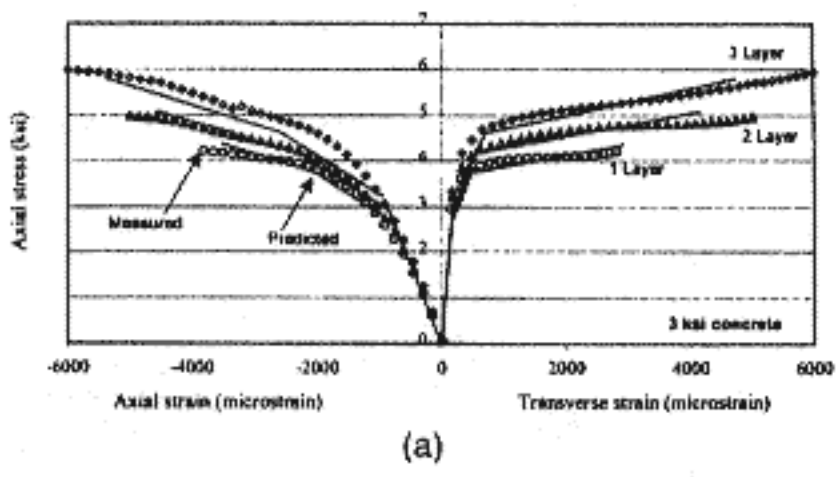

(a)

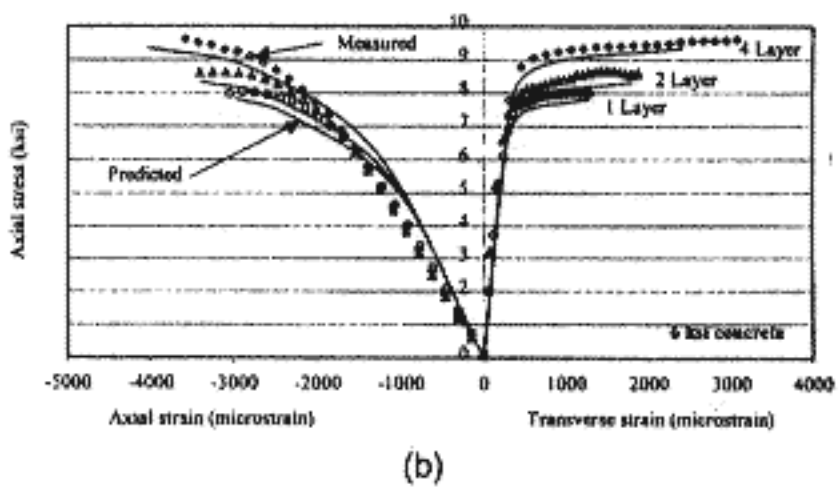

(b)

Fig. 10—Measured and predicted stress-strain response for: (a) 3 ksi concrete; and (b) 6 ksi concrete.

Validation of the model

The validity of the model was first verified by comparing the predicted values to the measured values obtained in laboratory tests. Figure 10(a) and (b) show the predicted and measured response for the 3 and 6 ksi concretes, respectively, wrapped with different numbers of layers of CFRP wrap. It is seen that the correlation between the measured and predicted values is good. To further validate the model, it was compared to results reported in other research studies. It must be noted that most of the research findings reported in the literature provide only the ultimate compressive strength of the confined concrete and, in some cases, the corresponding ultimate strain. A complete response model for rectangular columns retrofitted with FRP wrap is not available in the literature. Experimental results reported by a recent study[15] were compared with the results predicted by the proposed model (refer to Table 1). The comparison shows a good correlation between the measured and predicted values for the ultimate compressive strength of concrete confined by GFRP wrapping.

Table 2—Comparison between Rochette test results and predicted values by model

Description of tests	FRP layer number	FRP modulus, GPa	FRP thickness, mm	Test results		Ratio f_{cc}/f_{c0}	
				f_{c0}, MPa	f_{cc}, MPa	Measured	Predicted and Δ%
Five (152 x 152 x 500 mm) prisms wrapped with CFRP. Corner radius = 25 mm	3	82.7	0.9	42	42.4	1.01	1.18 (+14)
	4	82.7	1.2	43.9	50.9	1.16	1.23 (+6)
	5	82.7	1.5	43.9	47.85	1.09	1.29 (+15)
	4	82.7	1.2	35.8	52.27	1.46	1.31 (–14)
	5	82.7	1.5	35.8	57.64	1.61	1.39 (–16)
Four (152 x 152 x 500 mm) prisms wrapped with aramid composites. Corner radius = 25 mm	3	13.6	1.26	43	51.2	1.19	1.04 (–14)
	6	13.6	2.52	43	51.2	1.19	1.08 (–10)
	9	13.6	3.78	43	53.32	1.24	1.12 (–11)
	12	13.6	5.04	43	55	1.28	1.16 (–10)

Note: 1 in. = 25.4 mm; 1 MPa = 0.145 ksi; 1 GPa = 145 ksi; and Δ% = (predicted f_{cc}/f_{c0} – measured f_{cc}/f_{c0})/(predicted f_{cc}/f_{c0}) × 100.

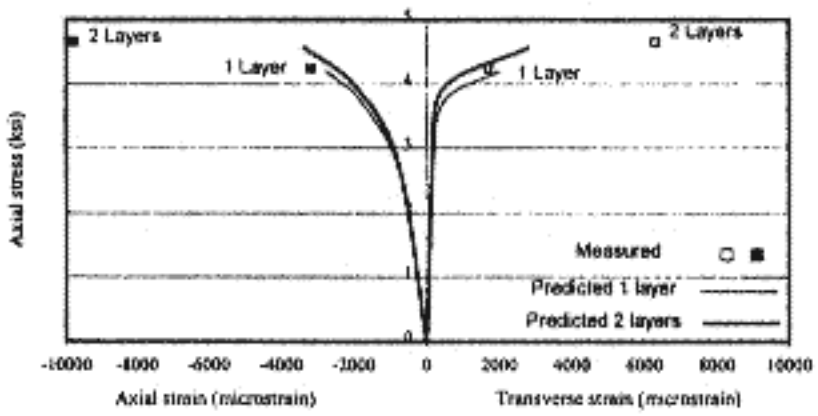

Fig. 11—Predicted stress-strain response versus measurements of ultimate stress and strains for concrete prisms confined by GFRP wrapping from Harries et al.[14]

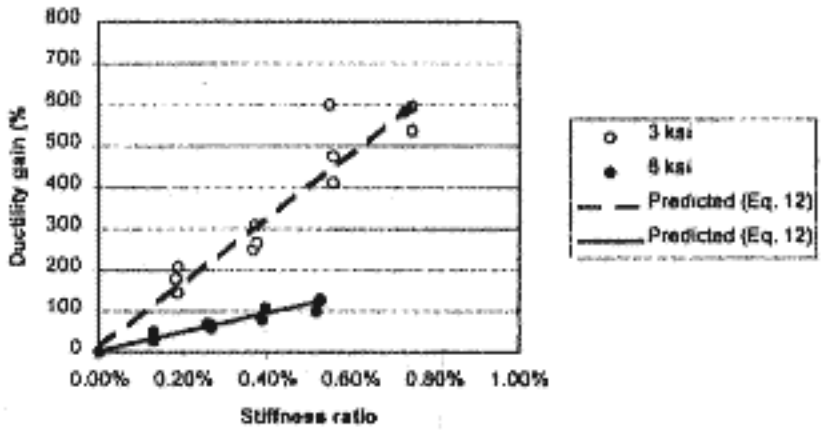

Fig. 12—Gain in ductility versus CFRP jacket to concentrate column stiffness ratio.

The values predicted by the model were also compared with test results reported by another study.[14] Figure 11 presents the measured ultimate compressive strength of confined concrete and corresponding strains for two series of tests on square concrete prisms of 6 in. × 6 in. (150 mm × 150 mm) confined with one and two layers of GFRP, together with the stress-strain response predicted by the model in continuous lines. A good correlation exists between the measured and predicted values for the specimens wrapped by one layer. The specimens confined with two layers showed a good correlation for the ultimate compressive strength of the confined concrete, but not as good for the corresponding strain.

Finally, a recent study[11] presented results of tests performed on rectangular prisms confined with various numbers of layers of CFRP and aramid fiber composites. Three corner radii were considered: 0.2, 1, and 1.5 in. (5, 25, and 38 mm). Only those results related to the corner radius of 1 in. (25 mm), however, are considered for discussion. Table 2 presents a comparison between the measured ultimate compressive strength of the confined concrete and the values predicted by the model. It can be seen that the difference between the measured values and the model varied between 6 and 18%. The difference between the measured and predicted values can be partially attributed to the scatter in test results reported by the authors. The measured strains in the composite were not reported for the corner radius of 1 in. (25 mm). The values reported for the specimens with corner radii of 0.2 in. (5 mm) and 1.5 in. (38 mm), however, were in the range of the values predicted by the model.

Aspect ratio effect

The ultimate compressive strength, the yield stress, the axial, and the transverse yield strains of the confined concrete were found to be independent of the aspect ratio. The ultimate axial and the ultimate transverse strains for specimens having an aspect ratio $a/b = 0.5$, however, were found to be overestimated by the model. Therefore, until further research is made available, it is suggested that the aspect ratio be greater than 0.6 when using the model to calculate the ultimate strains of confined rectangular short columns. In addition, the corner radii should be greater than or equal to 1 in. (25.4 mm) when using the proposed model. Clearly, the model can be further refined as more data is made available with regard to the effect of the corner radius.

Ductility response

A ductility can be defined as the area under the stress-strain diagram in the axial direction. The ductility of the short columns increased as the number of layers increased. Both the axial and the transverse strains at ultimate increased as the CFRP jacket stiffness increased. Figure 12 presents the gain in ductility versus the stiffness ratio k for both the 3 and the 6 ksi concretes. It can be observed that the increase in ductility due to the confinement provided by the CFRP layers is substantially greater for the 3 ksi concrete columns compared with the 6 ksi concrete columns. The ductility gain can be expressed by

$$\text{Ductility gain, \%} = 125 \times 10^8 k / f_{c0}^{1.5} \qquad (12)$$

where k is the effective confinement coefficient and f_{c0} is the ultimate compressive strength of the unconfined concrete, in psi.

CONCLUSIONS

This study presents a stress-strain response model in the axial and the transverse directions for short rectangular columns

strengthened by externally bonded FRP jacket. The model is based on test results from an extensive experimental investigation where a total of 90 rectangular short column specimens were instrumented and tested under uniaxial compression conditions. The findings can be summarized as follows: a) the stiffness of the applied FRP jacket is the key parameter in the design of external jacket retrofits. The enhancement of the performance of the confined concrete columns is governed by the ratio of FRP jacket stiffness in the lateral direction to the axial stiffness of the columns; b) the confinement provided by the FRP improves both the load-carrying capacity and the ductility of rectangular columns but to a lesser degree than for circular columns; c) the gain in performance (strength and ductility) due to the wrapping, with respect to the control (unwrapped specimen), was relatively greater for 3 ksi wrapped columns than for the corresponding 6 ksi concrete wrapped columns; and d) the increase in ultimate compressive strength of the confined concrete due to the wrapping was found to be independent of the unconfined concrete strength and of the column's aspect ratio.

The proposed model for stress-strain response in the axial and the transverse directions is trilinear. The coordinates of the points defining the models were determined in terms of the confinement coefficient k and the ultimate strength and ultimate strain of the unconfined concrete.

Some difference between the measured strains and the strains predicted by the model was observed in a number of specimens with an aspect ratio $a/b = 0.5$. Therefore, until further data is made available, it is suggested that the use of the model be limited to columns with aspect ratios ranging from 0.6 to 1.0.

ACKNOWLEDGMENTS

The financial support provided by the Natural Science and Engineering Council of Canada (NSERC) to the project is gratefully acknowledged.

REFERENCES

1. Ahmad, S. H.; Khaloo, A. R.; and Irshaid, A., "Behavior of Concrete Spirally Confined by Fiberglass Filaments," *Magazine of Concrete Research*, V. 43, No. 156, 1991, pp. 143-148.

2. Fardis, M. N., and Khalili, H. H., "Concrete Encased in Fiberglass-Reinforced Plastic," ACI JOURNAL, *Proceedings* V. 78, No. 6, Nov.-Dec. 1981, pp. 440-446.

3. Miyaushi, K.; Nishibayashi, S.; and Inoue, S., "Estimation of Strengthening Effects with Carbon Fiber Sheet for Concrete Column," *Non Metallic (FRP) Reinforcement for Concrete Structures*, Proceedings of the Third International Symposium, V. 1, Sapporo, Japan, 1997, pp. 217-232.

4. Samman, M.; Mirmiran, A.; and Shahawy M., "Model of Concrete Confined by Fiber Composites," *Journal of Structural Engineering*, Sept. 1998, pp. 1025-1031.

5. Spoelstra, M. R., and Monti, G., "FRP-Confined Concrete Model," *Journal of Composites for Construction*, V. 3, No. 3, Aug. 1999, pp. 884-888.

6. Seible, F.; Priestley, N.; Hegemier, G. A.; and Innamorato, D., "Seismic Retrofit of RC Columns with Continuous Carbon Fiber Jackets," *Journal of Composites for Construction*, V. 1, No. 2, 1997, pp. 52-62.

7. Chaallal, O.; Shahawy, M.; and Hassan, M., "Performance of Axially Short Columns Strengthened with CFRP Wrapping," *ASCE Journal of Composites for Construction*, 2002. (to be published)

8. Mirmiran, A., and Shahawy, M., "Behavior of Concrete Columns Confined with Fiber Composites," *Journal of Structural Engineering*, ASCE, V. 123, 1997, pp. 583-590.

9. Nanni, A., and Bradford, M. N., "FRP Jacketed Concrete under Uniaxial Compression," *Construction & Building Materials*, V. 9, No. 2, 1995, pp. 115-124.

10. Demers, M.; Hebert, D.; Labossière, P.; and Neale, K. W., "The Strengthening of Structural Concrete with an Aramid Woven Fiber/Epoxy Resin Composite," *Proceedings of Advanced Composite Materials in Bridges and Structures II*, Montreal, Quebec, Canada, Aug. 1995, pp. 435-442.

11. Rochette, P., and Labossière, P., "Axial Testing of Rectangular Column Models Confined with Composites," *Journal of Composites for Construction*, V. 4, No. 3, 2000, pp. 129-136.

12. Picher, F.; Rochette, P.; and Labossière, P., "Confinement of Concrete Cylinders with CFRP," *Proceedings of the First International Conference on Composites in Infrastructure*, ICCI '96, H. Saadatmanesh and M. R. Ehsani, eds., Tucson, Ariz., 1996, pp. 829-841.

13. Hosotani, M.; Kawashima, K.; and Hoshikima, J., "A Study on Confinement Effect of Concrete Cylinders by Carbon Fiber Sheets," *Non Metallic (FRP) Reinforcement for Concrete Structures*, Proceedings of the Third International Symposium, V. 1, Sapporo, Japan, 1997, pp. 209-216.

14. Harries, K. A.; Kestner, J.; Pessiki, S.; Sause, R.; and Ricles, J., "Axial Behavior of Reinforced Concrete Columns Retrofit with FRPC Jackets," *Fiber Composites in Infrastructure*, Proceedings of the Second International Conference on Composites in Infrastructure, ICCI '98, H. Saadatmanesh and M. R. Ehsani, eds., Tucson, Ariz., 1998, pp. 411-425.

15. Wang, Y. C., and Restrepo, J. I., "Investigation of Concentrically Loaded Reinforced Concrete Columns Confined with Glass Fiber-Reinforced Polymer Jackets," *ACI Structural Journal*, V. 98, No. 3, May-June 2001, pp. 377-385.

16. Mander, J. B., Priestley, M. J. N., and Park, R., "Theoretical Stress-Strain Model for Confined Concrete," *Journal of Structural Engineering*, ASCE, V. 114, No. 8, 1988, pp. 1804-1826.

國立雲林科技大學
九十二學年度研究所博士班招生考試試題

所別：工程科技研究所
科目：營建文獻評論

（附件2）

Residual Shear Strength Mobilized in First-Time Slope Failures

G. Mesri, M.ASCE,[1] and M. Shahien, A.M.ASCE[2]

Abstract: This paper presents a review of long-term stability of stiff clay and clay shale slopes, and detailed reanalyses of 99 case histories of slope failures in 36 soft clays to stiff clays and clay shales. We analyzed 107 sections using the observed actual slip surface. In a first-time slope failure in clay or shale, part or all of the slip surface is unsheared prior to the occurrence of the landslide. Most stiff clays and clay shales contain stratigraphic discontinuities such as bedding planes and laminations. The fully softened shear strength is shown to be the lower bound for mobilized shear strength in first-time slope failures in homogeneous soft to stiff clays and on the slip surfaces cutting across bedding planes and laminations. For many of the first-time slope failures it appears that part of the slip surface is at the residual condition. For excavated slopes, the residual condition could be present before the final slope is formed, or it may develop in response to excavation by progressive deformation along nearly horizontal surfaces including bedding planes or laminations. In addition to the permeability dependent rise in porewater pressure, and softening, delayed first-time failure of slopes in stiff clays and clay shales is caused by propagation of the residual condition into the slope, on horizontal or subhorizontal surfaces including stratigraphic discontinuities. The residual condition is present on the entire surface of reactivated landslides.

DOI: 10.1061/(ASCE)1090-0241(2003)129:1(12)

CE Database keywords: Clays; Laminates; Residual strength; Slope stability.

Introduction

Residual shear strength has been largely associated with reactivated landslides. It has been assumed that large displacements commonly associated with landslides have already presheared the entire slip surface to the residual condition. Compelling evidence and interpretation have accumulated during the past three decades, however, to suggest that residual conditions may also be present on part of the slip surface of first-time natural or excavated slope failures in stiff clays and clay shales. The geological history of stiff clays and clay shales, including deposition, consolidation, erosion, swelling, softening, and preshearing, may facilitate lithological and structural discontinuities, including laminations, bedding planes, and presheared surfaces, that fail to residual condition after small shear displacements as compared to the large movements commonly associated with reactivated landslides. In a first-time global slope failure, different elements along the slip surface may mobilize the intact, the fully softened, or the residual shear strength. Empirical data from laboratory tests are available for characterizing both the residual shear strength and the fully softened shear strength of stiff clay and clay shale compositions, and nonlinear shear strength-effective normal stress equations allow interpolation and extrapolation of the empirical information.

To assess the degree to which residual shear strength plays a role in landslides, stability analyses were carried out for 99 slope failures in 36 soft clays to stiff clays and clay shales. Reactivated landslides in 11 stiff clays and clay shales were analyzed in order to evaluate the empirical information on residual shear strength based on laboratory shear tests. First-time slope failures in 14 homogeneous soft to stiff clays were analyzed to compare the lower bound of the back-calculated mobilized shear strength on the observed slip surface to the empirical data on the fully softened shear strength from laboratory tests. Forty-six sections in 40 first-time slope failures in 14 stiff clays and clay shales were analyzed using the residual shear strength on part of the observed slip surface. In all cases, effective stress stability analyses were carried out using the observed actual slip surface.

Geological History

The geological history of stiff clays and clay shales in natural and excavated slopes has three distinct phases, notwithstanding intermittent deposition and erosion and multiple glacial advances and retreats at some areas. First is the phase of accumulation of silt- and clay-sized particles, consolidation under the weight of overburden, and aging over a period of up to millions of years, including in some cases bonding by siliceous, calcareous, or organic precipitates. In lacustrine environments annual horizontal varves develop with silt- and clay-rich laminations. Flocculation in saline or marine water, although hindering the segregation of silt- and clay-sized particles, does not prevent the formation of annual laminations of organic matter and calcium carbonate (Rubey 1930). Laminations and bedding planes also result from dramatic changes in climate and source material. Volcanic events deposit layers of ash that may alter into highly plastic clay seams.

Under the weight of overburden, including ice in some areas, that might range from 1 to 30 MPa, and the lapse of millions of

[1]Ralph B. Peck Professor of Civil Engineering, Univ. of Illinois at Urbana-Champaign, Urbana, IL 61801. E-mail: g-mesri@uiuc.edu

[2]Assistant Professor of Civil Engineering, Tanta Univ., Tanta, Egypt.

Note. Discussion open until June 1, 2003. Separate discussions must be submitted for individual papers. To extend the closing date by one month, a written request must be filed with the ASCE Managing Editor. The manuscript for this paper was submitted for review and possible publication on March 16, 2000; approved on May 7, 2002. This paper is part of the *Journal of Geotechnical and Geoenvironmental Engineering*, Vol. 129, No. 1, January 1, 2003. ©ASCE, ISSN 1090-0241/2003/1-12–31/$18.00.

years in a laterally constrained compression condition, plate-shaped or elongated particles reorient in the horizontal direction, especially in seams rich in clay minerals. Clay particle orientation in the horizontal direction or microlamination of mineralogy and particle size leads to planes of fissility parallel to the bedding in shales. Some argillaceous rocks are deformed, sheared, and weakened during the first phase by tectonic or glacial forces and horizontal compression that produce relative displacements along lithological discontinuities (Cruden and Tsui 1991; Imrie 1991). However, in general, during the first phase there is a gradual increase in shear strength with time until aging at the maximum overburden pressure is interrupted, e.g., by erosion of overburden and swelling. In summary, the first phase produces stiff clay and clay shale masses that frequently are stratified and include horizontal or subhorizontal weak layers that may range in thickness from a few tenths or hundredths to more than 10 mm.

The second phase is the period of erosion of overburden or retreat of ice, with or without significant reductions in horizontal restraints. This phase produces heavily overconsolidated stiff clay and clay shale. During this unloading phase, joints may form at regular spacing and random inclinations varying from vertical to horizontal, including subhorizontal shears. The removal of overburden and lateral support leads to undrained deformation, development of planes of parting parallel to laminations and bedding planes, and horizontal displacement along laminations and bedding separations (Singh et al. 1973; Imrie 1991). The decrease in effective overburden leads to primary and secondary swelling, and the breakdown of interparticle bonds and fissuring leads to softening and to further displacements along bedding planes. Mechanical and chemical weathering, including cycles of drying and wetting or freezing and thawing, accelerates the softening process (Chandler 1972; Graham and Au 1985). During the second phase, the shear strength of stiff clay or clay shale gradually deteriorates with time (Terzaghi 1936; Bjerrum 1967; Wilson 1970; Morgenstern 1977; Hutchinson 1988). The end result of complete softening in homogeneous clays and shales is the fully softened condition with a shear strength equal to that of the normally consolidated mineralogical composition of the stiff clay or clay shale (Henkel 1957; Skempton 1970). The so-called "intact" strength, defined by peak strength of undisturbed specimens, corresponds to a partially softened condition of stiff clay or shale during the second phase but before the fully softened condition is reached. Intact strength deteriorates with time also as a result of shear induced creep strains (Tavenas and Leroueil 1981). Thus the intact strength representative of a mass of stiff clay and clay shale is highly dependent on the degree of softening and on the duration of shearing.

During the second phase, shear strains may become localized on a continuous shear surface and take the stiff clay or clay shale to the residual condition at which plate-shaped and elongated particles are substantially oriented in the direction of shearing (Skempton and Petley 1967; Esu and Calabresi 1969). At the residual condition, a predominantly face to face interaction among clay particles minimizes short-range edge to face contact and interlocking, and thus decreases shearing resistance (Mesri and Cepeda-Diaz 1986). The drop in shearing resistance to the residual condition is facilitated on stratigraphic discontinuities such as bedding planes, laminations, and weak seams, because these features tend to localize shear strains and because the clay particles were already oriented parallel to stratigraphic planes during the first phase. The residual condition may be reached on the failure surface through a clay after a landslide movement, or along subhorizontal planes including stratigraphic discontinuities as a result of differential horizontal movement valleyward or seaward by undrained deformation including creep, and by swelling during and following erosion, downcutting, and removal of lateral support. A colluvium may form on a slope, and solifluction and downslope creep may lead to the residual condition at the contact surface of weathered colluvium and unweathered stiff clay or clay shale (Wilson 1970). A significant portion of the shear deformation leading to the residual condition is time-independent. However, because differential undrained creep and swelling also contribute to the localized shearing strain, the drop from intact strength to the residual strength is a time-dependent process (James 1970; Burland et al. 1978; Potts et al. 1997). In summary, structural discontinuities, including fissures and horizontal or subhorizontal planes at residual condition, may develop during the second phase.

The third phase begins when an eventually unstable slope is formed by such natural processes as fluvial downcutting, marine wave erosion, and landsliding, or by excavation. The age of an unstable slope is measured from the beginning of the third phase, whereas the age of the stiff clay or clay shale in the slope began with the first phase. At the beginning of the third phase the strength condition of the stiff clay or clay shale may range from intact to residual. For natural slopes, swelling, softening, and localization of shear strains may begin, continue, or accelerate during the third phase (Esu et al. 1984).

For excavated slopes or after rapid erosion, the removal of overburden and lateral support produce a drop in porewater pressure in the stiff clay or clay shale in the slope. With time the porewater pressure rises toward the steady seepage condition in the slope, which decreases the effective stress and causes swelling and a decrease in shear strength (Bishop and Bjerrum 1960; Muir Wood 1971; Vaughan and Walbancke 1973; Eigenbrod 1975; Bromhead and Dixon 1984; Chandler 1984a; Potts et al. 1997). Undrained deformation and swelling, especially at high horizontal stresses prior to excavation, are accompanied by softening due to the extension of fissures and by differential shear displacements toward the valley or excavation along bedding planes and laminations.

The dramatic range in shear strength from the intact condition to the residual condition is illustrated in Fig. 1 using data from triaxial compression, direct shear, and ring shear tests. The relationship between shear strength and effective normal stress is curved (Chandler 1969; Hutchinson 1969; Bishop et al. 1971; Marsland 1972; Morgenstern 1977; Chandler 1982; Lambe 1985; Stark and Eid 1994; Eid 1996; Stark and Eid 1997), and there is no shear strength at zero effective normal stress (Terzaghi et al. 1996). The intact strength envelope displays a pronounced curvature because swelling and softening intensify as effective normal stress decreases toward zero. The fully softened strength envelope (often defined for stiff clays and shales by peak strength of reconstituted normally consolidated specimens) displays a curvature because, even for a random arrangement of particles, high effective normal stresses promote face to face interaction of plate-shaped particles. The residual strength envelope is curved because a higher degree of particle orientation in the direction of shearing is possible at high effective normal stresses. Fig. 1(c) illustrates that there can be a wide variation in the intact strength at any effective normal stress because the stiff clay or clay shale may experience different degrees of softening during the second and third phases of its geological history. The effects of softening from weathering are to lower the intact strength envelope toward the fully softened strength (Chandler and Apted 1988). Because the number, spacing, and orientation of fissures have a pro-

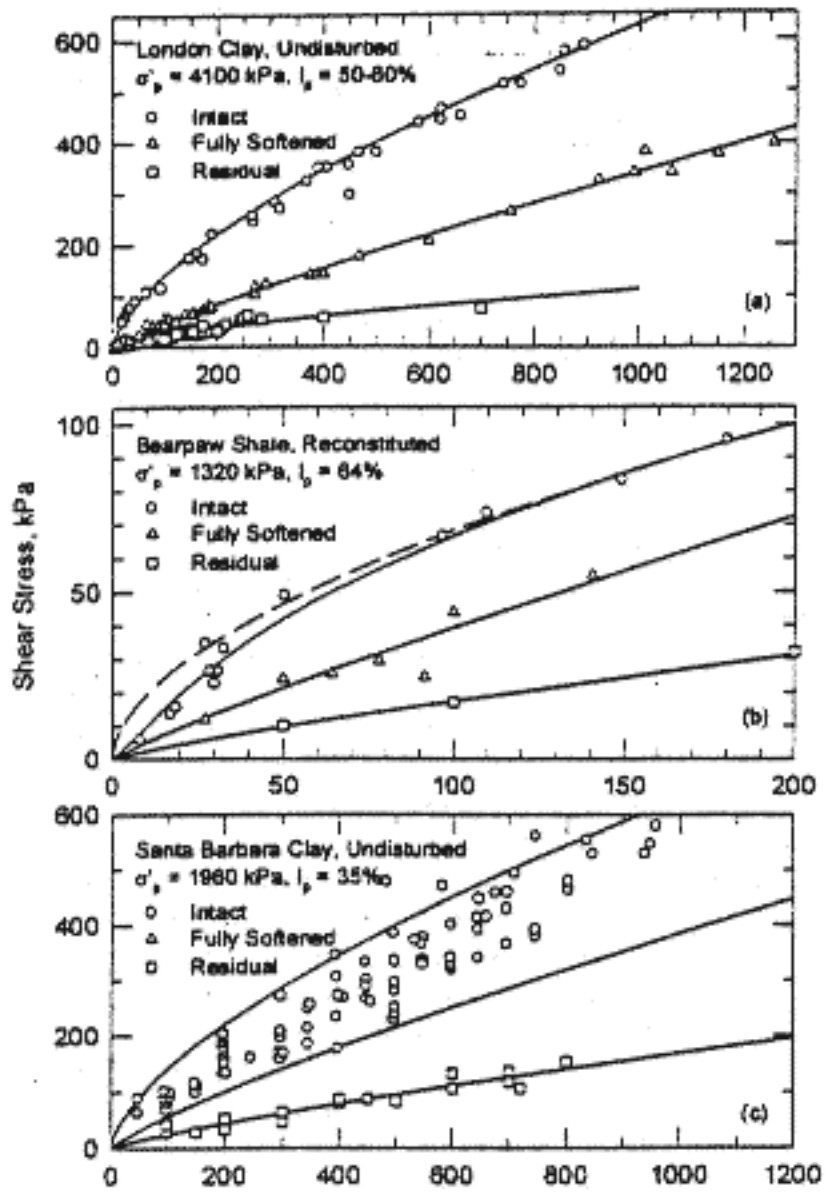

Fig. 1. Intact, fully softened, and residual shear strengths: (a) London clay (data from Bishop et al. 1965; Skempton 1977; Chandler 1984b; Skempton 1985; Eid 1996), (b) Bearpaw shale (data from Singh et al. 1973; Eid 1996), (c) Santa Barbara clay (data from Esu et al. 1984), no laboratory data on fully softened strength of Santa Barbara clay, the curve corresponds to $[\phi'_{fs}]_s$ from Fig. 2 for $I_p = 35\%$

nounced influence on intact strength, the measured peak value depends highly on the location of the sample in the slope and the size of the specimen that is tested (Marsland and Butler 1967; Chandler 1984a; Wu et al. 1987).

A convenient method for expressing a nonlinear relationship between shear strength and effective normal stress is in terms of values of a secant friction angle. The intact, fully softened, and residual shear strength are expressed by

$$s(i) = \sigma'_n \tan[\phi'_i]_s \quad (1a)$$

$$s(\mathrm{fs}) = \sigma'_n \tan[\phi'_{fs}]_s \quad (1b)$$

$$s(r) = \sigma'_n \tan[\phi'_r]_s \quad (1c)$$

where the secant friction angles $[\phi'_i]_s$, $[\phi'_{fs}]_s$, and $[\phi'_r]_s$ = functions of the effective normal stress σ'_n.

Empirical Data on $[\phi'_{fs}]_s$ and $[\phi'_r]_s$

The fully softened friction angle and the residual friction angle depend both on the nature of the particles and on the effective normal stress because the latter influences the arrangement of particles during consolidation and shear. The fully softened shear strength corresponds to a relatively random arrangement of particles with predominant edge to face interaction and interference, whereas the residual shear strength represents the face to face interaction of particles that are predominantly oriented parallel to the direction of shearing to the maximum extent possible for that composition (Mesri and Cepeda-Diaz 1986).

The magnitude of the drop in shear strength from the fully softened condition to the residual condition depends on the plasticity of the clay. The difference between $[\phi'_{fs}]_s$ and $[\phi'_r]_s$ maximizes at a plasticity index around 50%, approaching zero at very low plasticity where particle reorientation is not a factor and at very high plasticity where the predominant particle interaction even for a random fabric is face to face (Mesri and Cepeda-Diaz 1986).

For stiff clays and clay shales compositions containing plate-shaped clay minerals, a correlation should exist between both $[\phi'_{fs}]_s$ and $[\phi'_r]_s$ and index properties such as the liquid limit or plasticity index. These index properties are measures of the ability of the clay or shale constituents to hold water. As the particle size decreases and, therefore, as the particle surface area per unit weight increases, the liquid limit and plasticity index should increase. For plate-shaped clay minerals there is a correlation between particle size and plateyness: as particle size decreases, plateyness increases. A correlation between $[\phi'_{fs}]_s$ or $[\phi'_r]_s$ and liquid limit or plasticity index is expected because each is directly or indirectly related to one or both of the fundamental factors of particle size and plateyness (Mesri and Cepeda-Diaz 1986). However, such empirical correlations are not applicable to clays or shales that are composed of clay minerals that are not plate-shaped, such as attapulgite and allophane, or are exceptionally aggregated (Chandler 1984a; Mesri and Cepeda-Diaz 1986; Terzaghi et al. 1996).

There is considerable information in the literature on the relationship between $[\phi'_{fs}]_s$ and $[\phi'_r]_s$ and index properties (Kenney 1967b; Voight 1973; Kanji 1974; Seycek 1978; Lupin et al. 1981; Chandler 1984a; Skempton 1985; Mesri and Cepeda-Diaz 1986; Mesri and Abdel-Ghaffar 1993; Eid 1996). However, most empirical correlations between friction angles and index properties include significant scatter mainly because of (1) the effect of variable sample preparation (aggregation, disaggregation) on the measurement of index properties (Townsend and Banks 1974), (2) the influence of effective normal stress on friction angles, and (3) the presence of nonplatey or amorphous clay minerals. The empirical correlations by Stark and Eid (1994, 1997) in terms of the liquid limit, w_l, and clay size fraction, CF, include less scatter because all samples for both index tests and for the measurements of friction angles were prepared consistently following the procedure developed by Mesri and Cepeda-Diaz (1986), and because they included the influence of effective normal stress on friction angles. Because the record of a significant number of slope failures reinterpreted for the present study did not include reliable information on CF, the $[\phi'_{fs}]_s$ and $[\phi'_r]_s$ data of Stark and Eid (1994, 1997) were correlated with the plasticity index, I_p, as shown in Fig. 2. Further examination, however, has shown that for many clay and shale compositions, $I_p \approx (w_l)$ (CF), implying that, in fact, I_p to some extent encapsulates information on both w_l and CF.

The empirical equation proposed by Mesri and Abdel-Ghaffar (1993) for the intact strength envelope is rewritten as

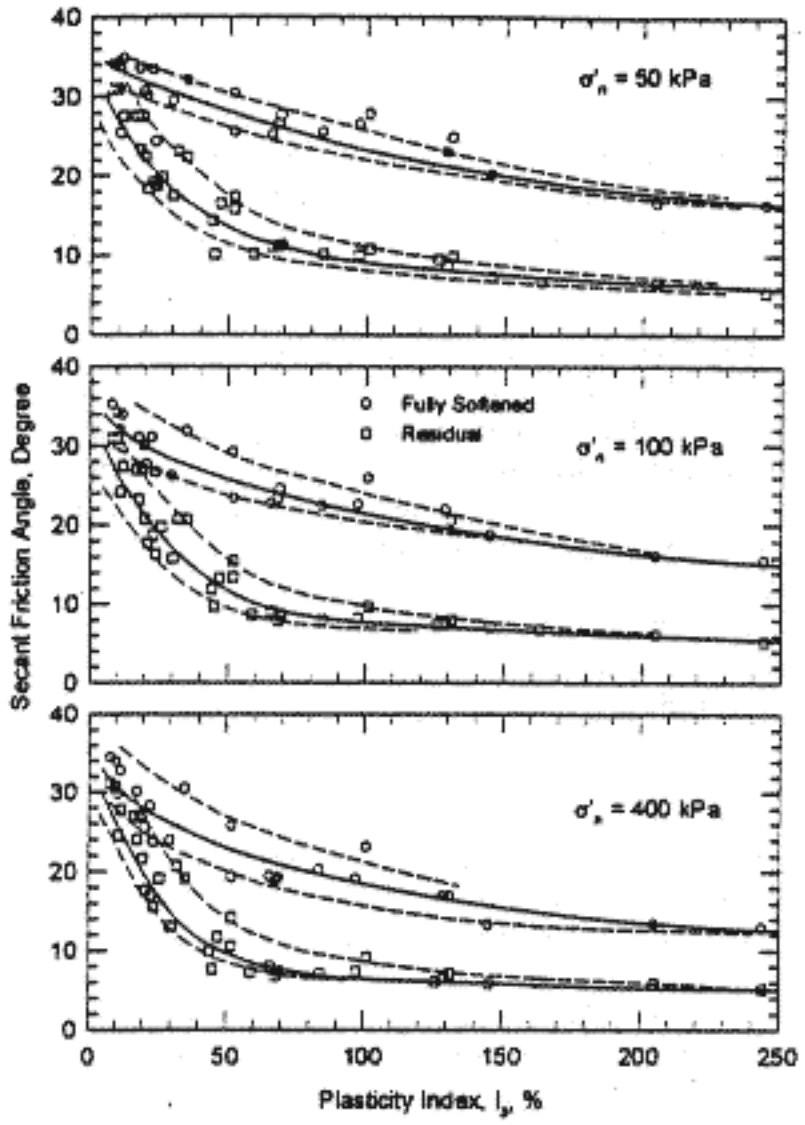

Fig. 2. Empirical information on fully softened strength and residual strength (data from Stark and Eid 1994; Eid 1996; and Stark and Eid 1997)

$$s(i) = \sigma_n' \tan[\phi_{fs}']_s^p \left[\frac{\sigma_p'}{\sigma_n'}\right]^{1-m} \quad (2)$$

where $[\phi_{fs}']_s^p$ = secant fully softened friction angle at $\sigma_n' = \sigma_p'$, and σ_p' = preconsolidation pressure. Eq. (2) together with $([\phi_{fs}']_s^p, m)$ values of (21°,0.65), (20°,0.77), and (28°,0.70) define the intact strength versus effective normal stress curves in Figs. 1(a–c), respectively [dashed curve in Fig. 1(b)]. Similar empirical equations can be used to describe the curvature of fully softened and residual shear strength envelopes

$$s(fs) = \sigma_n' \tan[\phi_{fs}']_s^{100} \left[\frac{100}{\sigma_n'}\right]^{1-m_{fs}} \quad (3a)$$

$$s(r) = \sigma_n' \tan[\phi_r']_s^{100} \left[\frac{100}{\sigma_n'}\right]^{1-m_r} \quad (3b)$$

where $[\phi_{fs}']_s^{100}$ and $[\phi_r']_s^{100}$ = secant fully softened and secant residual friction angles at $\sigma_n' = 100$ kPa. At any plasticity index, $(1-m_{fs})$ = slope of $\log(\tan[\phi_{fs}']_s / \tan[\phi_{fs}']_s^{100})$ versus $\log(100/\sigma_n')$, and $(1-m_r)$ = slope of $\log(\tan[\phi_r']_s / \tan[\phi_r']_s^{100}$ versus $\log(100/\sigma_n')$. In Figs. 1(a–c) the fully softened shear strength envelopes correspond to $([\phi_{fs}']_s^{100}, m_{fs})$ values of (24°,0.88), (22°,0.89), and (29°,0.92), respectively, and the residual shear strength envelopes correspond to $([\phi_r']_s^{100}, m_r)$ values of (10°, 0.85), (9°,0.85), and (14°,0.88), respectively. In the absence of data on fully softened strength for Santa Barbara clay, the lower limit of intact strength is used, which is consistent with $(\phi_{fs}')_s$ data in Fig. 2 for $I_p = 35\%$.

In summary, reliable empirical data on $[\phi_{fs}']_s$ and $[\phi_r']_s$ are now available, and in the absence of site-specific information, can be used to estimate shear strength for stability analysis.

Shear Strength Mobilized in Slope Failures

Experience has evolved to show that in general the shear strength that is mobilized in long-term stability of stiff clays and clay shales may not be equal to the drained shear strength measured in laboratory shear tests. In most laboratory shear tests during the early days of modern soil mechanics, small intact specimens were tested and a measurement of the intact strength was obtained. However, it quickly became apparent that in most field situations the mobilized shear strength, $s(\text{mob})$, was significantly less than the intact strength, $s(i)$. The classic example was described in the Fourth Rankine lecture by Skempton (1964) who recommended for the long-term stability of stiff fissured clay slopes use of the residual strength which had been already introduced by Tiedemann (1937) and Haefeli (1938, 1950). It is now generally accepted that only in homogeneous clays of low plasticity [plasticity index less than 20% (Chandler 1984a; Mesri and Abdel-Ghaffar 1993), or clay content less than 20% (Skempton 1985)], including glacial clays or heavily overconsolidated intact boulder clays and lightly overconsolidated soft to firm clays, is a mobilized strength available that is equal to or greater than the fully softened strength (Skempton and Brown 1961; Kenney 1969; Janbu 1977; Tavenas and Leroueil 1981). In these cases, progressive failure (Duncan 1996) is not a significant factor as there is little difference between the residual friction angle and fully softened friction angle (Mesri and Cepeda-Diaz 1986).

In nonfissured plastic clays an average mobilized shear strength significantly higher than the fully softened strength may not be available because progressive failure along a global slip surface may occur (Peck 1967). Skempton (1970) recommended a mobilized strength equal to the fully softened shear strength for slopes excavated in homogeneous stiff fissured clays in which there has been no previous sliding (Henkel 1957). Following Skempton (1970) it was widely assumed that the fully softened strength is the lower bound for first-time slides in homogeneous stiff fissured clays (James 1970; Skempton 1977, Cancelli 1981; Chandler 1984b). Skempton (1977) assumed that displacements preceding first-time slides are sufficient to cause some progressive failures which reduce the mobilized strength toward the fully softened value, but the movements are not sufficient to reduce the strength to the residual condition.

Subsequent analyses of a number of first-time slope failures in stiff fissured clays in terms of the average effective normal stress and average shear stress acting on the whole slip surface at the time of the failure have led to the conclusion that the mobilized shear strength of fissured clays may be at an intermediate value between the fully softened strength and residual strength (James 1970; Chandler 1984a; Mesri and Abdel-Ghaffar 1993; Potts et al. 1997; Stark and Eid 1997). This possibility had been examined by Bishop (1971) in terms of residual factors along the slip surface. These analyses appear to contradict Skempton's hypothesis that for the displacements which typically precede a first-time slide in stiff clays, the fully softened shear strength is the lower limit.

If a slope failure or landslide has already occurred, any subsequent movement on the existing slip surface is controlled by the residual shear strength. Localized shear displacements have reduced shearing resistance to the residual condition along the en-

tire slip surface. Therefore a shear strength equal to the residual shear strength is available on the preexisting shear surface of old landslides (Skempton 1964; Early and Skempton 1972; Palladino and Peck 1972; Chandler 1984a). Brooker and Peck (1993) define a reactivated slide as one in which the shearing resistance on the failure surface is everywhere reduced to the residual strength. This means that the entire landslide mass is already separated from the stable ground by a slip surface that has reached the residual condition.

Good agreements have been generally obtained between the mobilized residual friction angle back-calculated for reactivated slides and values measured by laboratory tests, for example, on natural shear surfaces obtained from the field or precut planes in multiple reversal direct shear tests or in ring shear tests (Skempton 1964; Palladino and Peck 1972; Blondeau and Josseaume 1976; Chandler 1984a,b; Skempton 1985).

Residual Condition in First-Time Slides

It has been recognized that in geological settings other than reactivated landslides, a potential slip surface may incorporate a previously sheared segment that is at the residual condition (James 1970; Skempton 1970; Wilson 1970; Thomson 1971a,b; Parry 1972; Morgenstern 1977; 1990; Dixon and Bromhead 1991; Imrie 1991; Brooker and Peck 1993). In other words, a first-time slide need not be seated completely in previously unsheared stiff clay or shale (Morgenstern 1977). For the deep-seated Miramar landslide at Herne Bay, Bromhead (1978) used residual strength along the horizontal London clay-Oldhaven Beds and back-calculated a mobilized strength equal to or greater than the fully softened strength along the steep rear part of the observed slip surface. The residual condition might have been present for a long time during phase two, or it may actually develop by progressive deformation in response to the erosion or excavation that leads to the first-time failure (Bjerrum 1967; Peck 1967; Hutchinson 1969; Yudhbir 1969; Wilson 1970; Bishop 1971; Bromhead 1978; Imrie 1991; Potts et al. 1997).

Shear planes on which localized shear displacements have reduced the shearing resistance to the residual condition may exist within otherwise stable slope masses. They may be produced by old landslides buried beneath younger sediments, tectonic folding, glacial shearing, periglacial solifluction, valley rebound, or downslope creep of weathered colluvium on parent stiff clay or clay shale (Skempton and Petley 1967; Clarke et al. 1970; Wilson 1970; Morgenstern 1977). These preexisting shear surfaces have inclinations that may range from horizontal to vertical. In the latter case the shear surface approximately parallels existing topography. However, by far the most common sheared surfaces that are at the residual condition are horizontal or subhorizontal. Stiff clay and clay shale deposits are seldom isotropic and homogeneous. More often they are anisotropic and stratified, and slope movements follow discontinuities such as bedding surfaces or the contact between soft and stiff layers (Dixon and Bromhead 1991).

Slope formation by erosion or excavation in bedded and laminated flat-lying sedimentary layers leads to differential lateral expansion, swelling, and creep. Horizontal or nearly horizontal depositional discontinuities such as bedding planes and partings, laminations, bentonite seams, and abrupt transitions from high to low organic or calcite content (Rubey 1930; Anson and Hawkins 1999) are uniform and continuous in the horizontal direction, and reach the residual condition after horizontal displacements that are much smaller than those resulting from prior landslides. In addition to the existence of high horizontal stresses in highly overconsolidated stiff clays and clay shales and occasional high porewater pressures at permeable–impermeable boundaries, shearing is localized into thin shear bands and shear zones, and plate-shaped particles already lie essentially parallel to bedding planes and laminations. The planes of fissility, caused by differences in lithology or by orientation of clay particles parallel to the bedding, localize shear displacements. According to Obermeir (1984), in the montmorillonite facies of Cretaceous Potomac deposits the subhorizontal bedding-plane partings caused by rebound from erosion unloading are commonly offset horizontally a few millimeters even in nearly level ground; and the few millimeters of relative movement along the two sides of some subhorizontal breaks have been sufficient to make slickensides in the highly plastic clays.

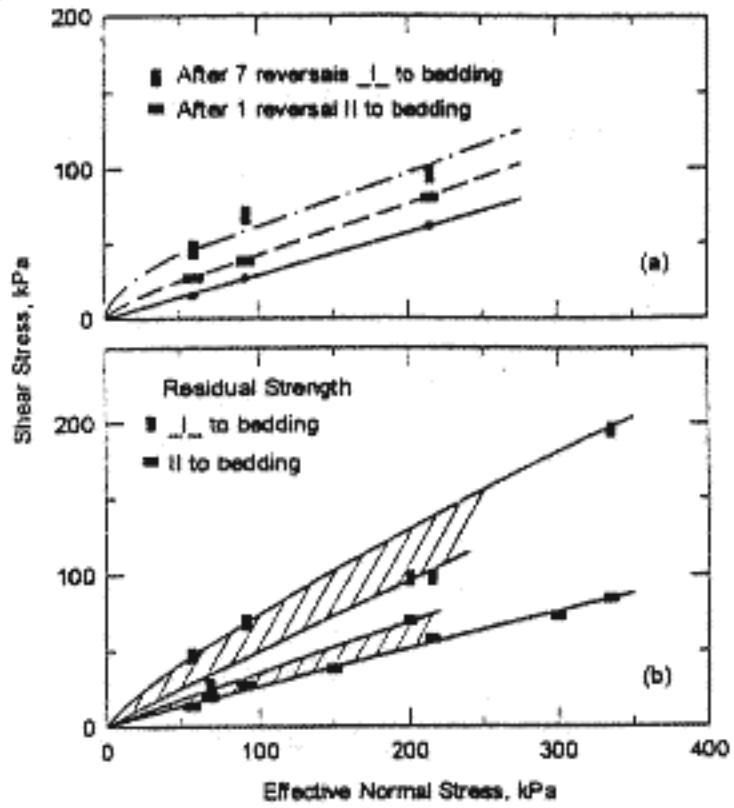

Fig. 3. Oxford clay, influence of direction of shearing on (a) displacement required to reach residual condition defined by solid circles (data from James 1970), (b) residual shear strength (data from James 1970; Parry 1972; Burland et al. 1977)

Because the concept of the residual shear strength has previously been generally limited to reactivated landslide failure surfaces on which previous displacements of several meters are readily possible, a careful examination of the minimum displacement required to reach the residual condition has not been carried out. For thick fault zones with multiple slip surfaces, a large displacement to the residual condition is required because total relative displacement is distributed among slip surfaces (Skempton 1966). It has been frequently assumed that the displacement was not great enough as to reach the residual condition (James 1971). However, as has been pointed out by Morgenstern (1977), large deformations may not be necessary in bedded deposits where shearing is restricted to bedding planes or interfaces. The displacement required to reach the residual, however, is expected to depend on the initial degree of clay particle orientation parallel to the bedding, the thickness of the shear zone, and the direction of shearing (Matheson 1972). The shear strength of clays along bedding planes can fall from the intact to the residual condition as a result of quite modest displacements, and on preexisting shear surfaces the residual strength is recovered at virtually zero dis-

placement (Skempton 1966, 1985). Direct shear tests carried out by James (1970) parallel and perpendicular to the bedding, Fig. 3(a), show that seven reversals of the shear box made perpendicular to the bedding produced less reduction in shear strength of the clay than one reversal along the bedding. Furthermore, data reported by Parry (1972) show that the residual strength parallel to lamination may be significantly less than the residual strength perpendicular to laminations, Fig. 3(b). Apparently, horizontal shearing follows seams of high clay content and high plasticity, whereas the shear planes cutting across the laminations include clay-rich as well as silt-rich seams of high and low plasticity. The residual condition at the toe is reached partly because shear strains to peak and residual condition seem to decrease with the decrease in effective normal pressure (Peck 1967), and shearing may progress predominantly from the toe toward the top of the slope as a result of swelling and shear stress distribution related to lateral unloading (Skempton and LaRochelle 1965; de Beer 1967, 1969; Bishop 1971; Osaimi and Clough 1979; Brooker and Peck 1993; Potts et al. 1997; Cooper et al. 1998).

Skempton and Petley (1967) concluded that movements of not more than 5 mm are sufficient to bring the strength along the joints to the residual condition and polish the joint surface. For the direct shear tests on Oxford clay specimens taken from near the base of Saxon brickpit, only about a 4 mm displacement was required to drop the shear strength on the bedding planes to a value near the residual condition (Burland et al. 1977). An assumed shear band thickness of 0.2 mm [depth of striations produced by typical silt-sized particles (Rubey 1930; Anson and Hawkins 1999)] leads to a shear strain to residual condition, including rotation and distortion, of 20. For a similar initial clay fabric and shear strain, for a shear band thickness of 1 or 10 mm in the field, a horizontal displacement of 20 or 200 mm would be required to reach the residual condition. In fact, inward horizontal displacements of up to 200 mm were observed just below the base level of the 29 m deep excavation to a horizontal distance of 0.69 –1.04 times the slope height, and the associated bedding plane was very polished and striated (Burland et al. 1977). In this case the residual condition on a bedding plane apparently developed during excavation to a significant distance from the face of the pit. Morgenstern (1990) mentions even larger observed lateral movements for excavations and natural slopes. According to James (1970), who analyzed about 90 slope failures in stiff clays and clay shales, it is unusual to find a slip surface extending below the level of the base of the cuttings in overconsolidated clays. This observation can be interpreted to mean that residual conditions on bedding planes and laminations encountered in first-time slides frequently develop during the excavation. A slip plane lower than the base level may develop when a preexisting shear band or an exceptionally weak seam such as a bentonite layer is located below the base of the excavation. This was the case for the Edmonton Convention Center excavation described by Morgenstern (1990). Because the shear band adjacent to Saxon brickpit (Burland et al. 1977) was located near the base of the pit, it probably developed by progressive deformation in response to the excavation. Unfortunately, however, in this case the band was also close to the base of Oxford clay on Kelleways beds which could have been geologically presheared (Morgenstern 1990).

In the Selborne cut-slope experiment in Gault clay (Cooper et al. 1998), starting shortly after slope cutting, 10–20 mm of horizontal displacements were measured on location of a near-horizontal eventual slip surface, while the movements nearer the center and back of the slope were negligible. Postfailure examination disclosed that the planar basal part of the slip surface parallel to the bedding formed as a single, highly polished, and strongly striated slickenside just above the slope toe, whereas the upper part across the bedding displayed a much wider and rougher zone of shearing with little polishing.

In summary, in first-time slope failures in stiff clays and clay shales, the residual condition may exist on horizontal or subhorizontal surfaces, including bedding planes, laminations, or other stratigraphic and structural discontinuities. Parry (1972) expected that for first-time slides in strongly laminated Oxford clay the use of the fully softened shear strength on the laminations might lead to a design on the unsafe side. According to Morgenstern (1990) in developing the site exploration strategy in bedded stiff clays and mudstones, it is prudent to assume at the outset that preshearing exists, and that only modest slips at low angle dips are needed to create residual conditions (Morgenstern 1989). Brooker and Peck (1993) concluded that beneath and behind valley floors where bedding-plane shears could exist, they should be assumed to be present with strengths at residual values, unless their absence can be conclusively demonstrated. In a discussion of the failure of Carsington Dam (Skempton and Vaughan 1995) Skempton stated that "residual strength can indeed play a part in first-time slides in clay fills and cuttings." In a first-time slope failure in stiff clays and clay shales part or all of the global slip surface is unsheared prior to the occurrence of the landslide; however, part of the slip surface may be at the residual condition.

Reanalyses of Slope Failures

Stability analyses were carried out for 99 slope failures in 36 soft clays to stiff clays and clay shales listed in Tables 1–3. 107 sections were analyzed. In all cases the observed actual slip surface was used together with the observed or assumed groundwater conditions or porewater pressures quoted in the original references. Analyses were carried out in terms of effective stress at failure using the reported porewater pressure condition. Most of the porewater pressure data correspond to values of the average porewater pressure ratio $\bar{r}_u$ (the average value of $r_u = u/\sigma_v$ along the slip surface) in the range of 0.2–0.4, near long-term steady condition. The stability analyses were carried out using Spencer's method (1967) as coded in the computer program *UTEXAS3* (Shinoak Software, Austin, Tex.) together with curved relationship between shear strength and effective normal stress. Three-dimensional side effects were not considered in stability analysis because information on the three-dimensional geometry of the slopes was not available. The residual strength condition was assumed to be present over the whole failure surface of reactivated slides and also over the bedding or lamination plane segment or basal planer part of the observed slip surface for the first-time slides. The residual shear strength for first-time slides was selected using the empirical data in Fig. 2 together with the reported plasticity index of the slope material (unless explained otherwise). For homogeneous slopes and on the back scarp of first-time failures, a mobilized strength was back-calculated to correspond to a factor of safety of 1 for the entire slip surface. In most cases the back-calculated mobilized strength was in fact at or near the fully softened condition.

Reanalysis of the Santa Barbara slope failure (Esu et al. 1984) is introduced in Fig. 4 as a means of describing the format used in Figs. 4–9 and 11–16. The stratigraphy and slope geometry are defined in Fig. 4(a) together with the observed slip surface and groundwater surface as indicated by the piezometric level. In some cases the porewater pressure at failure is defined in terms of

Table 1. Reactivated Slides Used to Calibrate Residual Strength from Laboratory Test

No.	Slope failure	Slope material	I_p(%)	$\bar{r}_u$	Reference
1	Lyme Regis 1962, UK	Lower Lias clay[a]	30–45+	0.31	James (1970)
2	Jackfield, Wales, UK	Heavily overconsolidated clay/shale	25	0.39	Henkel and Skempton (1955); Skempton (1964)
3	Portuguese Bend, California, USA	Altamira Bentonitic Tuff	61	0.18	Morriam (1960); Skempton and Hutchinson (1969); James (1970); Wilson (1970); Vonder Linden (1972); Ehlig (1987); Stark and Eid (1994); Eid (1996)
4	Trending Bluff (3 s), California, USA	Santiago formation	45	0.013–0.28	Stark and Eid (1992, 1994); Eid (1996)
5–12	Seattle Freeway (8 slides), Seattle, USA	Lawton clay	15–40	0.10–0.20	Wilson and Johnson (1964); Wilson (1970); Palladino and Peck (1972)
13	Putney-Chirton, UK	Gault clay	40–60	0.30	James (1970)
14,15	Folkestone Warren-Slips W2 & W4, UK	Gault clay	40–60	0.06, 0.20–0.36	Hutchinson (1969)
16–19	Miramar 1953, 1956, 1966, 1979 Herne Bay, Kent, UK	Brown and Blue London clay	50–60	0.37–0.43	Hutchinson (1965a,b, 1980); Hutchinson and Hughes (1968); Bayley (1972); Bromhead (1972, 1978)
20–21	Queen's Avenue 1966, 1970, Herne Bay, Kent, UK	Brown and Blue London clay	50–60	0.34–0.36	Hutchinson (1965b, 1980); Bromhead (1978)
22	Beacon Hill 1966, Herne Bay, Kent, UK	Brown and Blue London clay	50–60	0.43	Wise (1957); Hutchinson (1965b, 1980); Bayley (1972); Bromhead (1978)
23	Guildford, UK	Brown London clay[b]	50–60		Skempton and Petley (1967); Chandler (1969)
24–28	Hadleigh 2, 3, 5, 8, 12, UK	Brown London clay[b]	50–60		Hutchinson and Gostelow (1976)
29	Barnsdale, Leicestershire, UK	Lias clay[a]	30–45+	0.36	Chandler (1976, 1982)
30	Daventry, Northamptonshire, UK	Lias clay[b]	30–45+		Biczysko and Starzewski (1977a,b)
31	Gretton, Northamptonshire, UK	Lias clay	30–45+	0.45	Chandler et al. (1973); Chandler (1982)
32	Hambleton, Leicestershire, UK	Lias clay	30–45+	0.33	Chandler (1976, 1982)
33	Rockingham, Northamptonshire, UK	Lias clay	30–45+	0.44	Chandler (1971, 1982)
34	Uppingham, Leicestershire, UK	Lias clay	30–45+	0.48	Chandler (1970)
35	Wansford, Cambs, UK	Lias clay	30–45+	0.35	Chandler (1979, 1982)
36	Wardley, Leicestershire, UK	Lias clay	30–45+	0.48	Chandler (1982)
37	Weedon, Northamptonshire, UK	Lias clay	30–45+	0.43	Chandler et al. (1973); Chandler (1982)
38–42	Chiusi della Verna (5 slides), Tuscany, Italy	Clay shale[c]	20–25	0.30–0.60	Canuti et al. (1994)
42a[d]	Matsue, Japan	Tertiary Mudstone	60	0.28	Nakamori et al. (1996)

[a]True range of I_p for lias clay is probably 50–60%.

[b]Reported mobilized strength data from back-analysis, no data on $\bar{r}_u$ reported.

[c]True range of I_p for the clay shale is probably 25–40%.

[d]Matsue was initially classified as first-time slide.

$\bar{r}_u$. The dotted line in Fig. 4(a) indicates the piezometric level, and the dashed line the observed slip surface. The segment assumed to be at the residual condition is shown by a bold solid line. Fig. 4(b) shows the values of secant friction angles. The continuous curves correspond exactly to the mean line used to fit the empirical data on fully softened and residual shear strengths in Fig. 2 at a plasticity index of 35%, interpolated or extrapolated with the help of Eqs. (3*a*) and (3*b*). The hollow squares in Fig. 4(b) indicate values of $[\phi'_r]$, used to define the residual shear strength on the segment of the slip surface at the residual condition. The hollow circles represent values of $[\phi'_i]$, back-calculated for a factor of safety of 1 for the entire slip surface; for the Santa Barbara slope failure the back-calculated $[\phi'_i]$, are close to the empirical $[\phi'_{fs}]$, from Fig. 2. Fig. 4(c) shows by continuous curves the fully softened and residual strength envelopes corresponding to $I_p = 35\%$ obtained from Fig. 2. The hollow squares represent the mobilized residual strengths at points on the observed slip surface assumed to be at the residual condition, and hollow circles represent the mobilized shear strength back-calculated at points on the rest of the observed failure surface. Whenever available, residual strengths back-calculated from reactivated slides in the same clay or shale are shown as large solid squares, and laboratory data on residual and fully softened or intact strengths are represented by small solid squares and circles, respectively. Fig. 4(c) shows that in the case of Santa Barbara clay the laboratory residual shear strengths are in excellent agreement with empirical data used to calculate the mobilized residual strength. The back-calculated shear strength on the rest of the failure surface agrees with the fully softened condition defined by the empirical data in Fig. 2 and is much less than most of the intact strength (solid circles) from laboratory tests.

Reactivated Landslides

Reactivated landslides in 11 stiff clays and clay shales were analyzed in order to evaluate the empirical information in Fig. 2 on the residual shear strength. Additional data on mobilized residual

Table 2. First-Time Slides in Unstratified Low-Plasticity Stiff Clays and in Homogeneous Soft to Firm Clays with Mobilized Shear Strength Equal or Greater than Fully Softened Strength from Laboratory Tests

No.	Slope failure	Slope material	I_p(%)	F_u	Reference
43	Kimola canal, Finland	Slightly overconsolidated glacial clay sediments	25–40	0.58	Kankare (1969a,b)
44	Cut slope failure, China	Brown fissured clay	20	0–0.33	Li and Zhao (1984)
45,46	Ukuwela excavation slope failure, (2 slides), Sri Lanka	Talus/weathered residual clayey silt-clayey sand	19–29	0	Balasubramaniam et al. (1977)
47	Selset, Yorkshire, UK	Boulder clay, uniform without fissures or joints	13	0.40	Skempton and Brown (1961)
48	Selnes, Norway	weathered/quick clay	5–7	0.50	Kenney (1966, 1967a)
49	Lodalen, Norway	Dry crust/insensitive firm comparatively homogeneous marine clay/thin silt layers	10–20	0.36	Sevaldson (1956); Kenney (1966)
50	Drammen riverbank failure, Norway	Sensitive normally to slightly overconsolidated clay	10–17	0.35	Kjaernsli and Simons (1962); Kenney (1966)
51	Ullensaker, Norway	Stiff fissured/quick clay	6	0.55	Stabell and Höy (1954); Bjerrum (1955); Kenney (1966); Kenney and Drury (1973)
52	Saint-Vallier, 1, Québec, Canada	Brownish fissured crust/fairly homogeneous gray clay with occasional stones or sand	37	0.23	Lefebvre and LaRochelle (1974); Lefebvre (1981)
53	Saint-Louis 2, Québec, Canada	Sandy layer/gray clay with light tone bands alternating with dark bands	25	0.42	Lefebvre and LaRochelle (1974); Lo and Lee (1974); Lefebvre (1981)
54, 55	Lachute 1 & 2, Montreal, Canada	Silty clay	32–39	0.51–0.60	Lefebvre (1981); Silvestri (1980)
56	Rosemere, Montreal Canada	Silty clay	33	0.42	Lefebvre (1981)
57	Breckenridge, Canada	Sandy silt/clay	38	0.63	Crawford and Eden (1967)
58	Orleans, Ontario, Canada	Soft clay with some silt layers/firm clay	20–40	0.58	Eden and Jarrett (1971)

shear strength from previous back-analyses of reactivated slides in London clay and Lias clay were utilized to evaluate the laboratory information and to select residual strength for analyses of first-time slope failures. The back-calculated residual strength data, to be introduced subsequently, correspond to 45 sections in 43 reactivated slides (Table 1). The example in Fig. 5 shows that the mobilized residual shear strength back-calculated for the porewater pressure range suggested by Hutchinson (1969) are within the range defined by the empirical data in Fig. 2 for a range of I_p of 40–60%. The laboratory values of residual strength for Gault clay are slightly higher than those defined by the empirical data in Fig. 2 and back-calculated mobilized strength.

Ten reactivated and eight first-time slope failures in Lias clay were analyzed, including the reactivated landslide at Lyme Regis shown in Fig. 6 (Tables 1 and 3). For Lias clay, laboratory values of residual shear strength as well as of fully softened shear strength are significantly smaller than corresponding strengths from the empirical data in Fig. 2 for I_p in the range of 30–45%. The mobilized residual strengths back-calculated by Chandler (1984b) and those calculated here for Lyme Regis failure shown in Fig. 6 are smaller than the residual strength from the empirical data for I_p of 30–45%. A much better agreement is obtained between shear strengths from empirical data using an I_p range of 50–60% and from laboratory measurements for both fully softened and residual conditions. In this case, there is also good agreement between the empirical data and back-calculated residual shear strength. One possible explanation of low reported values of I_p is incomplete disaggregation of Lias clay prior to the measurement of Atterberg limits as compared to that assumed in the empirical correlations in Fig. 2. In other words, the values of I_p in the range of 30–45% may underestimate the actual plasticity index of Lias clay in the shear zone.

For the Atterberg limit tests carried out to develop the empirical correlations in Fig. 2, stiff clay and clay shale samples were ball-milled according to the method recommended by Mesri and Cepeda-Diaz (1986). Complete disaggregation of Atterberg limit samples is especially required for the correlations between residual friction angle and liquid limit or plasticity index. It appears that either clay mineral aggregates disaggregate in the shear zone or coarser particles migrate out of the thin shear band (Skempton and Petley 1967; Chandler 1969; Morgenstern 1990). Furthermore, the shear bands in the field are expected to be localized in the most plastic lithologic seams in horizontally bedded clays such as the Lias clay. According to James (1970), Lias clay may contain localized montmorillonitic bands which allow "failures to occur at greatly reduced strengths." This view is supported by the back-analyses of reactivated slope failures in Lawton clay with reported I_p values in the range of 15–40%. The back-calculated residual strengths for the slip surfaces in Fig. 7 as well as other slips (Palladino and Peck 1972) are near the values predicted from the empirical correlation for I_p=40%. Chandler (1984a), aware of the discrepancy for Lias clay between mobilized friction angles and reported Atterberg limits, suggested that for some clays it may be difficult to establish the plasticity index relevant to the landslide, or that the Lias clay landslides moved at a time when porewater pressures were higher than assumed in back-analyses. The latter suggestion, however, does not explain for Lias clay the discrepancy between laboratory measurements of residual and fully softened friction angles and values from the empirical correlations for I_p of 30–45%. It is also possible that Atterberg-limit measurements for Lias clay are influenced by the calcareous nature of the layered clay.

For the Tertiary mudstone of Matsue landslide, the reported value of plastic limit w_p is unusually low and the corresponding value of plasticity index I_p is inconsistent with the reported value of residual friction angle from reversal direct shear tests on undisturbed samples (Nakamori et al. 1996). However, Fig. 8 shows that the back-calculated mobilized shear strength on the entire

Table 3. First-Time Slides in Stiff Clays and Clay Shales with Segment of Slip Surface at Residual Condition

No.	Slope failure	Slope material	I_p(%)	$\bar{r}_u$	Slope age (years)	Reference
59	Northolt, 1, 3, 6, 9, 11, UK	London clay	50–60	0.14,0.25,0.25, 0.25,0.27	35	DeLory (1957); Henkel (1957); James (1970); Chandler and Skempton (1974); Abdel-Ghaffar (1990); Mesri and Abdel-Ghaffar (1993)
60	Upper Holloway, UK	London clay	50–60	0.34	82	DeLory (1957); James (1970)
61	Fareham, UK	London clay	50–60	0.29	58	James (1970)
62	Whitstable, UK	London clay	50–60	0.30	99	James (1970, 1971)
63	Whembley, UK	London clay	50–60	0.35	13	Skempton (1948, 1977); DeLory (1957); James (1970)
64	West Action 8 and 9, UK	London clay	50–60	0.30	46	James (1970); Chandler and Skempton (1974)
65	Tulse Hill, UK	London clay	50–60	0.30	101	James (1970)
66	Grove Park, UK	London clay	50–60	0.16	98	James (1970)
67	Wood Green, UK	London clay	50–60	0.36	55	DeLory (1957); Henkel (1957); James (1970)
68	Grange Hill, UK	London clay	50–60	0.30	50	James (1970); Chandler and Skempton (1974)
69	Cuffley, UK	London clay	50–60	0.30	40	James (1970); Chandler and Skempton (1974)
70	Crews Hill, UK	London clay	50–60	0.30	47	James (1970); Chandler and Skempton (1974)
71	St. Helier, UK	London clay	50–60	0.28	22	James (1970); Skempton (1977)
72	Kingsbury 1, UK	London clay	50–60	0.30	16	James (1970); Skempton (1977)
73	Sudbury Hill South and North, UK	London clay	50–60	0.30,0.32	46	Chandler and Skempton (1974); Skempton (1977)
74	New Cross Cutting, UK	London clay	50–60	−0.46	3	Gregory (1944); Skempton (1977)
75	Ridgemont, UK	Chalkey Boulder clay	27–36	0.30	105	James (1970)
76	Verney Junction, UK	chalkey Boulder clay	41	0.30	103	James (1970)
77	Dauntsey, UK	Oxford clay	45–50	0.27	121	James (1970)
78	Peterborough, UK	Oxford clay/Callow	45–50/30	0.37	?	Petley (1966); James (1970)
79	Hullavington, UK	Oxford clay	33	0.15–0.30	57	Cassel (1948); James (1970)
80	Ampthill, UK	Oxford clay	31–42	0.30	90	James (1970)
81	Bincombe, UK	Oxford clay	31–42	0.30	41	James (1970)
82	Haddenham, UK	Kimmeridge clay	50	0.32	55	James (1970)
83	Hunsbury Hill, UK	Upper Lias clay	32	0.43	85	Hollingworth and Taylor (1951); James (1970); Chandler (1974); Abdel-Ghaffar (1990)
84	Barrowden, UK	Upper Lias clay	31	0.38	83	Chandler (1974); Abdel-Ghaffar (1990)
85	Heyford, UK	Upper Lias clay	28	0.28	126	Chandler (1974); Abdel-Ghaffar (1990)
86	Seaton, UK	Upper Lias clay	29	0.38	68	Chandler (1974); Abdel-Ghaffar (1990)
87	Stowehill, UK	Upper Lias clay	31	0.30	118	James (1970); Chandler (1972, 1974); Abdel-Ghaffar (1990)
88	Wellingborough, UK	Upper Lias clay	31	0.20	105	Chandler (1974); Abdel-Ghaffar (1990)
89	Wothrope B, UK	Upper Lias clay	41	0.43	6	James (1970); Chandler (1974); Abdel-Ghaffar (1990)
90	Ardley, UK	Upper Lias clay	31	0.27	52	James (1970); Chandler (1974); Abdel-Ghaffar (1990)
91	Haslemere, UK	Atherfield clay	21	0.30	104	James (1970)
92	Lesueur, Edmonton, Canada	Bentonitic clay shale	170	0.24	?	Thomson (1970, 1971a,b); Abdel-Ghaffar (1990)
93	Amuay, Venezuela	Brown Fat	40	0.38	?	Lumbe (1973, 1985); Lumbe et al. (1981); Abdel-Ghaffar (1990)
94	Albedosa, St. Cristoforo, Italy	Lugagnano clay	26	0.47	?	Cancelli (1981); Abdel-Ghaffar (1990)
95	Santa Barbara, Italy	Santa Barbara clay	35	0.22	?	Esu et al. (1984); Abdel-Ghaffar (1990)
96	Wettern, Brussels	Loam/Blue clay	12/88	0.22	37	Marivoet (1948); Abdel-Ghaffar (1990);
97	Selborne, UK	Gault clay	40–50	0.16		Cooper et al. (1998)
98	Akistu, Japan	Tertiary Mudstone	60	0.27–0.40	?	Nakamori et al. (1996)

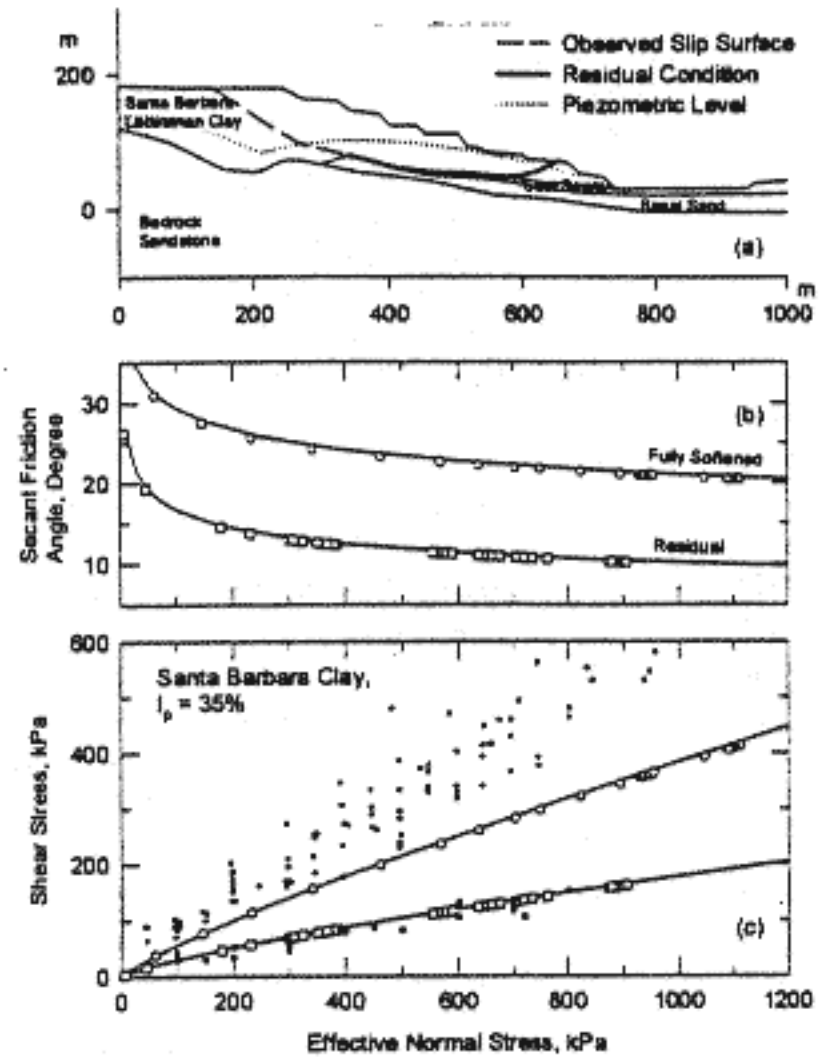

Fig. 4. Santa Barbara landslide, case 95, Table 3 (continuous curves represent mean of empirical data in Fig. 2 with $m_{fs}=0.92$ and $m_r=0.88$ for $I_p=35\%$)

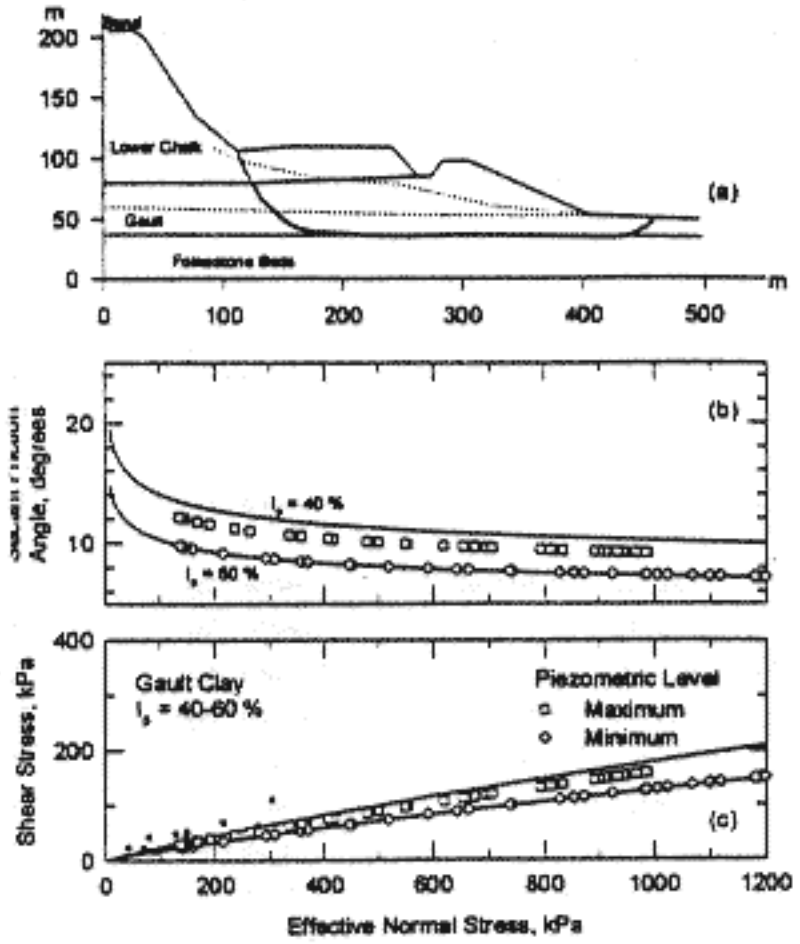

Fig. 5. Reactivated slide at Folkestone Warren, Kent, case 15, W4 slide, Table 1 (continuous curves represent mean of empirical data in Fig. 2 with $m_r=0.86$ to 0.85 for $I_p=40-60\%$)

observed slip surface is consistent with laboratory residual shear strength from undisturbed samples as well as with $[\phi_r']_r$ data from Fig. 2 for an I_p range of 30–40%.

First-Time Slides in Homogeneous Clays

First-time slope failures in 14 homogeneous clays were analyzed to permit comparing the lower bound of the back-calculated mobilized shear strength on the observed slip surface to the empirical information in Fig. 2 on the fully softened strength. These include unstratified low-plasticity stiff clays and homogeneous soft to firm clays. Sixteen sections in as many slides were analyzed (Table 2). In all cases the mobilized shear strength was equal or greater than the fully softened shear strength from the empirical information in Fig. 2 together with the plasticity index of the clay. An example of first-time slide in a homogeneous clay of low plasticity is shown in Fig. 9 (Skempton and Brown 1961; Skempton 1964; Chandler 1984a). For the boulder clay at Selset the mobilized shear strength (hollow circles) is significantly higher than the fully softened strength determined from the empirical data in Fig. 2 for $I_p=13\%$ (solid line). The back-calculated mobilized shear strength is equal to the upper bound of the intact or peak strength from laboratory tests (dashed line and solid circles, Skempton and Brown 1961). A similar conclusion was reached by Chandler (1984a). The so-called homogeneous slopes, for which the mobilized shear strength is equal to or greater than the fully softened strength and frequently near the intact strength, are generally either stiff clays of low plasticity such as glacial clays, or are soft to firm clays of low to medium plasticity such as those

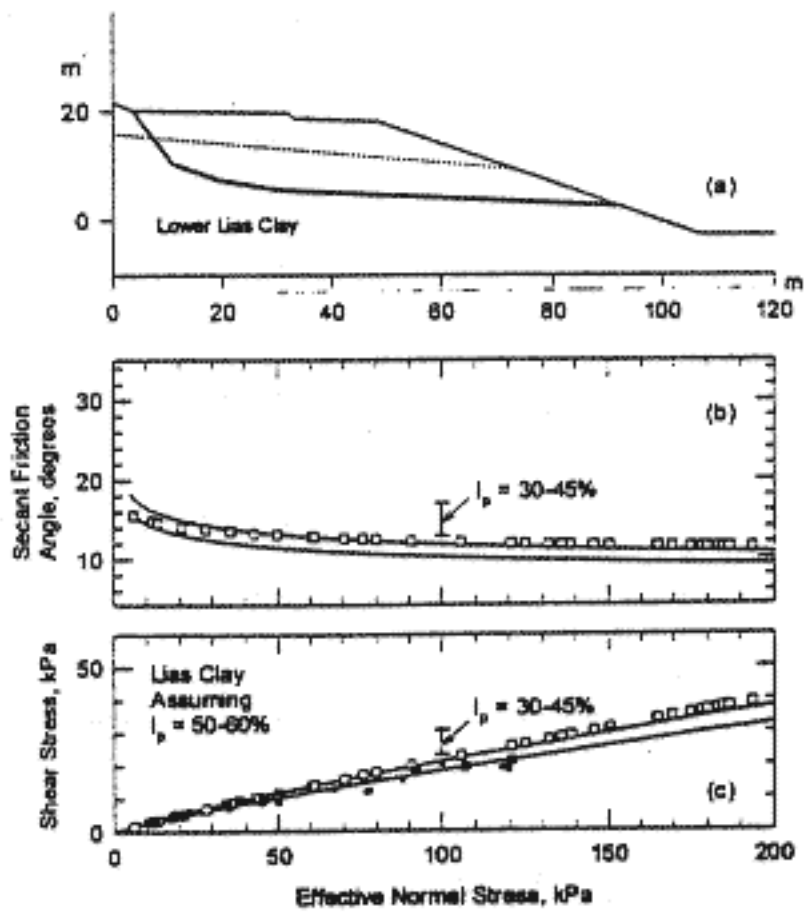

Fig. 6. Reactivated slide at Lyme-Regis, case 1, Table 1 (continuous curves represent mean of empirical data in Fig. 2 with $m_r=0.85$ for $I_p=50-60\%$)

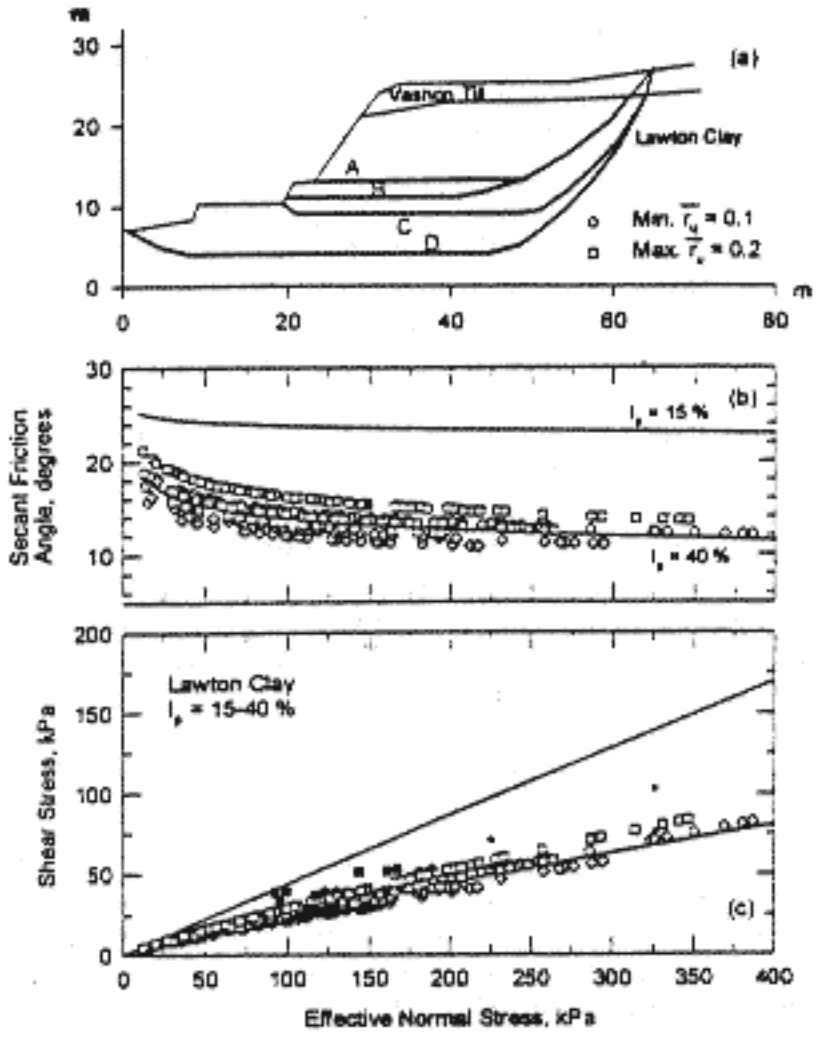

Fig. 7. Reactivated slides, Seattle Freeway, case 5, Table 1 (continuous curves represent mean of empirical data in Fig. 2 with m_r = 0.98–0.86 for I_p = 15–40%)

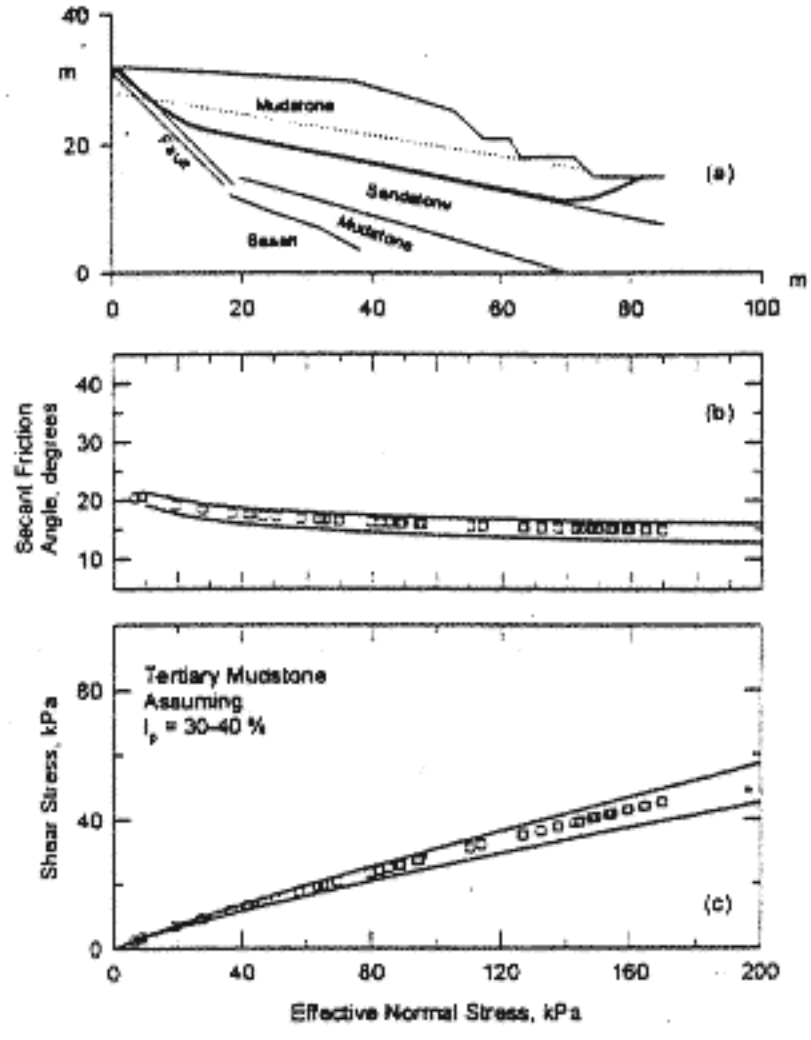

Fig. 8. Reactivated slide at Matsue, case 42a, Table 1 (continuous curves represent mean of empirical data in Fig. 2 with m_r = 0.90–0.86 for I_p = 30–40%)

from eastern Canada and Norway. For clays of eastern Canada mobilized strength is near the large-strain strength (Lefebvre 1981; Mesri and Abdel-Ghaffar 1993).

First-Time Slides Mobilizing Residual Shear Strength

Forty-six sections in 40 first-time slope failures in 14 stiff clays and clay shales were analyzed using the residual shear strength on part of the observed slip surface (Table 3). The residual condition was assumed on the segment of the observed slip surfaces passing through presheared bands or stratigraphic discontinuities such as bedding planes, laminations, and weak seams. A parametric finite element analysis of progressive failure of hypothetical cut slopes in stiff fissured London clay, conducted by Potts et al. (1997) with swelling and strain softening, predicted residual conditions along the horizontal part of the eventual slip surface. Twenty examples of first-time slope failures reanalyzed here are shown in Fig. 10 to indicate the residual and nonresidual segments of the observed slip surface, and additional landslides are described in detail.

The first-time slope failure in the stiff clay of lowest plasticity index among the cases in Table 3 is shown in Fig. 11 (James 1970). A residual shear strength from empirical data for I_p = 21% on the horizontal part of the observed failure surface leads to a mobilized strength on the curved part that is equal to the fully softened strength from empirical data for I_p = 21% for Atherfield clay. Similar behavior was back-calculated for Santa Barbara clay, Fig. 4, Lugagnano clay, Fig. 12, and Oxford clay, Fig. 13. The back-calculated shear strength on the curved part of the slip surface of Albedosa landslide (Cancelli 1981) corresponds to the fully softened condition defined by the empirical data for I_p = 26%, and is within the range of laboratory test results shown by the dashed lines. A mobilized residual shear strength from the empirical data for I_p of 45–50% on the horizontal portion of the observed slip surface in Oxford clay at Dauntsey (James 1970) results in a back-calculated mobilized shear strength on the back scarp that is equal to the fully softened strength from empirical data for I_p in the range of 45–50%, Fig. 13.

For the Tertiary mudstone from Akitsu landslide in Fig. 14 (Nakamori et al. 1996), the unusually low reported value of w_p leads to an I_p = 60% that is inconsistent with the measured residual friction angle. The residual shear strength from laboratory reversal direct shear tests on undisturbed samples is equal to residual shear strength from Fig. 2 for an I_p range of 30–40%. A stability analysis of the Akitsu landslide using a mobilized shear strength at the interface between mudstone and sandstone equal to the residual strength from laboratory tests on undisturbed samples leads to a mobilized strength on the back scarp equal to the fully softened strength from Fig. 2 for I_p of 30–40%. The back-calculated mobilized strength is somewhat smaller than intact or peak shear strength from the laboratory tests on undisturbed specimens [solid circles in Fig. 14(c)].

The 9 m deep Selborne cutting in Gault clay (Fig. 15) was brought to failure by porewater pressure recharge to model a coastal slope (Cooper et al. 1998). The slope was isolated at its ends by means of low-friction panels to produce plane strain deformation and to minimize side shear effects on the sliding mass. According to Cooper et al. (1998) "the failure of the slope took place as a result of a progressive failure mechanism, with movements initiating at the toe of the slope at an early state in the experiment." The slip surface has a planar near-horizontal section

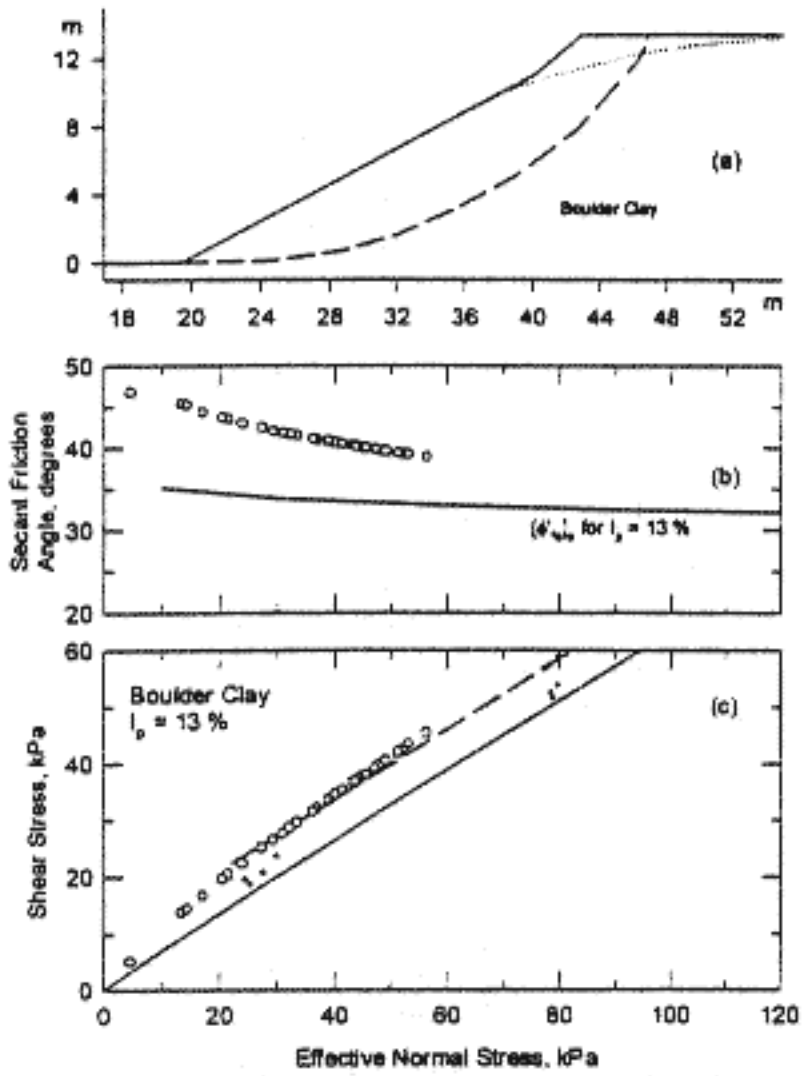

Fig. 9. First-time slope failure at Seiset, case 47, Table 2 (continuous curves represent mean of empirical data in Fig. 2 with $m_{fs}=0.95$ for $I_p=13\%$)

as it emerges just above the slope toe. Postfailure excavation revealed that "the lower part of the slip surface in Gault clay formed a single highly polished, strongly striated slickenside," whereas the curved part passing across the bedding included wider shear zones (up to a 20 mm wide disturbed zone) with a slip surface that was much rougher, with little polishing (Cooper et al. 1998). It was also reported that by the time slip occurred appreciable (up to greater than 10 mm) displacement had taken place along an extension of the basal failure surface into the slope.

Triaxial compression tests on undisturbed specimens of soliflucted clay, upper and lower weathered clays, and unweathered clay defined the peak (intact) strength of Gault clay. The intact strength range from soliflucted clay to unweathered clay, including also upper and lower weathered clays, is shown in Fig. 15 together with the range of fully softened strength from triaxial compression tests on reconstituted specimens of different zones. Reversal direct shear tests on precut specimens, ring shear tests, as well as direct shear tests on slip surfaces recovered during postfailure excavation, defined the residual shear strength of Gault clay. The measured residual strengths in Fig. 15 are within the range defined by empirical data in Fig. 2 for $I_p=40-50\%$. The stability analysis depicted in Fig. 15 was carried out using the actual slip surface, $\bar{r}_u=0.16$, and the measured residual shear strength on the planar near-horizontal section. The back-calculated mobilized shear strengths on the curved part of the slip surface are near the upper bound of the measured fully softened strength range, and are very close to the range defined by empirical data on $[\phi'_{fs}]_s$ in Fig. 2 for $I_p=40-50\%$.

Twenty-two sections were analyzed for 16 slope failures in London clay (Table 3). One example is shown in Fig. 16. In general, a residual shear strength from the empirical data for $I_p=50-60\%$ on the horizontal part of the observed slip surface results in a back-calculated mobilized shear strength on the curved part that is identical to the fully softened strength from empirical data for I_p of 50–60%. The fully softened and residual shear strengths from the empirical data are similar to the corresponding strength from laboratory tests, although the latter data display a considerable range. The mobilized shear strength from the 16 slope failures are compared in Fig. 17 with those from the empirical data for I_p of 50–60%, as well as with laboratory test results. The back-calculated mobilized shear strength on the curved part of the observed failure surfaces are near the fully softened strength from empirical data, except for the Upper Holloway failure (James 1970) where the stability analysis probably does not adequately account for the construction of the retaining structure and hence gives mobilized strengths that are too high.

Friction Angles Mobilized in Slope Failures

Values of the secant residual friction angle back-calculated for reactivated landslides (solid squares), and those used for first-time slides over the part of the observed failure surface assumed to be at residual condition (hollow squares), are compared in Fig. 18 with the range of empirical information on residual friction angle (Fig. 2). Most of the values of the mobilized residual friction angle are within the range defined by the empirical data based on laboratory tests. This should be expected for the values corresponding to first-time slides because selection of the mobilized residual strength in those cases was based on the empirical information in Fig. 2. It is of greater practical interest, however, that most of the back-calculated friction angles for reactivated slides are within the range defined by the empirical correlations. In a few cases the back-calculated values of $[\phi'_r]_s$ plot slightly below the lower boundary of the empirical correlation. This is probably the result of assuming porewater pressures that are lower than the true field values. For example, for the three sections of the Trending Bluff slope failures, the porewater pressures reported by Eid (1996) correspond to values of $\bar{r}_u$ equal to 0.013, 0.074, and 0.28. Values of $\bar{r}_u$ equal to 0.30, 0.40, and 0.48, respectively, would result in $[\phi'_r]_s$ values within the empirical range. Alternatively, the mobilized $[\phi'_r]_s$ could correspond to an actual I_p higher than the reported value, especially within higher plasticity bedding planes and laminations. In fact, the lower boundary of the empirical correlation between secant residual friction angle and plasticity index may be considered a conservative lower bound for the mobilized residual strength on the entire slip-surface of reactivated landslides and on the slip-surface segment of first-time slope failures assumed to be at the residual condition.

Fig. 18 also includes the values of back-calculated secant friction angles over the entire slip surface of first-time slides in homogeneous slopes (solid circles) and over the back scarp or the curved segments of observed slip surfaces not at the residual condition for first-time slides (hollow circles). These secant friction angles are either within the range defined by empirical information on fully softened shear strength from Fig. 2 or in some instances (cases 44–47, 49, 52, 56, and 57) are somewhat above it. In the latter cases no particular trend in behavior can be deduced in relation to the plasticity index of the clay. There are very few reported cases of well-defined first-time slope failures in low-plasticity unstratified stiff clays, such as the Selset (Skempton and Brown 1961), for which the mobilized shear strength is near the

國立雲林科技大學
九十二學年度研究所博士班招生考試試題

所別：工程科技研究所
科目：營建文獻評論

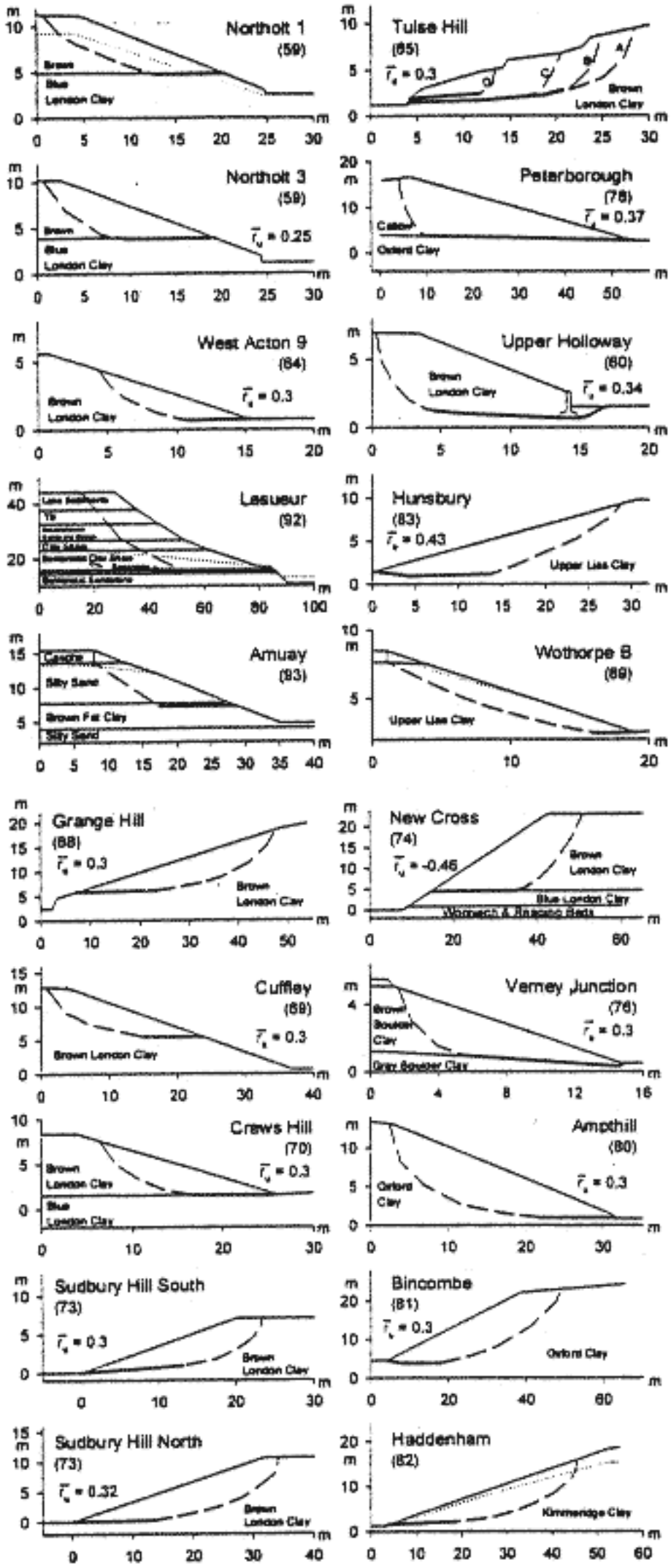

Fig. 10. Examples of first-time slope failures showing assumed segment of observed slip surface at residual condition (case no. in Table 3)

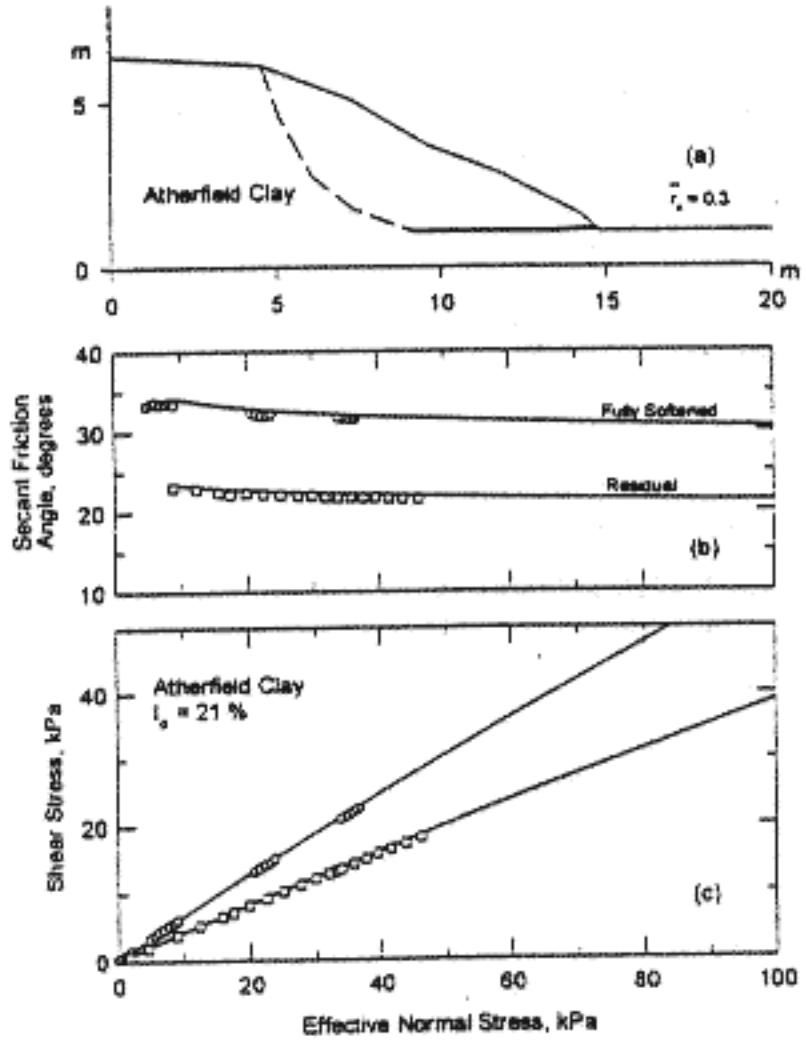

Fig. 11. First-time slide at Haslemere, case 91, Table 3 (continuous curves correspond to mean of empirical data in Fig. 2 with m_{fs} = 0.94 and m_r = 0.95 for I_p = 21%)

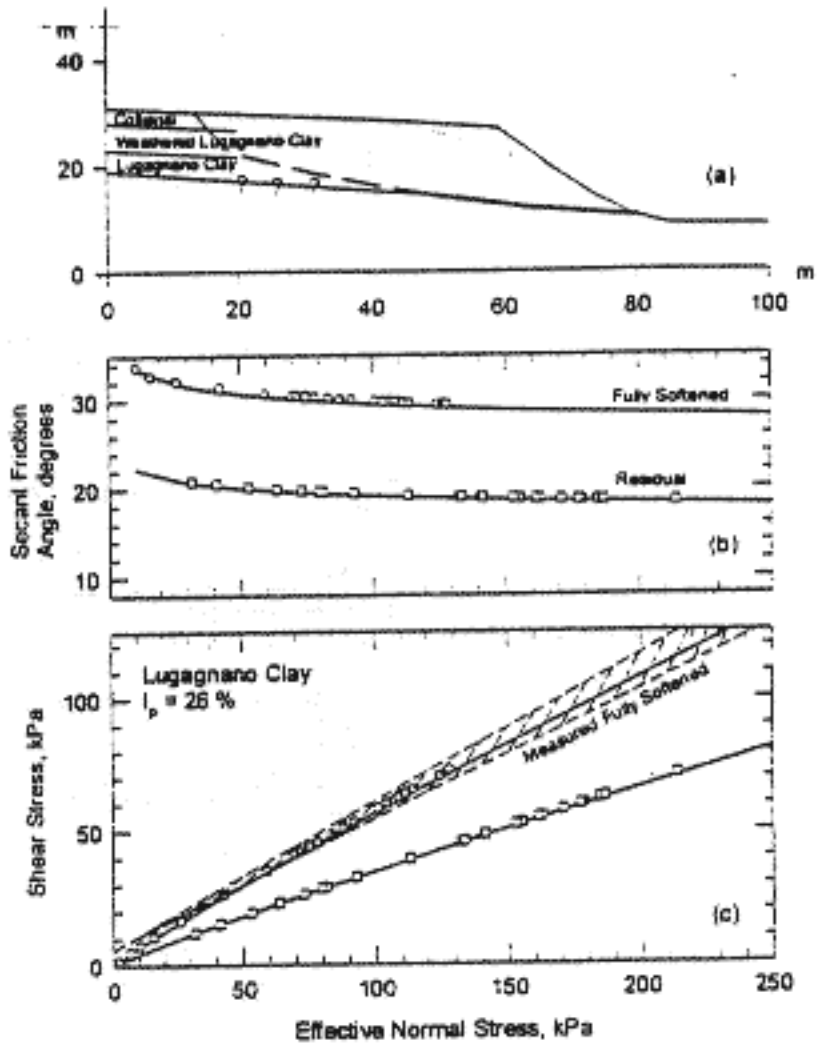

Fig. 12. First-time slide at Albedosa, case 94, Table 3 (continuous curves represent mean of empirical data in Fig. 2 with m_{fs} = 0.93 and m_r = 0.93 for I_p = 26%)

intact strength from laboratory tests. For slope failures in soft to firm clays in eastern Canada (cases 52, 56, and 57), the mobilized shear strength, which is equal to the large-strain strength from laboratory tests (Lefevbre 1981; Mesri and Abdel-Ghaffar 1993), is always higher than the fully softened strength from the empirical correlation between $[\phi'_{fs}]_r$ and I_p in Fig. 2. In general, for first-time slope failures in unstratified low plasticity soft to stiff clays, the fully softened strength from Fig. 2 is a conservative lower bound for the mobilized strength. For first-time slope failures in stiff fissured clays and clay shales, the fully softened strength from Fig. 2 is an appropriate measure of shear strength mobilized over the segments of slip surface cutting across laminations or bedding planes. In Fig. 18, for Lesueur landslide, the mobilized secant friction angles, on both the segment of the slip surface at the residual condition and on the back scarp, have been recorded at the same plasticity index. However, the I_p = 170%, which corresponds to the bentonitic clay seam at the residual condition of the horizontal basal slip surface, overestimates the plasticity index of the back scarp cutting across layers of lake deposits, tills, clay shales, and sands and gravels.

Delayed Failure of Slopes

After a slope is formed during the third phase of the geological history of a stiff clay or clay shale that is stratified, bedded, laminated, or retains high horizontal stresses, but not yet sheared to the residual condition, the propagation at the residual condition of a shear zone inward from the face of the slope should partly depend on the age of the slope. Although part of the undrained lateral expansion that may lead to the residual condition on bedding planes, laminations, and weak seams is time-independent, swelling, softening, and creep which are time-dependent also contribute to development of the residual condition (Morgenstern 1990; Potts et al. 1997). Therefore there may be a correlation between the length of the slip surface that is at the residual condition and the age of the slope. A possible relationship between L_r/L_t, where L_r = segment of the slip surface at residual condition and L_t = total length of the observed slip surface, and age of the slope is examined in Fig. 19 for the cases in Table 3. The age of slopes at the right end of Fig. 19 is unknown. The relationship between L_r/L_t and age of the slope at failure may be complicated by geometry of the slope (Terzaghi et al. 1996, p. 192), by particular stratigraphic features of the ground, by shear surfaces already at residual condition from the second geological phase, by K_0 magnitudes that survive the second phase, by weathering conditions, and by changes in topography of the slope and extreme groundwater conditions that trigger failure (Janbu et al. 1977; Morgenstern 1977; Potts et al. 1997). These factors complicate the definition of the age of a slope involved in first-time failures. In other words, time is not the only element controlling the length of the slip surface at residual condition. Finite element analyses conducted by Matheson (1972) and Potts et al. (1997) predicted that the length of the horizontal slip surface at residual condition, which starts at the toe of the slope, increases with the coefficient of earth pressure at rest, K_0. Fig. 19 suggests a rough trend of increasing L_r/L_t with age of the slope for first-time failures. The Lias clay slope failures at Seaton (86) and Heyford (85) correspond to very shallow slips; for such a small range of effective normal stress on the slip surface, an alternative interpretation of

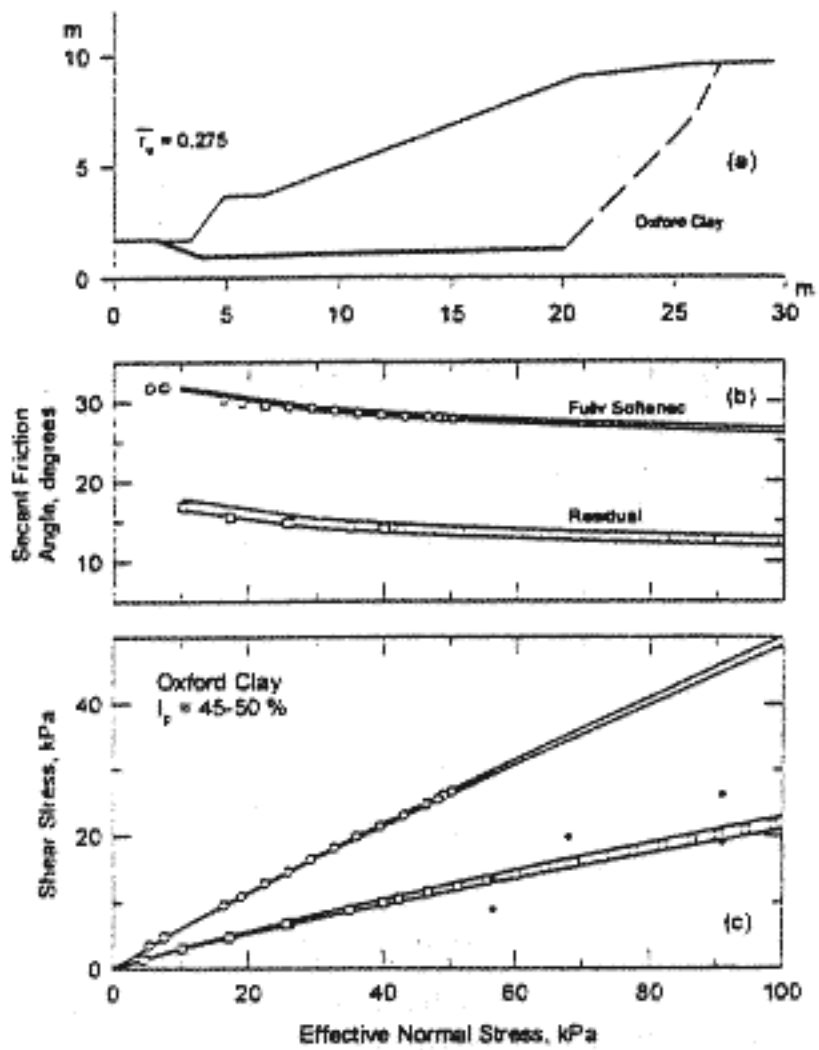

Fig. 13. First-time slide at Dauntsey, case 77, Table 3 (continuous curves represent mean of empirical data in Fig. 2 with m_{fs} = 0.91–0.90 and m_r = 0.86–0.85 for I_p = 45–50%)

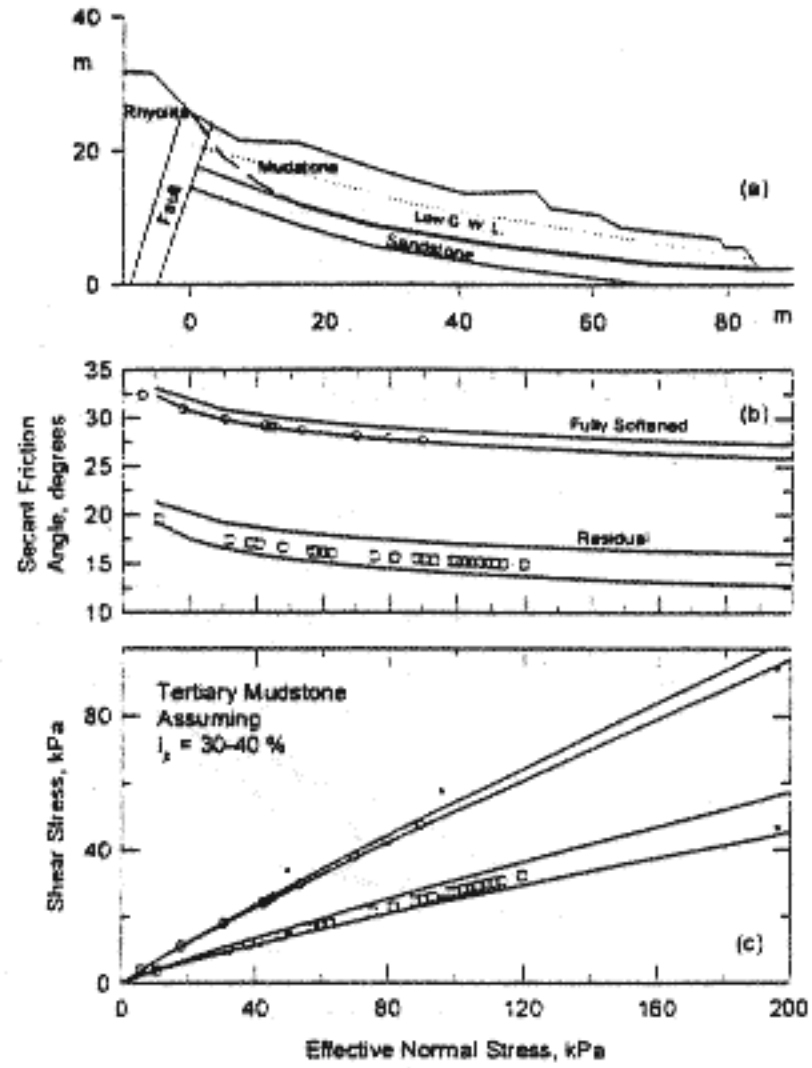

Fig. 14. First-time slide at Akitsu, case 98, Table 3 (continuous curves represent mean of empirical data in Fig. 2 with m_{fs} = 0.92–0.91 and m_r = 0.90–0.86 for I_p = 30–40%)

the slope failures, leading to higher values of L_r/L_t, is possible. In the latter interpretation, a residual condition is assumed on the observed shallow brecciated slip surface parallel to the slope as a result of deep freezing and thawing and of subsequent downslope creep.

The magnitude and range of values of L_r/L_t are analogous to those of the residual factor R defined by Skempton (1964). However, L_r/L_t, which defines the portion of the slip surface along which the mobilized shear strength has fallen to the residual value, does not include values of mobilized shear strength between the residual and fully softened strength, whereas R, which is defined in terms of average mobilized shear strength along the whole slip surface, does. Skempton (1964) summarized the values of R for a number of clay conditions in slopes. They suggest an increase in R with an increase in degree of weathering, fissuring, jointing, and age of the slope. The increase in L_r/L_t with age of slope reflects time-dependent propagation of the residual condition into the slope as a result of localized swelling, softening, and shear deformation.

It is well known that the delayed first-time failure of slopes in stiff clays and clay shales is caused by (a) time-dependent equilibration of porewater pressures and associated decrease in effective stress and swelling, and (b) softening. A third factor should be added, namely (c) development and time-dependent increase in length of a shear zone at the residual condition on layer boundaries, bedding planes, laminations, weak seams, or planes parallel to high geostatic stresses in the slope. However, the life of a slope can be abruptly interrupted by unusual weather events producing severe erosion or extreme groundwater conditions, or by placement of a fill at the head of the slope.

Conclusions

The following conclusions are based on a review of long-term stability of stiff clay and clay shale slopes, and detailed reanalyses of 99 slope failures in 36 soft clays to stiff clays and clay shales. Stability analyses were carried out for 107 sections.

1. Most stiff clays and clay shales are not homogeneous. They are usually stratified and may include hard to soft or permeable to impermeable layer interfaces, bedding planes and separations, laminations, or thin weak continuous seams.

2. Erosion and unloading, including removal of lateral support, lead to swelling, fissuring, and softening. The end result of softening is the fully softened condition with a shear strength equal to that of the normally consolidated mineralogical composition of the stiff clay or clay shale. Any state of stiff clay or clay shale before the fully softened condition is reached is said to be an "intact" condition. The intact condition is quite variable, because different degrees of fissuring and softening are possible. Stiff clay and shale masses may include sheared zones in which plate-shaped clay mineral particles are parallel-oriented to the maximum extent possible in the direction of shearing. This is the residual condition.

3. The relationships between shear strength and effective normal stress for all conditions of stiff clays and shales—intact, fully softened, and residual—are curved, and there is no shear strength at zero effective normal stress. A convenient method for describing the nonlinear intact, fully softened, and residual shear strength envelopes is to employ secant friction angles $[\phi'_i]_s$, $[\phi'_{fs}]_s$, and $[\phi'_r]_s$, respectively, that are functions of the effective normal

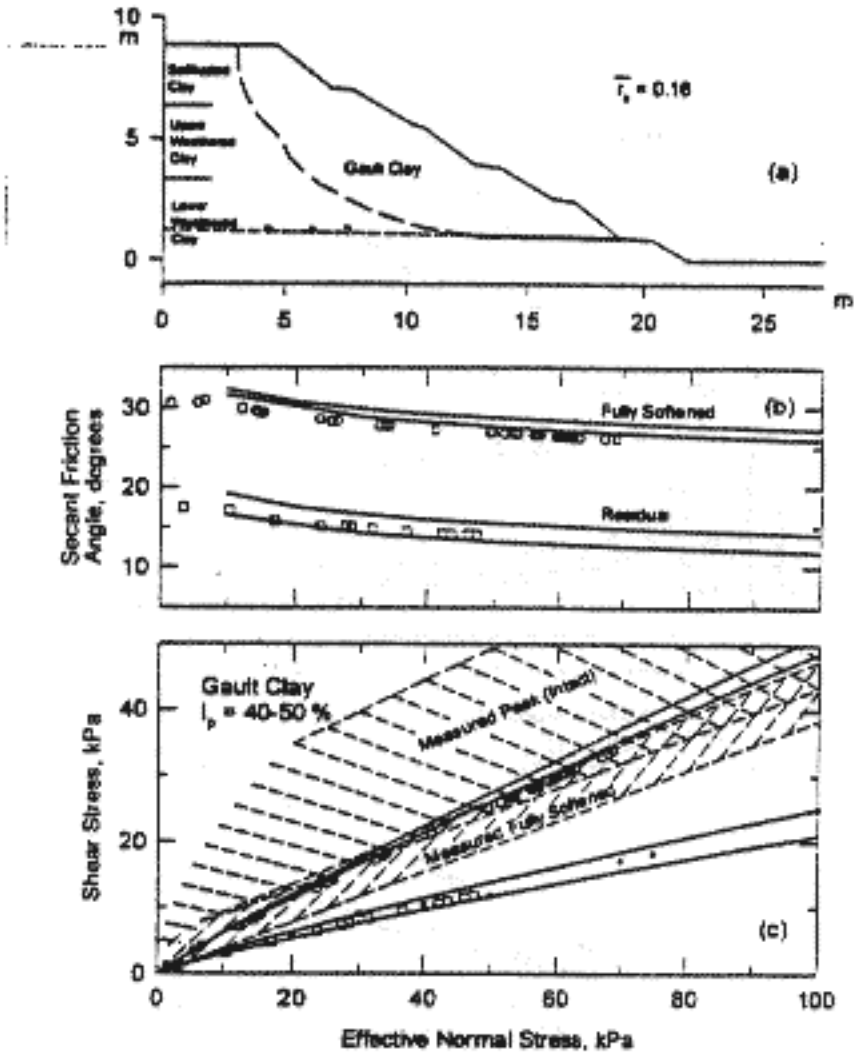

Fig. 15. First-time slide at Selborne, case 97, Table 3 (continuous curves represent mean of empirical data in Fig. 2 with m_{fs} = 0.91–0.90 and m_r = 0.86–0.85 for I_p = 40–50%)

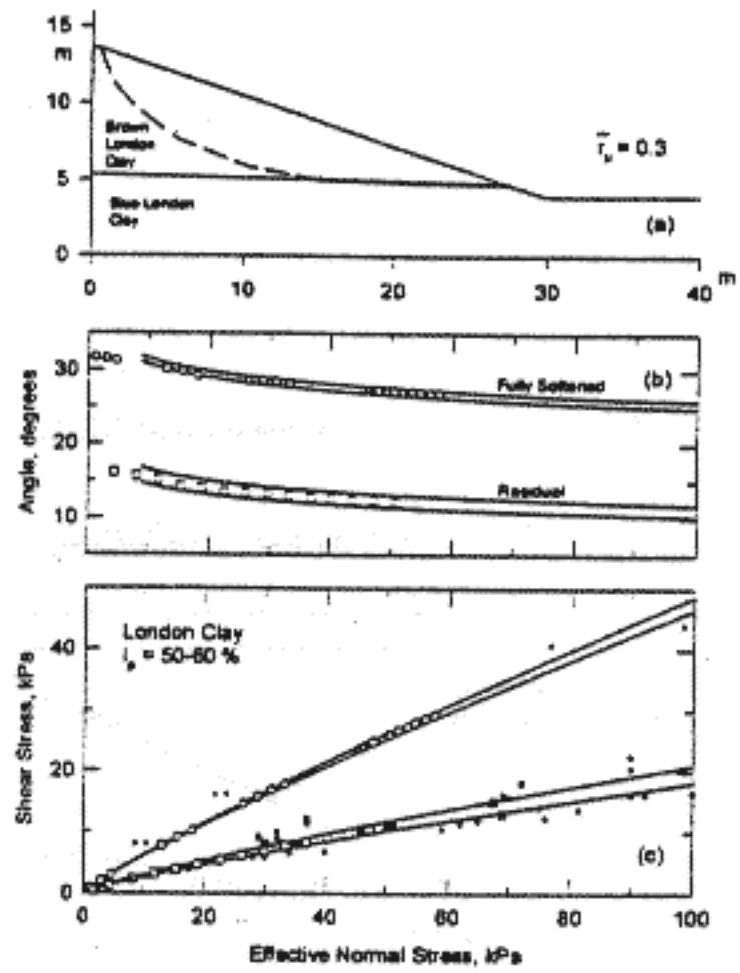

Fig. 16. First-time slide at Whitstable, case 62, Table 3 (continuous curves represent mean of empirical data in Fig. 2 with m_{fs} = 0.90–0.89 and m_r = 0.86–0.84 for I_p = 50–60%)

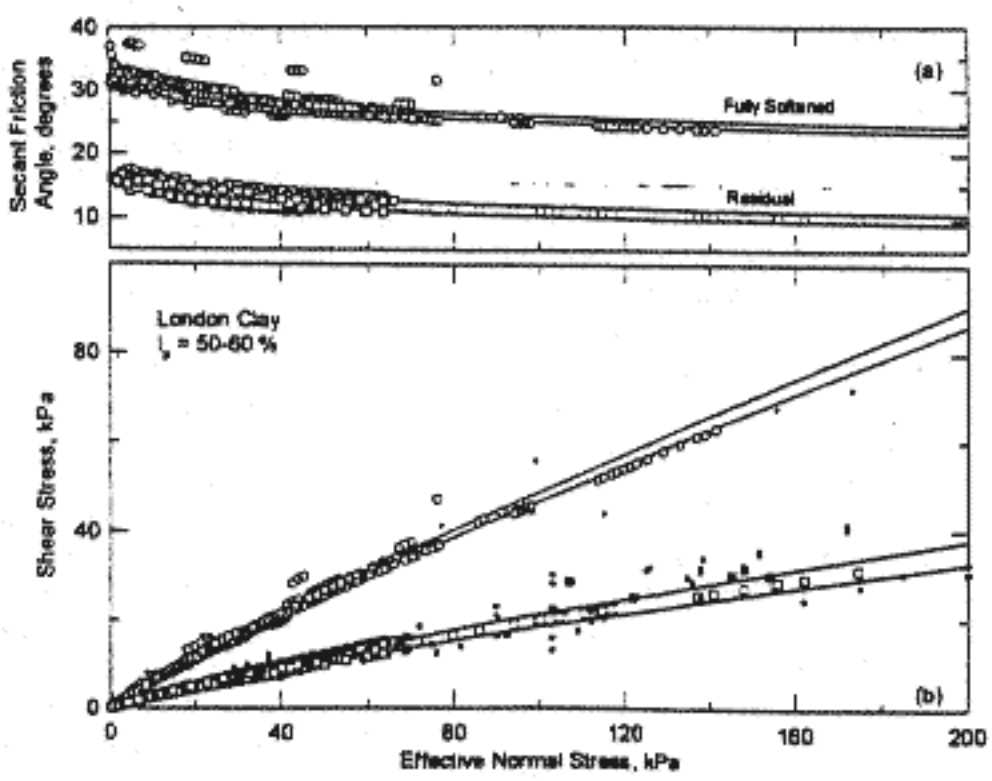

Fig. 17. London clay experience: mobilized strength from first-time slope failures (Table 3) as well as reactivated slope failures (Table 1) compared to shear strength from laboratory tests as well as from empirical correlation in Fig. 2 (laboratory data from Bishop et al. 1965; Skempton 1977; Chandler 1984b; Skempton 1985)

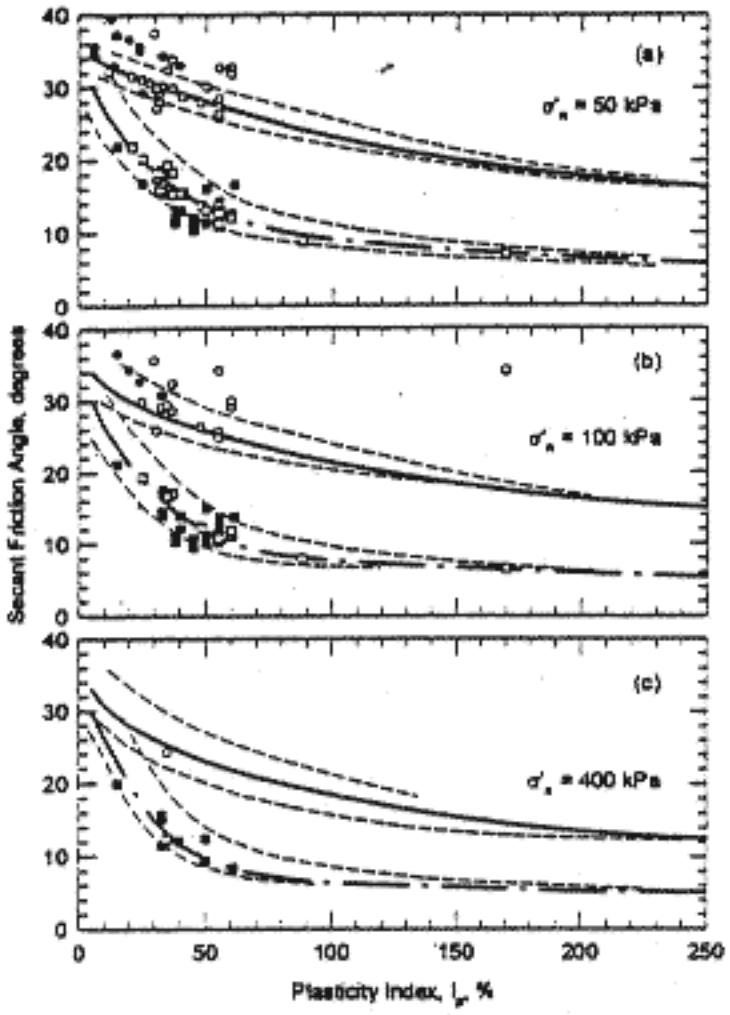

Fig. 18. Mobilized friction angles back-calculated from reactivated and first-time slope failures compared to the range from empirical information

stress (e.g., Fig. 2). There is now reliable empirical information on secant fully softened and secant residual friction angles of stiff clays and clay-shale mineralogical compositions characterized by Atterberg's plasticity index in a practical range of effective normal stresses (Figs. 2 and 18). However, caution should be exercised in the use of empirical correlations for friction angles because for certain stiff clay, shale, and mudstone compositions, sample preparation may have a significant effect on Atterberg limits. Also, the plasticity index of weak seams may be different from that of the scarp cutting across the laminations.

4. On reactivated slip surfaces of landslides in stiff clays and clay shales the residual condition has been reached, and the mobilized shear strength is equal to the residual shear strength from laboratory reversal direct shear or ring shear tests, independent of time after initial failure.

5. In first-time slope failures in unstratified stiff clays of low plasticity, the mobilized strength is equal to the intact strength from laboratory specimens because there is little postpeak reduction in strength.

6. The fully softened shear strength is the lower bound for mobilized strength in first-time slope failures in homogeneous soft to stiff clay slopes and on the part of the slip surface cutting across bedding planes and laminations in stiff fissured clays and shales.

7. Part of the slip surface for first-time slope failures may be at the residual condition. In stiff clays and shales either the residual condition already exists along bedding planes and laminations before a cut is made or it develops by progressive deformation. Sufficient strain energy to reach the residual condition is available along nearly horizontal surfaces, including bedding planes and laminations. When shearing strain is localized in thin weak bands, and clay particles are already substantially oriented parallel to the direction of shearing, rather small displacements will cause the clay to reach the residual condition.

8. Delayed first-time failure of slopes in stiff clays and clay shales is caused by (1) time-dependent rise of porewater pressure toward the steady seepage condition, swelling, decrease in effective stress and shear strength, (2) fissuring and softening, and (3) development and propagation of the residual condition into the slope on nearly horizontal surfaces, including layer boundaries, bedding planes and partings, laminations, or weak seams (Fig. 19).

9. Selection of potential slip surfaces for stability analyses of natural and excavated slopes should be based on a knowledge of geology. Special attention should be directed toward structural features such as presheared surfaces produced by old landslides, tectonic or glacial deformation, or downslope creep, as well as to lithological details such as horizontal or subhorizontal bedding planes, laminations, and weak seams that are likely to drop to the residual condition after relatively small shear displacements, measured in millimeters or centimeters as opposed to meters as commonly assumed for homogeneous clays or across laminations. For existing slopes, locating the position and shape of the critical slip surface by trial and error may be aided by observations of movements. In the absence of well-defined weak surfaces, including preexisting shear surfaces, the planar basal portion of the critical slip surface in stiff clays and shales should be selected parallel to the bedding and at the level of the base of the slope.

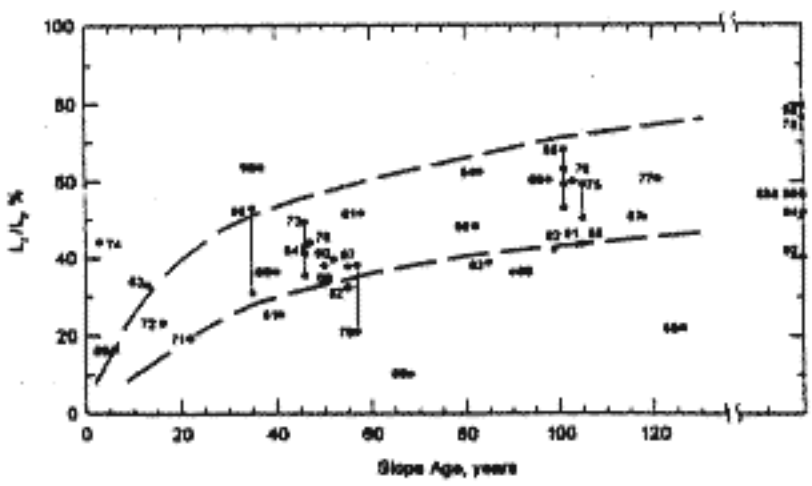

Fig. 19. Ratio of slip surface segment assumed at residual condition to total slip surface length plotted against age of slope

Notation

The following symbols are used in this paper:

CF = clay size fraction (% less than 2 μm);
I_p = Atterberg plasticity index;
K_0 = coefficient of earth pressure at rest;
L_r = segment of slip surface at residual condition;
L_t = total length of observed actual slip surface;
m = parameter defining curvature of intact strength envelope;
m_{fs} = parameter defining curvature of fully softened strength envelope;
m_r = parameter defining curvature of residual strength envelope;
r_u = porewater pressure ratio (u/σ_v);
$\bar{r}_u$ = average value of r_u along slip surface;

$s(i)$ = intact shear strength (peak shear strength of undisturbed specimens);
$s(\text{fs})$ = fully softened shear strength (shear strength of reconstituted, normally consolidated specimens);
$s(r)$ = residual shear strength (shear strength of presheared surfaces, from precut surfaces of intact or reconstituted specimens);
w_l = Atterberg liquid limit;
w_p = Atterberg plastic limit;
σ_n' = effective normal stress;
σ_p' = preconsolidation pressure;
$[\phi_i']_s$ = secant friction angle defining nonlinear relationship between intact shear strength and effective normal stress;
$[\phi_{fs}']_s$ = secant fully softened friction angle defining nonlinear relationship between fully softened shear strength and effective normal stress;
$[\phi_r']_s$ = secant residual friction angle defining nonlinear relationship between residual shear strength and effective normal stress;
$[\phi_{fs}']_s^p$ = secant fully softened friction angle corresponding to $\sigma_n' = \sigma_p'$;
$[\phi_{fs}']_s^{100}$ = secant fully softened friction angle corresponding to $\sigma_n' = 100$ kPa; and
$[\phi_r']_s^{100}$ = secant residual friction angle corresponding to $\sigma_n' = 100$ kPa.

References

Abdel-Ghaffar, M. E. M. (1990). "The meaning and practical significance of the cohesion intercept in soil mechanics." PhD thesis, Univ. of Illinois at Urbana-Champaign, Ill.

Anson, R. W. W., and Hawkins, A. B. (1999). "Analysis of a sample containing a shear surface from a recent landslip, south Cotswolds, UK." *Geotechnique*, 49, 33–42.

Balasubramaniam, A. S., Munasinghe, N. T. K., Tennekoon, B. L., and Karunaratne, G. P. (1977). "Stability of cut slopes for installation of penstocks." *Proc., Int. Symposium on the Geotechnics of Structurally Complex Formations*. Associazione Geotecnica Italiano, Italy, 1, 29–39.

Bayley, M. J. (1972). "Cliff stability at Herne Bay." *Civ. Eng. Public Works Rev.*, , 67, 788–792.

Biczysko, S. J., and Starzewski, K. (1977a). "Daventry bypass landslip." *Ground Eng.*, 10(1), 23–25.

Biczysko, S. J., and Starzewski, K. (1977b). "Daventry bypass landslip." *Ground Eng.*, 10(3), 6–7.

Bishop, A. W. (1971). "The influence of progressive failure on the choice of the method of stability analysis." *Geotechnique*, 2, 168–172.

Bishop, A. W., and Bjerrum, L. (1960). "The relevance of the triaxial test to the solution of stability problems." *ASCE Research Conf. on Shear Strength of Cohesive Soils*, Boulder, Colo., 437–451.

Bishop, A. W., Green, G. E., Garga, V. K., Andresen, A., and Brown, J. D. (1971). "A new ring shear apparatus and its application to the measurement of residual strength." *Geotechnique*, 21(4), 273–328.

Bishop, A. W., Webb, D. L., and Lewin, P. I. (1965). "Undisturbed samples of London clay from the Ashford common shaft: Strength-effective stress relationships." *Geotechnique*, 15, 1–31.

Bjerrum, L. (1955). "Stability of natural slopes in quick clay." *Geotechnique*, 5(1), 101–119.

Bjerrum, L. (1967). "Progressive failure in slopes of overconsolidated plastic clay and clay shales." *J. Soil Mech. Found. Div., Am. Soc. Civ. Eng.*, 93(5), 3–49.

Blondeau, F., and Josseaume, H. (1976). "Mesure de la resistance au asaillement residuelle en laboratoire." *Bull. Liasion Lab. Ponts Chauss., Numero Special II*, 90–106.

Bromhead, E. N. (1972). "A large coastal landslide at Herne Bay, Kent." *Arup J.*, 7, 12–14.

Bromhead, E. N. (1978). "Large landslides in London clay at Herne Bay, Kent." *Q. J. Eng. Geol.*, 11, 291–304.

Bromhead, E. N., and Dixon, N. (1984). "Porewater pressure observations in the coastal cliffs at the Isle of Sheppey, England." *Proc., 4th Int. Symposium on Landslides*, Toronto, 1, 385–390.

Brooker, E. W., and Peck, R. B. (1993). "Rational design treatment of slides in overconsolidated clays and clay shales." *Can. Geotech. J.*, 30, 526–544.

Burland, J. B., Longworth, T. I., and Moore, J. F. (1977). "A study of ground movement and progressive failure caused by a deep excavation in Oxford clay." *Geotechnique*, 27, 557–591.

Burland, J. B., Longworth, T. I., and Moore, J. F. A. (1978). "A study of ground movement and progressive failure caused by a deep excavation in Oxford clay." *Geotechnique*, 28(3), 357–358.

Canceili, A. (1981). "Evaluation of slopes in overconsolidated clays." *Proc., 10th Int. Conf. on Soil Mechanics and Foundation Engineering*, A. A. Balkma, Rotterdam, 3, 377–380.

Canuti, P., Casagli, N., and Garzonio, C. A. (1994). "Large-scale mudslides in structurally complex clay shales in the Northern Apennines (Italy)." *Proc., 13th Int. Conf. on Soil Mechanics and Foundation Engineering*, Oxford & IBH, New Delhi, India, 2, 1110–1114.

Cassel, F. L. (1948). "Slips in fissured clays." *Proc., 2nd Int. Conf. on Soil Mechanics and Foundation Engineering*, International Society of Soil Mechanics and Foundation Engineering, 2.

Chandler, R. J. (1969). "The effect of weathering on the shear strength properties of Keuper Marl." *Geotechnique*, 19, 321–334.

Chandler, R. J. (1970). "A shallow slab slide in the Lias clay near Uppingham, Rutland." *Geotechnique*, 20, 253–260.

Chandler, R. J. (1971). "Landsliding on the Jurassic escarpment near Rockingham, Northampton." *Slopes: form and process, International Bulletin of Geology, Special Publication No. 3*, 111–128.

Chandler, R. J. (1972). "Lias clay: weathering processes and their effect on shear strength." *Geotechnique*, 22, 403–431.

Chandler, R. J. (1974). "Lias clay: the long-term stability of cutting slopes." *Geotechnique*, 24, 21–38.

Chandler, R. J. (1976). "The history of stability of two Lias clay slopes in the Upper Gwash Valley, Rutland." *Philos. Trans. R. Soc. London, Ser. A*, 283, 463–491.

Chandler, R. J. (1979). "Stability of a structure constructed in a landslide: selection of soil strength parameters." *Proc., 7th European Conf. on Soil Mechanics and Foundation Engineering*, 3, 175–181.

Chandler, R. J. (1982). "Lias clay slope sections and their implications for the prediction of limiting or threshold slope angles." *Earth Surf. Processes Landforms*, 17, 427–438.

Chanlder, R. J. (1984a). "Recent European experience of landslides in overconsolidated clays and soft rocks." *Proc., 4th Int. Symposium on Landslides*, Toronto, 1, 61–81.

Chandler, R. J. (1984b). "Delayed failure and observed strengths of first-time slides in stiff clays." *Proc., 4th Int. Symposium on Landslides*, Toronto, 2, 19–25.

Chandler, R. J., and Apted, J. P. (1988). "The effect of weathering on the strength of London Clay." *Q. J. Eng. Geol.*, 21, 59–68.

Chandler, R. J., Pachakis, M., Mercer, J., and Wrightman, J. (1973). "Four long-term failures of embankments founded on areas of landslip." *Q. J. Eng. Geol.*, 6, 405–422.

Chandler, R. J., and Skempton, A. W. (1974). "The design of permanent cutting slopes in stiff fissured clays." *Geotechnique*, 24(4), 457–466.

Clarke, C. L., James, P. M., and Morgenstern, H. (1970). "Foundation conditions at Munda Dam." *Proc., 2nd Int. Conf. Rock Mechanics*, Beigrade, 13, 6–15.

Cooper, M. R., Bromhead, E. N., Petley, D. J., and Grant, D. I. (1998). "The Selborne cutting stability experiment." *Geotechnique*, 48(1), 83–101.

Crawford, C. B., and Eden, W. J. (1967). "Stability of natural slopes in sensitive clays." *J. Soil Mech. Found. Div., Am. Soc. Civ. Eng.*, 93(4), 419–436.

Cruden, D. M., and Tsui, P. C. (1991). "Some influences of ice thrusting in geotechnical engineering." *Q. J. Eng. Geol., Spec. Publ. No. 7*, 127–137.

國立雲林科技大學
九十二學年度研究所博士班招生考試試題

所別：工程科技研究所
科目：營建文獻評論

de Beer, E. (1967). "Discussion." *Proc., Geotech. Conf.*, Oslo, 2, 184–186.

de Beer, E. (1969). "Experimental data concerning clay slopes." *Proc., 7th Int. Conf. on Soil Mechanics and Foundation Engineering*, Mexico, 2, 517–525.

DeLory, F. A. (1957). "Long term stability in slopes in overconsolidated clays." PhD thesis, Univ. of London, London.

Dixon, N., and Bromhead, E. N. (1991). "The mechanics of first-time slides in the London clay cliff at the Isle of Sheppey, England." *Slope Stability Eng.*, 277–282.

Duncan, J. M. (1996). "State of the art: limit equilibrium and finite element analysis of slopes." *J. Geotech. Eng.*, 122(7), 577–596.

Early, K. R., and Skempton, A. W. (1972). "Investigations of the landslide at Walton's Wood, Straffordshire." *Q. J. Eng. Geol.*, 5, 19–42.

Eden, W. J., and Jarrett, P. M. (1971). "Landslide at Orleans, Ontario." *Tech. Paper No. 321*, Division of Building Research Council of Canada, Ottawa.

Ehlig, P. L. (1987). "The Portuguese Bend landslide stabilization project." *Geology of Palos Verdes Peninsula and San Pedro Bay*, P. J. Fischer, ed., Society of Economic Paleontologists and Mineralogists and American Association of Petroleum Geologists, Los Angeles, Part 2, 17–24.

Eid, H. T. (1996). "Drained shear strength of stiff clays for slope stability analyses." PhD thesis, Univ. of Illinois at Urbana-Champaign, Ill.

Eigenbrod, K. D. (1975). "Analysis of the pore pressure changes following the excavation of a slope." *Can. Geotech. J.*, 12, 420–440.

Esu, F., and Calabresi, G. (1969). "Slope stability in an overconsolidated clay." *Proc., 7th Int. Conf. in Soil Mechanics and Foundation Engineering*, Mexico, 2, 555–563.

Esu, F., Di Stefano, D. M., Grisolia, M., and Tancredi, G. (1984). "Stability of a high cut in overconsolidated lacustrine deposits." *Proc., 4th Int. Symposium on Landslides*, Univ. of Toronto Press, Toronto, 2, 63–68.

Graham, J., and Au, V. C. (1985). "Effects of freeze-thaw and softening on a natural clay at low stresses." *Can. Geotech. J.*, 22(1), 69–78.

Gregory, C. H. (1844). "On railway cuttings and embankments, with an account of some slips in the London clay, on the line of the London and Croydon railway." *Min. Proc. Inst. C. E.*, 3, 135–145.

Haefeli, R. (1938). "Mechanische Eigenschaften von Lockergesteinen (Mechanical properties of loose stones)." *Schweizerische Bauzeitung*, III, 299–303, 321–325.

Haefeli, R. (1950). "Investigation and measurements of the shear strengths of saturated cohesive soils." *Geotechnique*, 2(3), 186–208.

Henkel, D. J. (1957). "Investigations of two long-term failures in London clay slopes at Wood Green and Northolt." *Proc., 4th Int. Conf. on Soil Mechanics and Foundation Engineering*, 2, 315–320.

Henkel, D. J., and Skempton, A. W. (1955). "A landslide at Jackfield, Shropshire, in heavily overconsolidated clay." *Geotechnique*, 5, 131–137.

Hollingworth, S. E., and Taylor, J. H. (1951). *The Northampton sand ironstone: stratigraphy, structure and reserves*, Her Majesty's Stationery Office, London.

Hutchinson, J. N. (1965a). "The stability of cliffs composed of soft rocks with particular reference to the coasts of SE England." PhD thesis, Univ. of Cambridge, England.

Hutchinson, J. N. (1965b). "A survey of the coastal landslides of Kent." *Building Research Station, Note EN/35/65*.

Hutchinson, J. N. (1969). "A reconsideration of the coastal landslides at Folkestone Warren, Kent." *Geotechnique*, 19, 6–38.

Hutchinson, J. N. (1980). "Large landslides in London clay at Herne Bay, Kent." *Q. J. Eng. Geol.*, 13, 63–64.

Hutchinson, J. N. (1988). "Morphological and geotechnical parameters of landslides in relation to geology and hydrology," *Proc., 5th Int. Symp. Landslides*, Lausanne, Balkema, Rotterdam, The Netherlands, 1, 69–78.

Hutchinson, J. N., and Gostelow, T. P. (1976). "The development of an abandoned cliff in London clay at Hadleigh, Essex." *Philos. Trans. R. Soc. London, Ser. A*, 283, 557–604.

Hutchinson, J. N., and Hughes, M. J. (1968). "The application of micropaleontology to the location of a deep seated slip surface in the London clay," *Geotechnique*, 18, 508–510.

Imrie, A. S. (1991). "Stress-induced response from both natural and construction-related processes in the deepening of the Peace River Valley, B.C." *Can. Geotech. J.*, 28(5), 718–728.

James, P. M. (1970). "Time effects and progressive failure in clay slopes." PhD thesis, Univ. of London, London.

James, P. M. (1971). "The role of progressive failure in clay slopes." *Proc., 1st Australia-New Zealand Conf. on Geomechanics*, 1, Melbourne, Australia, 344–348.

Janbu, N. (1977). "Slopes and excavations in normally consolidated and lightly overconsolidated clays." *Proc., 9th Int. Conf. in Soil Mechanics and Foundation Engineering*, Tokyo, 2, 549–566.

Janbu, N., Kjekstad, O., and Senneset, K. (1977). "Slide in overconsolidated clay below embankment." *Proc., 9th Int. Conf. on Soil Mechanics and Foundation Engineering*, 2, 95–102.

Kanji, M. A. (1974). "The relationship between drained friction angles and Atterberg limits of natural soils," *Geotechnique*, 24(4), 671–674.

Kankare, E. (1969a). "Geotechnical properties of the clays at the Kimola canal area with special reference to the slope stability." PhD thesis, State Institute for Technical Research at Helsinki, Helsinki, Finland.

Kankare, E. (1969b). "Failures at Kimola floating canal in southern Finland." *Proc., 7th Int. Conf., on Soil Mechanics and Foundation Engineering*, 2, 609–616.

Kenney, T. C. (1966). "Shearing resistance of natural quick clays." PhD thesis, Univ. of London, London.

Kenney, T. C. (1967a). "Slide behavior and shear resistance of a quick clay determined from a study of the landslide at Selnes, Norway." *Proc., Geotech. Conf.*, 1, 57–64.

Kenney, T. C. (1967b). "Influence of mineralogical composition on the residual strength of natural soils." *Proc., Oslo Geotech. Conf. Shear Strength of Natural Soils and Rocks*, Oslo, 1, 123–129.

Kenney, T. C. (1969). "Stability of natural slopes and embankment foundations," *Proc., 7th Int. Conf. in Soil Mechanics and Foundation Engineering*, Mexico, 3, 381–385.

Kenney, T. C., and Drury, P. (1973). "Case record of the slope failure that initiated the retrogressive quick-clay landslide at Ullensaker, Norway." *Geotechnique*, 23(1), 33–47.

Kjaernsli, B., and Simons, N. (1962). "Stability investigations of the north bank of the Drammen river." *Geotechnique*, 12(2), 147–167.

Lambe, T. W. (1973). "Up to date methods of investigating the strength and deformability of soils (laboratory and field testing of soils for their strength, deformative and rheological properties)," *Proc., 8th Int. Conf. on Soil Mechanics and Foundation Engineering*, 3, 3–25.

Lambe, T. W. (1985). "Amuay Landslides." The First Terzaghi Oration, *Proc., 11th Int. Conf. on Soil Mechanics and Foundation Engineering*, Golden Jubilee Volume, 137–158.

Lambe, T. W., Silva, F., and Marr, W. A. (1981). "Instability of Amuay Cliffside." *J. Geotech. Eng. Div., Am. Soc. Civ. Eng.*, 107(11), 1505–1520.

Lefebvre, G. (1981). "Fourth Canadian geotechnical colloquium: strength and slope stability in Canadian soft clay deposits." *Can. Geotech. J.*, 18(3), 420–442.

Lefebvre, G., and LaRochelle, P. (1974). "The analysis of two slope failures in Champlain sea clays." *Can. Geotech. J.*, 11(1), 89–108.

Li, T. D., and Zhao, Z. S. (1984). "A method of back analysis of the shear strength parameters for the first-time slide of the slope of fissured clay." *Proc., 4th Int. Symposium on Landslides*, 2, 127–129.

Lo, K. Y., and Lee, C. F. (1974). "An evaluation of the stability of natural slopes in plastic Champlain clays," *Can. Geotech. J.*, 11(1), 165–181.

Lupin, J. F., Skinner, A. E., and Vaughan, P. R. (1981). "The drained residual strength of cohesive soils," *Geotechnique*, 31, 181–213.

Marivoet, L. (1948). "Control of stability of a sliding slope in a railway cut near Wetteren," *Proc., 2nd Int. Conf. on Soil Mechanics and Foundation Engineering*, 2, 38–42.

Marsland, A. (1972). "The shear strength of fissured clay." *Stress-Strain Behavior of Soils, Rosco Memorial Symposium*, Foulis, Henley-on-Thames, U.K., 59–68.

Marsland, A., and Butler, M. E. (1967). "Strength measurements on stiff

fissured Barton Clay from Rawley, Hampshire." *Proc., Geotechnical Conf.*, 1, Oslo, 139–145.
Matheson, D. S. (1972). "Geotechnical implications of valley rebound." PhD thesis, Univ. of Alberta, Edmonton, Canada.
Mesri, G., and Abdel-Ghaffar, M. E. M. (1993). "Cohesion intercept in effective stress-stability analysis." *J. Geotech. Eng.*, 119(8), 1229–1249.
Mesri, G., and Cepeda-Diaz, A. F. (1986). "Residual shear strength of clays and shales." *Geotechnique*, 36, 269–274.
Morgenstern, N. R. (1977). "Slopes and excavations," State of the Art Report, *Proc., 9th Int. Conf. on Soil Mechanics and Foundation Engineering*, 2, 567–581.
Morgenstern, N. R. (1989). "Recent experience with dam foundations on clay-shale in western Canada." Special Lecture, *Proc., 12th Int. Conf. on Soil Mechanics and Foundation Engineering*, 4, 2201–2208.
Morgenstern, N. R. (1990). "Instability mechanisms in stiff soils and weak rocks." *Proc., 10th Southeast Asian Geotechnical Conf.*, Taipei, 27–36.
Morriam, R. (1960). "Portuguese Bend Landslide, Palos Verdes Hills, California." *J. Geol.*, 68, 140–153.
Muir Wood, A. M. (1971). "Engineering aspects of coastal landslides." *Price Inst. Civ. Eng.*, 50, 257–276.
Nakamori, K., Yang, P., and Sokobiki, H. (1996). "Strength characteristics of undisturbed landslide clays in tertiary mudstone." *Soils Found., J. Jpn. Geotech. Soc.*, 36(3), 75–83.
Obermeir, S. F. (1984). "Engineering geology of Potomac formation deposits in Fairfax county, Virginia, and vicinity, with emphasis on landslides." *Geological Survey Bulletin 1556*, U.S. Dept. of the Interior, Washington, D.C., 5–48.
Osaimi, A. E., and Clough, G. W. (1979). "Pore pressure dissipation during excavation." *J. Geotech. Eng. Div., Am. Soc. Civ. Eng.*, 105(4), 481–498.
Palladino, D. J., and Peck, R. B. (1972). "Slope failures in an overconsolidated clay, Seattle, Washington." *Geotechnique*, 22, 563–595.
Parry, R. H. G. (1972). "Some properties of heavily overconsolidated Oxford clay at a site near Bedford." *Geotechnique*, 22, 485–507.
Peck, R. B. (1967). "Stability of natural slopes." *J. Soil Mech. Found. Div., Am. Soc. Civ. Eng.*, 93(SM4), 403–417.
Petley, D. J. (1966). "The shear strength of soils at large strains." PhD thesis, London Univ., London.
Potts, D. M., Kovacevic, N., and Vaughan, P. R. (1997). "Delayed collapse of cut slopes in stiff clay." *Geotechnique*, 47(5), 953–982.
Rubey, W. W. (1930). "Lithologic studies of fine-grained upper cretaceous sedimentary rocks of the black hills region." *United States Geological Survey, Prof. Paper 165-A*.
Sevaldson, R. A. (1956). "The slide in Lodalen, October 6th, 1954." *Geotechnique*, 6(4), 167–182.
Seycek, J. (1978). "Residual shear strength of soils." *Bull. Int. Assoc. Eng. Geol.*, 17, 73–75.
Silvestri, V. (1980). "The long-term stability of a cutting slope in an overconsolidated clay." *Can. Geotech. J.*, 17(3), 337–351.
Singh, R., Henkel, D. J., and Sangrey, D. A. (1973). "Shear and K_o swelling of overconsolidated clay." *Proc., 8th Int. Conf. on Soil Mechanics and Foundation Engineering*, 1.2, 367–376.
Skempton, A. W. (1948). "The rate of softening in stiff fissured clays, with special reference to London clay." *Proc., 2nd Int. Conf. on Soil Mechanics and Foundation Engineering*, 2, 50–53.
Skempton, A. W. (1964). "Long-term stability of clay slopes." *Geotechnique*, 14(2), 77–101.
Skempton, A. W. (1966). "Bedding-plane slip, residual strength and the Vaiont Landslide." *Geotechnique*, 16(1), 82–84.
Skempton, A. W. (1970). "First time slides in overconsolidated clays." *Geotechnique*, 20, 320–324.
Skempton, A. W. (1977). "Slope stability of cuttings in Brown London clay." *Proc., 9th Int. Conf. on Soil Mechanics and Foundation Engineering*, 3, 261–270.
Skempton, A. W. (1985). "Residual strength of clays in landslides, folded strata and the laboratory." *Geotechnique*, 35, 3–18.
Skempton, A. W., and Brown, J. D. (1961). "A landslide in boulder clay at Selset, Yorkshire." *Geotechnique*, 11(4), 280–293.
Skempton, A. W., and Hutchinson, J. N. (1969). "Stability of natural slopes and embankment foundations." *Proc., 7th Int. Conf. on Soil Mechanics and Foundation Engineering*, State-of-the-Art Volume, Mexico City, 291–340.
Skempton, A. W., and La Rochelle, P. (1965). "The Bradwell Slip, a short term failure in London clay." *Geotechnique*, 15, 221–242.
Skempton, A. W., and Petley, D. J. (1967). "The strength along structural discontinuities in stiff clays." *Proc., Geotechnical Conf.*, Oslo, 2, 29–47.
Skempton, A. W., and Vaughan, P. R. (1995). "The failure of Carsington Dam." Discussion, *Geotechnique*, 45(1), 719–739.
Spencer, E. (1967). "A method of analysis of the stability of embankments assuming parallel inter-slice forces." *Geotechnique*, 17, 11–26.
Stabell, O., and Höy, E. (1954). "Det störe eksamen sarbeidet i geoteknikk." *Norwegian Geotechnical Institute Internal Rep. No. F.32*, Norway.
Stark, T. D., and Eid, H. T. (1992). "Comparison of field and laboratory residual strengths." *Proc., ASCE Spec. Conf. on Stability and Performance of Slopes and Embankments-II, A 25-Year Perspective, Geotechnique, Special Publication No. 31*, (1), 876–889.
Stark, T. D., and Eid, H. T. (1994). "Drained residual strength of cohesive soils." *J. Geotech. Eng.*, 120(5), 856–871.
Stark, T. D., and Eid, H. T. (1997). "Slope stability analyses in stiff fissured clays." *J. Geotech. Geoenviron. Eng.*, 123(4), 335–343.
Tavenas, F., and Leroueil, S. (1981). "Creep and failure of slopes in clays." *Can. Geotech. J.*, 18(1), 106–120.
Terzaghi, K. (1936). "Stability of slopes of natural clay." *Proc., 1st Int. Conf. on Soil Mechanics and Foundation Engineering*, 1, 161–165.
Terzaghi, K., Peck, R. B., and Mesri, G. (1996). *Soil mechanics in engineering practice*, 3rd Ed., Wiley, New York.
Thomson, S. (1970). "Riverbank stability study at the University of Alberta, Edmonton." *Can. Geotech. J.*, 7, 157–168.
Thomson, S. (1971a). "The Lesuer landslide, a failure in Upper Cretaceous clay shale." *Proc. 9th Annual Engineering Geology and Soils Engineering Symposium*, Boise, Idaho, 257–287.
Thomson, S. (1971b). "Analysis of a failed slope." *Can. Geotech. J.*, 8(4), 596–599.
Tiedemann, B. (1937). "Uber die Schubfestigkeit bindiger Boden." *Bautechnik*, 15, 433–435.
Townsend, F. C., and Banks, D. C. (1974). "Preparation effects on clay shale classification indexes." *Proc., ASCE National Meeting, Water Resources Engineering*, Los Angeles, 1–36.
Vaughan, P. R., and Walbancke, H. J. (1973). "Pore-pressure changes and delayed failure of cutting slopes in overconsolidated clay." *Geotechnique*, 23, 531–539.
Voight, B. (1973). "Correlation between Atterberg plasticity limits and residual shear strength of natural soils." *Geotechnique*, 23, 265–267.
Vonder Linden, K. (1972). "An analysis of the Portuguese Bend landslide, Palos Verdes Hills, California." PhD thesis, Stanford Univ., Stanford, Calif.
Wilson, S. D. (1970). "Observational data on ground movements related to slope instability." *J. Soil. Mech. Found Div., Am. Soc. Civ. Eng.*, 96(SM5), 1521–1544.
Wilson, S. D., and Johnson, K. A. (1964). "Slides in overconsolidated clays along the Seattle freeway." *Proc., 2nd Annual Engineering Geology and Soil Engineering Symposium*, 29–42.
Wise, E. V. A. (1957). "The stability of natural slopes in overconsolidated fissured clay." MSc thesis, Imperial College, London Univ., London.
Wu, T. H., Williams, R. L., Lynch, J. E., and Kulatilake, H. S. W. (1987). "Stability of slopes in Red Conemaugh Shale of Ohio." *J. Geotech. Eng.*, 113(3), 248–264.
Yudhbir (1969). "Engineering behavior of heavily overconsolidated clays and clay shales with special reference to long-term stability." PhD thesis, Cornell Univ., Ithaca, N.Y.

國立雲林科技大學
九十二學年度研究所博士班招生考試試題
所別：工程科技研究所
科目：營建文獻評論

（3件1）

IMPACT OF TOTAL QUALITY MANAGEMENT ON HOME-BUYER SATISFACTION

By Zeljko M. Torbica[1] and Robert C. Stroh[2]

ABSTRACT: Providing superior quality and keeping customers satisfied are rapidly becoming the ways construction companies differentiate themselves from competitors. Many companies are, however, frustrated in their efforts to improve quality and customer satisfaction through the implementation of total quality management (TQM). The primary objective of this study was to increase understanding of how TQM affects home-buyer satisfaction. For the first time an empirical study has confirmed that implementation of TQM is positively associated with home-buyer satisfaction. Supplier quality management has emerged as the most important factor in shaping home-buyer satisfaction, but it is the area in which home builders do not practice extensively.

INTRODUCTION

Quality began to emerge as a key management focus in the United States in the early 1980s. In the construction industry the need for such attention has long been presented based on all available evidence (Tucker 1990). Many studies have presented a rather unfavorable picture of the industry performance [see, e.g., Modern (1983), Wiggins (1988), Davis et al. (1989), and Tucker (1990)]. Providing superior quality is rapidly becoming the way for companies to differentiate themselves from competitors and win more projects. To meet this quality challenge, many companies are adopting new management practices that focus on the continuous improvement of product and service quality. All of these practices have come to be known as total quality management (TQM). The search for the universal definition of TQM has yielded inconsistent results. We define TQM as a comprehensive company-wide effort dedicated to customer satisfaction through continuous improvement.

CONTROVERSY SURROUNDING TQM

TQM has evolved as a business philosophy with worldwide appeal and was seen as a universal cure for all organizational ills. The media have been sending mixed messages about the actual impact of TQM initiatives on business performance, and an increasing number of criticisms and accounts of failed efforts appeared in the literature. Some studies have stressed positive impacts of TQM efforts, reporting significant improvements in outcomes such as market share, cost, and profits (Schoefler et al. 1974; Peters and Waterman 1982; Rehder and Ralston 1984; Burati et al. 1991; "Management" 1991; McKim and Kiani 1995). Other studies have expressed criticism concerning the effectiveness of TQM initiatives ("The Cracks" 1992; Wilkinson et al. 1995; Lackritz 1997), and an increasing number of firms begin to question the link between TQM effort and economic returns and competitiveness. Such conflicting signals imply that general understanding about quality is becoming increasingly complex and puzzling.

Construction industry shares a similar experience with other industries with respect to confusing results of TQM initiatives. Although many companies have a hard time acknowledging this point publicly, the results of most quality programs have fallen short of expectations. For many of them, quality initiatives turned out to be just another burden on the bottom line. Some companies even began questioning the basic tenets of TQM. Is TQM as a business philosophy flawed or do the flaws lie in the implementation of TQM?

Empirical evidence of the success or failure of TQM practice in the construction industry is surprisingly scarce. The literature is full of prescriptions that offer various remedies to improve the quality of products and services. Most of these recommendations are, however, anecdotal. There is a need for more research to systematically assess and document the results of TQM and to identify the factors that contribute to its success or failure.

CUSTOMER SATISFACTION AS PERFORMANCE CRITERIA

Companies need assurance that their improvement efforts are organized and that their priorities are on the right track (Kelvin and Lynch 1992). Organizational efforts toward continuous improvement should be focused on creating performance measurement systems that provide relevant, factual information on core business processes and key activities (Miller 1992). The distinguishing characteristic of this study is that it utilizes customer satisfaction for evaluation of quality and, ultimately, for assessment of success of a company's TQM program. This is in line with Juran's call for new measures for quality:

> Unsuccessful companies did not develop new measures for quality in order to provide the executives with essential information on quality. Or, alternatively, unsuccessful companies focused exclusively on financial measures (sales, profits, ROI) and they lacked some essential measures of quality (measures of customer satisfaction, competitive quality). Lacking such measures, they learned of their quality problems only after severe damage had already been done. (Juran 1993, p. 37)

Quality improvement is difficult to achieve unless quality is accurately and periodically measured. One reason for that difficulty is the lack of good overall measures of quality in its broadest sense. Companies say they have difficulty even making a baseline assessment of their quality ("TQM" 1995). Consequently, TQM remains a mystery to many top managers in the construction industry, and many are not even interested in getting involved.

The challenge is to design valid external measures, but to report and use the results to drive internal organizations to improve quality performance, and ultimately to increase profitability. Customer satisfaction, as an external measure, can

[1]Asst. Prof., Dept. of Constr. Mgmt., Florida Int. Univ., 2912 College Ave., Davie, FL 33314. E-mail: torbicaz@fiu.edu
[2]Dir., Shimberg Ctr. for Affordable Housing, Univ. of Florida, M. E. Rinker Sr. School of Build. Constr., P.O. Box 115703, Gainesville, FL 32611-5703. E-mail: stroh@ufl.edu

Note. Discussion open until November 1, 1999. To extend the closing date one month, a written request must be filed with the ASCE Manager of Journals. The manuscript for this paper was submitted for review and possible publication on June 26, 1998. This paper is part of the *Journal of Construction Engineering and Management*, Vol. 125, No. 3, May/June, 1999. ©ASCE, ISSN 0733-9634/99/0003-0198–0203/$8.00 + $.50 per page. Paper No. 18655.

provide the strategic intelligence needed to direct the quality improvement effort. It is true that most home builders do customer surveys. But too often there is no structure that ties customer satisfaction to internal business processes. In this study we attempt to find answers to the following questions:

1. How to organize a TQM effort that will allow achievement of the highest home-buyer satisfaction?
2. What level of home-buyer satisfaction may be expected from a particular organizational or managerial TQM approach?

By determining how TQM affects customer satisfaction and which TQM factors correlate the most with customer satisfaction, builders can focus their activities on the most promising areas.

CUSTOMER SATISFACTION MODEL

Before we can elaborate on a model of customer satisfaction, it is necessary to provide simple, conceptually sound definitions of customer. The simplest available definition of a customer is "one who pays the bill" (Austin and Peters 1985)—a "paying" customer. Another type of customer, equally important, is one who uses a product or service—a "user" customer. Most facilities have been designed and built for a client other than the user. It is very important to make the distinction between the two types of customers for they use different sets of criteria against which they judge their satisfaction. This study is unique in that it deals with single-family house buyers who both purchase and live in their homes; that is, the home-buyer population represents both types of customers—paying and user customers.

Fig. 1 shows a model depicting the relationships between a company's TQM practice and home-buyer satisfaction. According to the proposed model, the TQM system, if observed and managed in a structured fashion, will lead to achieving higher house and service quality, which will eventually lead to improved home-buyer satisfaction.

Rarely are market offerings either all products or all services but most often they are a blend of the two (Brown and Fern 1981). Every product and service must be designed, produced, and delivered in the context of a total package of products and services—it is the "total offering" that generates the total degree of customer satisfaction. The customer satisfaction model used in the present study assumes that the relevant elements of home-buyer satisfaction extend beyond the house itself. Several studies have suggested that satisfaction depends not only upon the product itself but also upon the experience surrounding the acquisition of the product (Hempel 1977). The price home buyers pay for a house is more than the price for bricks—it is a price for the product, including the service they get from home builder before, during, and after construction. In fact, the quality of service may be the only factor that sets a builder apart from other builders who are offering similar homes for similar market segments ("Customer" 1988).

Making a distinction between product and service components of satisfaction is methodologically appropriate for satisfaction does not appear to involve some form of compensatory judgment where poor performance on one dimension is balanced by good performance on another, and vice versa (Swan and Combs 1976). We further break down the product component of customer satisfaction into two dimensions: satisfaction with the house design and the house itself. We theorize that design of a product plays a major role in shaping customer satisfaction. In summary, our model anticipates that home-buyer satisfaction is affected by three distinct dimensions of home-builder's total offering: house design, house, and service.

RESEARCH METHODOLOGY

No large-scale study to date has attempted to measure the extent of TQM practice in the home-building industry and to relate that to specific measures of company performance. This study investigates the nature and strength of the link between TQM and home-buyer satisfaction. We asked the following questions:

- How does TQM affect home-buyer satisfaction?
- What aspects of TQM are the most highly related to home-buyer satisfaction?
- What areas of improvement will have the greatest impact on home-buyer satisfaction?

By gaining a better understanding of the relationship between TQM practice and customer satisfaction, and by knowing which aspect of TQM practice has the greatest impact on customer satisfaction, management actions can be orchestrated in such a way that product and service receive maximum customer satisfaction evaluation. To gather the necessary data we had to conduct two separate surveys, the TQM Survey and the Customer Satisfaction Survey.

TQM SURVEY

Based on an exhaustive review and synthesis of the quality literature, Saraph et al. (1989) identified eight critical areas of managerial planning and action that must be practiced to achieve effective quality management in a company. The eight critical factors identified are as follows:

1. The role of divisional top management and quality policy
2. The role of the quality department
3. Quality-related training
4. Product/service design
5. Supplier quality management

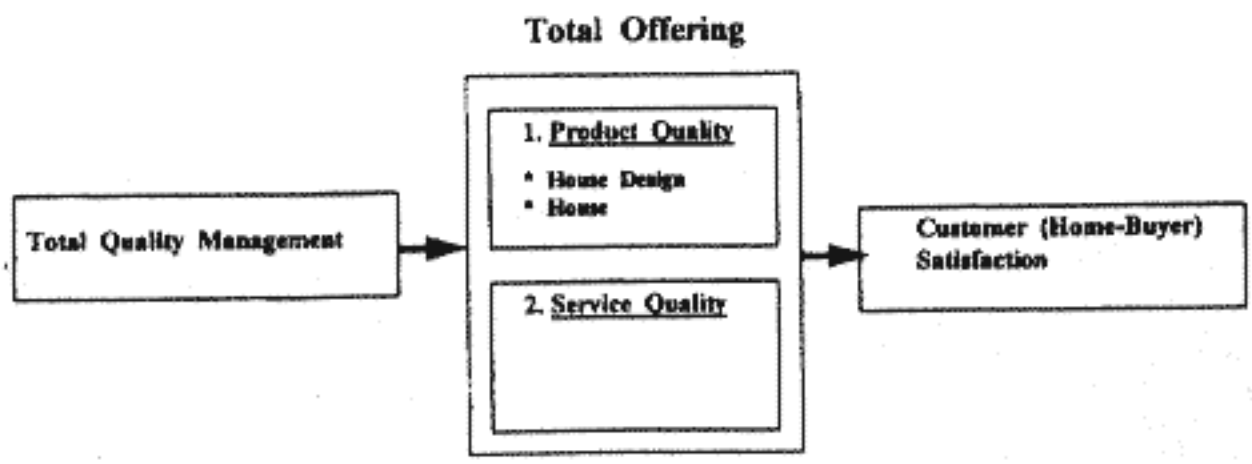

FIG. 1. Customer (Home-Buyer) Satisfaction Model

6. Process management and operating procedures
7. Quality data and reporting
8. Employee relations

The writers developed an instrument to assess critical factors of quality management containing several operational measures for each of the factors—a total of 78 items. The instrument is considered to be a relatively quick method to self-assess the extent of company TQM practice.

Survey Questionnaire

A customized version of an instrument developed by Saraph et al. (1989) was used to gather data about the TQM program of home builders. The modifications included minor alterations of the wording of some questions to make them more uniform and easily understood. The items were critically reviewed for their clarity and content by a variety of industry practitioners and academicians. Seven items were deleted from the original questionnaire due to the lack of applicability to the home-building industry, resulting in an instrument with 71 statements. To enable respondents to indicate the extent of current practice of each item by their business unit, a five-point Likert-type interval-rating scale was used.

Survey Administration

The *Florida Trend* ("Top" 1996) list of the top 50 Florida home builders served as the sample frame from which 20 companies were randomly selected. Telephone contact with the company president or division-level manager sought agreement to participate in the survey. In addition to willingness to participate in the survey, the companies had to agree to provide a complete list of customers who had moved into their new home between August and October 1995. These telephone contacts resulted in agreements with 16 home builders to serve as the survey sample.

A set of five questionnaires was sent to each company contact. It was left to the discretion of the contact person to select the five company personnel that had the best perspective on internal TQM practices and that would complete the questionnaire. Respondents rated their perceptions regarding the extent of implementation of TQM in a business unit. All 80 questionnaires (16 companies × 5 questionnaires) were completed and returned yielding a 100% response rate. Each of the 16 companies also provided their customer list for the specified time period so that the second survey (i.e., home-buyer satisfaction survey) could be initiated.

Survey Data

The TQM survey resulted in a data set consisting of 80 observations on 71 items representing eight critical factors of TQM. Two items were excluded from analysis for having more than 30% of "not applicable" responses, resulting in a final data set of 80 observations on 69 items.

Eight companies provided a negative answer to the question: Does your business unit have a separate quality department/group/unit? Consequently, the assessment for Factor 2 (F2) ("role of the quality department") was not provided by these companies. To have a balanced data set for all companies we excluded F2 from further analysis. This action is considered to be methodologically appropriate, because the authors of the instrument claim that the critical factors of TQM could be used independently or in combination (Saraph et al. 1989).

For each respondent within a company, scores for seven critical factors of TQM were calculated. The factor scores were the mean of the individual's responses for the items within each factor. A mean was then obtained for each company on each of the seven critical factors of TQM by averaging scores of five individuals on that factor. This process resulted in a 7D vector (F1, F3, F4, F5, F6, F7, F8) that can be considered as a company TQM profile. A total company score of TQM (TOTALTQM) was then obtained by adding up the average score on each of the seven factors and then dividing by 7.

CUSTOMER SATISFACTION SURVEY

The customer satisfaction model used in the present study views customer satisfaction as a composite, 3D satisfaction with house design, house, and service. To measure the extent of home-buyer satisfaction, a special instrument, called HOMBSAT (HOMe-Buyer SATisfaction), was developed. The instrument contains several operational measures for each of the dimensions—a total of 51 items: 14 items representing the design dimension; 16 items representing the house dimension; and 21 items representing the service dimension [see Torbica (1997)]. The measures proposed were empirically based and tested and shown to be reliable and valid. More detailed discussion on the development and testing of the HOMBSAT can be found in Torbica (1997).

Survey Administration

Once the names and addresses for the targeted home buyers were obtained, the home-buyer satisfaction survey was ready for administration. Data were collected from home buyers regarding their level of satisfaction with design, house, and service. Response to all items on the HOMBSAT instrument were in the form of a seven-point Likert-like interval rating scale. A total of 545 questionnaires were distributed, and 295 of them were completed and returned with the overall response rate of 54.2%. Given the nature of study, and the length of the questionnaire (11 pages), it was considered to be a high to very high return rate.

Survey Data

The number of home buyers who returned the questionnaire varied between 15 and 20 per company. To have a balanced data set, we retained only 15 respondents for each company for further analysis. For those companies that were represented with more than 15 respondents, responses from 15 randomly selected home buyers were retained for analysis.

Measures of home-buyer satisfaction were obtained for each individual home buyer by calculating the home-buyer's average score on each of the three HOMBSAT dimensions. The scores were the mean of the individual's responses for the items within each dimension. Scores for DESIGN, HOUSE, and SERVICE for each company were then obtained by averaging the individual home-buyer scores for that company. A total company score for home-buyer satisfaction (SATIS) was obtained by adding up the average score on each of the three dimensions and then dividing by 3.

DATA ANALYSES

In this section we discuss the results from several analyses that were conducted on the empirical data obtained from two surveys. The data were analyzed with the aid of the SPSS computer software package (*SPSS 7.5* 1997).

Relationship between TQM and Home-Buyer Satisfaction

The thesis of this study is that home-buyer satisfaction is determined by a company's TQM practice. We asked the following questions:

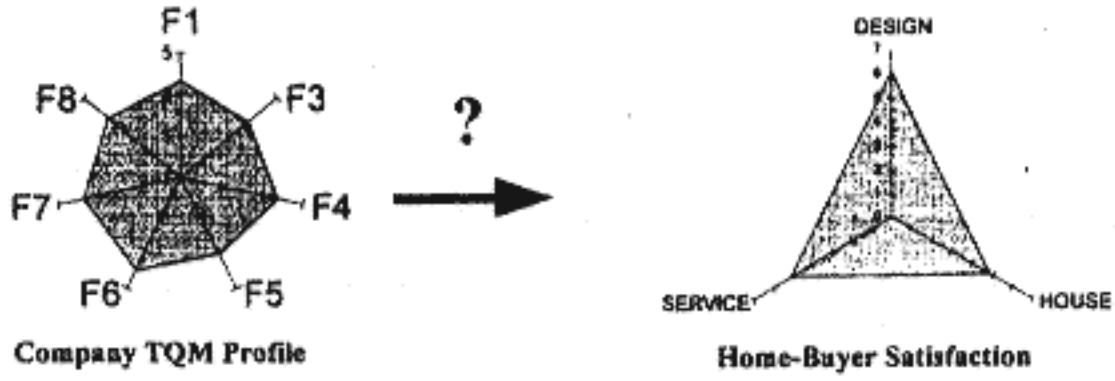

Home- Buyer Satisfaction $= f$(F1, F3, F4, F5, F5, F6, F7, F8)

FIG. 2. What Is Relationship between TQM and Home-Buyer Satisfaction

TABLE 1. Statistically Significant Regression Models

Dependent variable (1)	Regression Model (2)
SATIS	SATIS = 3.882 + 0.426*(TOTALTQM) R^2 = 0.311; s_e = 0.246; D-W = 2.2; F = 5.876; p < 0.031
SATIS	SATIS = 3.251 + 0.067(F1) + 0.555*(F5) R^2 = 0.541; s_e = 0.2091; D-W = 2.138; F = 7.058; p < 0.009 $SATIS_s$ = 0.667*(F5) + 0.112(F1)
DESIGN	DESIGN = 5.076 + 0.278*(TOTALTQM) R^2 = 0.208; s_e = 0.2108; D-W = 2.624; F = 3.409; p < 0.088
DESIGN	DESIGN = 4.823 + 0.231(F5) + 0.137(F8) R^2 = 0.300; s_e = 0.2062; D-W = 2.687; F = 2.574; p < 0.117 $DESIGN_s$ = 0.347(F5) + 0.3(F8)
HOUSE	HOUSE = 3.296 + 0.573*(F5) R^2 = 0.391; s_e = 0.2544; D-W = 1.600; F = 8.356; p < 0.013
SERVICE	SERVICE = 2.342 + 0.718*(TOTALTQM) R^2 = 0.379; s_e = 0.3568; D-W = 2.225; F = 7.936; p < 0.015
SERVICE	SERVICE = 1.280 + 0.760*(F5) + 0.142(F6) + 0.145(F8) R^2 = 0.577; s_e = 0.3203; D-W = 2.037; F = 4.992; p < 0.020 $SERVICE_s$ = 0.597*(F5) + 0.166(F8) + 0.11(F6)

Note: Independent variables are as follows: F1 = role of divisional top management and quality policy; F3 = quality-related training; F4 = product/service design; F5 = supplier quality management; F6 = process management and operating procedures; F7 = quality data and reporting; F8 = employee relations; TOTALTQM = (F1 + F3 + F4 + F5 + F6 + F7 + F8)/7; SATIS = (DESIGN + HOUSE + SERVICE)/3.

- How does TQM affect home-buyer satisfaction?
- Can home-buyer satisfaction be predicted by TQM factors?
- What factors of TQM are the most highly related to home-buyer satisfaction?

This is graphically presented in Fig. 2.

After the close investigation of the combined data set, one company was excluded from further analysis for having very unusual responses. Simple and multiple regression analysis were performed on the data set, using scores for seven critical factors of TQM and total company score of TQM (TOTALTQM) as independent variables, and scores for four measures of home-buyer satisfaction, DESIGN, HOUSE, SERVICE, and SATIS, as dependent variables.

The analysis was performed in three steps as follows. We first conducted a simple regression analysis where each of the four measures of home-buyer satisfaction were regressed on the company total quality score of TQM (TOTALTQM). Next, for each of the four measures of home-buyer satisfaction seven simple linear regression analyses were performed with seven factors of TQM used as independent variables. In the third step, multiple regression was performed for each measure of home-buyer satisfaction for which two or more critical factors were found to be significant predictors. Multiple regression was used to determine the relative importance of each of significant predictors. Table 1 summarizes the results of the statistical analysis. Only models that were found to be significant are shown. Each regression model is accompanied by the following five statistics: R^2, s_e, D-W (Durbin-Watson statistic), F-value, and p-value. The asterisk (*) indicates a two-tailed coefficient that is statistically significant at the 0.05 level. Both regular and standardized regression equations, designated by subscript s, are shown.

Implications

We developed several regression models to predict the impact of critical factors of TQM on different aspects of home-buyer satisfaction. The models that link TQM with home-buyer satisfaction can help managers in pinpointing areas requiring action to improve design, house, and service quality. By identifying and prioritizing specific areas for improvement, top management can allocate its resources efficiently, targeting those areas that are in immediate need of improvement.

For the first time an empirical study has confirmed that the implementation of TQM practices is positively associated with home-buyer satisfaction. We have shown that home-buyer satisfaction can be successfully predicted by means of an regression equation in which 31% of the variance in a company's home-buyer satisfaction (SATIS) is explained by the total company TQM score (TOTALTQM) [regression model (1)]. This lends strong credence to the hypothesized relationship between TQM and home-buyer satisfaction. With the exception of F3 (training), all other critical factors of TQM have demonstrated lesser or greater potential for predicting home-buyer satisfaction. F5 (supplier quality management) has emerged as the most important factor in shaping all three aspects of home-buyer satisfaction. The implication is that subcontractors and suppliers are critical members of the building team. They have to be included in the creation of performance standards. It also suggests that home builders should pay more attention in generating a list of approved suppliers and subcontractors. An interesting finding is that we failed to find a significant association between F3 (training) and home-buyer satisfaction. One possible explanation is that training, perhaps, has not been fully implemented in home building.

Current Level of Industry Practice of TQM

The responses to the survey of home builders provided a snapshot of TQM practiced by large Florida home builders. The actual scores on the TQM factors are used as measures of the degree with which home builders practice TQM. Our

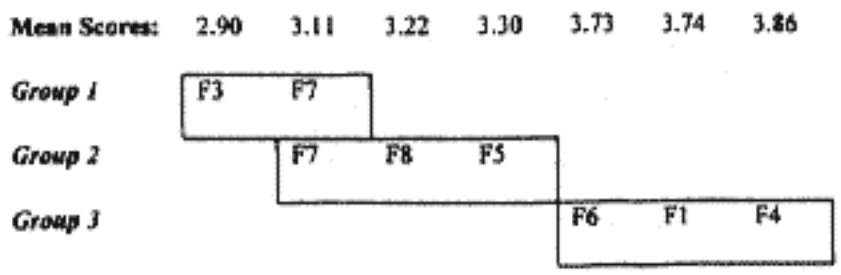

FIG. 3. Duncan Comparison of Critical Factors' Mean Scores

survey data illustrate clear patterns where companies stress certain TQM practices but ignore others. Using an analysis of variance technique (ANOVA) and the Duncan test, it was determined that critical factors of TQM can be grouped into three categories with respect to current level of practice. F3 (training) and F7 (quality data and reporting) are practiced significantly (95% confidence) less than other critical TQM factors. Slightly better performance is associated with F8 (employee relations) and F5 (supplier quality management). The respondents reported that significantly more commonly practiced factors were "product/service design" (F4), "role of divisional top management and quality policy" (F1), and "process management and operating procedures" (F6). These relationships are illustrated in Fig. 3.

Implications

The study findings clearly indicate that there is a gap between the levels of importance that critical factors have in affecting different aspects of home-buyer satisfaction and the levels of home builders' practice of each of the factors. These gaps are graphically shown in Fig. 4 where we match the importance of factors, that were found to be significant predictors of home-buyer satisfaction, with the current level of industry performance regarding these factors.

In constructing Fig. 4 we assigned significance and performance scores to each factor in accordance with the following rules: The most important factor in the regression model (Table 1) receives Score 3; the next one in importance receives Score 2; and the third factor in importance receives Score 1. Similarly, Score 3 was assigned to factors that belong to Group 3 (the highest practiced factors), and Score 2 is assigned to factors from Group 2. Because none of factors from Group 1 was found to be a significant predictor of any measure of home-buyer satisfaction, they are not included in the graphs.

The implication is that there is a gap between the importance that F5 (supplier quality management) has in affecting home-buyer satisfaction and the current level of industry practice of that factor. Because this is the area with greatest potential for competitive advantage, home builders should pay more attention and focus their improvement effort toward practicing F5 (supplier quality management).

RECOMMENDATIONS FOR FUTURE RESEARCH

The initial research findings that emerged from this study are encouraging, but a great deal of further research remains to be done. There are several types of future studies that would build on the results of this research. First, the model developed in this study that links TQM practice and home-buyer satisfaction can be extended to study how TQM influences customer satisfaction in a field other than home building. Building construction, engineering construction, and heavy and highway construction sectors of the industry can be investigated, as well, using specifically designed instruments that will reflect the unique nature of customers for each of the sectors.

Second, much work needs to be done with regard to linking TQM and additional operating and financial performance measures, such as net profit margin, return on investment (ROI), and employee satisfaction, to mention but a few. These alternative measures could be used in conjunction with home-buyer satisfaction to evaluate company performance, to give a more

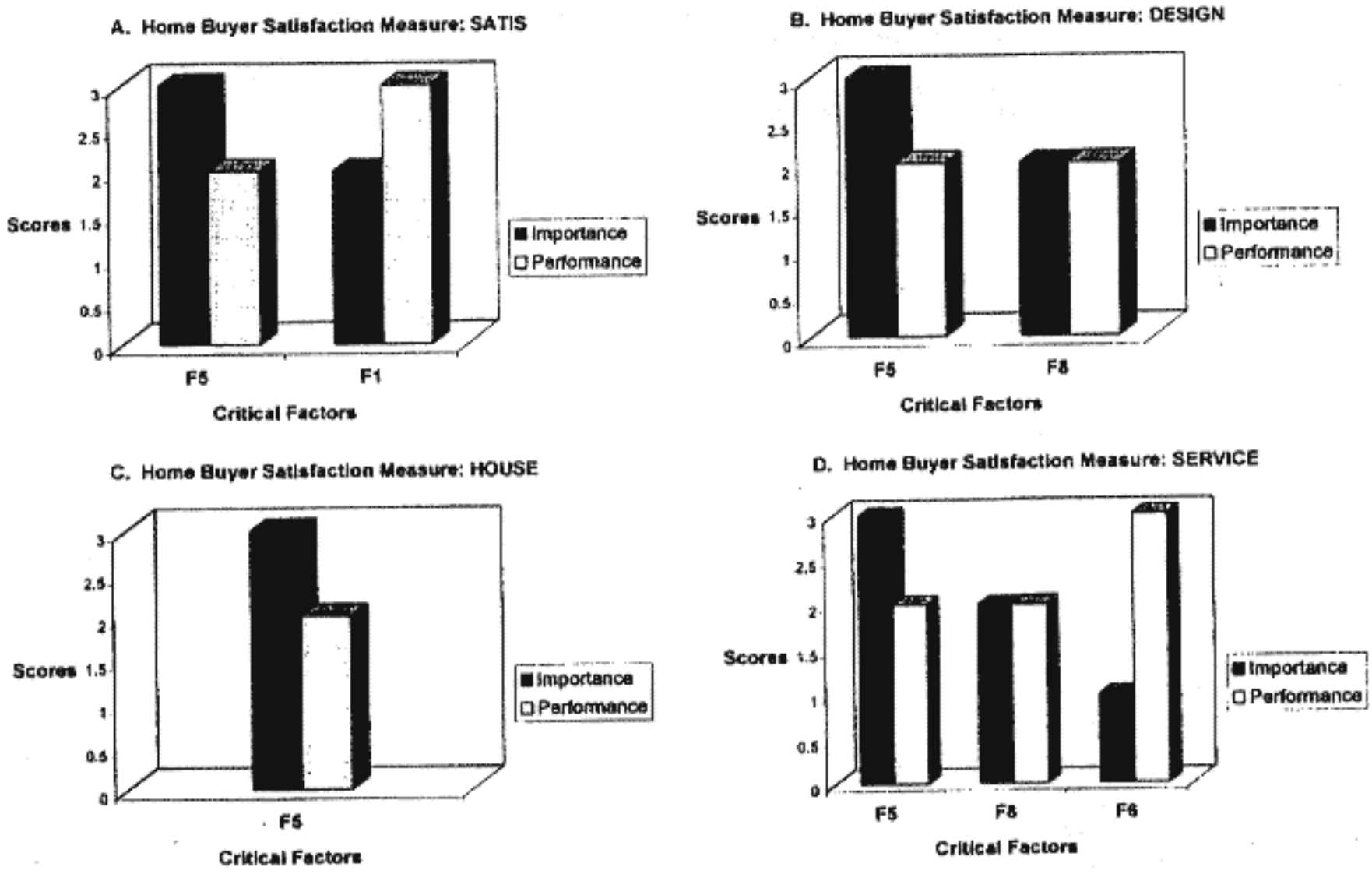

FIG. 4. Comparison of Importance and Levels of Performance for Critical Factors of TQM for Four Customer Satisfaction Measures

complete indication of the success or failure of TQM initiatives.

This study only examined internal TQM factors to evaluate their impact on home-buyer satisfaction. However, many external factors might influence home-buyer satisfaction, such as income, age, level of education, and neighborhood. Perhaps future research should consider the impact of these external factors on home-buyer satisfaction. These additional studies should be conducted with larger sample sizes, which will improve the power of the statistical analyses.

CONCLUSIONS

This study has resulted in new insights regarding TQM and home-buyer satisfaction. Most of the previous research about TQM has been descriptive. This is the first study that links TQM practices with single-family detached home-buyer satisfaction. The research results found a significant relationship between TQM practice and home-buyer satisfaction in a population of medium to large Florida home builders. This is especially interesting in light of the recent critique of effectiveness of TQM initiatives. Our results suggest that home builders with well established TQM programs will have more success in delivering high home-buyer satisfaction; the higher level of actual practice of critical factors of TQM, the higher the home-buyer satisfaction. Supplier quality management has emerged as the most potential predictor of home-buyer satisfaction, and home builders should focus their improvement efforts more toward that critical area.

APPENDIX. REFERENCES

Austin, N., and Peters, T. (1985). *A passion for excellence.* Warner Books, New York.
Brown, J. R., and Fern, E. F. (1981). "Goods vs. service marketing: A divergent perspective." *Marketing of services*, J. H. Donnelly and W. R. George, eds., America Marketing Association, Chicago, 205–212.
Burati, J. L., Michael, F. M., and Satyanarayana, N. K. (1991). "Quality management in construction industry." *J. Constr. Engrg. and Mgmt.*, ASCE, 117(2), 341–359.
"The cracks in quality." (1992). *Economist*, April 18, 67–68.
Davis, K., Ledbetter, W. B., and Burati, J. L. (1989). "Measuring design and construction quality costs." *J. Constr. Engrg. and Mgmt.*, ASCE, 115(3), 385–400.
Hempel, D. J. (1977). "Consumer satisfaction with the home buying process: Conceptualization and measurement." *Conceptualization and measurement of consumer satisfaction and dissatisfaction*, K. H. Hunt, ed., Marketing Science Institute, Cambridge, Mass.
Juran, J. M. (1993). "Why quality initiatives fail." *J. Business Strategy*, 14(4), 35–38.
Kelvin, F. C., and Lynch, R. L. (1992). "For good measure." *CMA Mag.*, April, 20–23.
Lackritz, J. R. (1997). "TQM within FORTUNE 500 corporations." *Quality Progress*, February, 69–72.
McKim, R. A., and Kiani, H. (1995). "Applying total quality management to the North American construction industry." *Cost Engrg.*, 37(3), 24–28.
Miller, J. A. (1992). "The new activity performance measures." *CMA Mag.*, April, 34.
Modern Management Systems. (1983). "Business Roundtable's Construction Industry Cost Effectiveness Project." *Rep. A6*, The Business Roundtable, New York.
Peters, T. J., and Waterman, R. W., Jr. (1982). *In search of excellence: Lessons from America's best run companies.* Harper & Row, New York.
Rehder, R., and Ralston, F. (1984). "Total quality management: A revolutionary management philosophy." *SAM Advanced Mgmt. J.*, Summer, 24–34.
Saraph, V. J., Benson, P. G., and Schroeder, G. R. (1989). "An instrument for measuring the critical factors of quality management." *Decision Sci.*, 20(4), 810–829.
Schoeffler, S., Buzzell, R., and Heany, D. (1974). "Impact of strategic planning on profit performance." *Harvard Business Rev.*, March–April, 137–145.
SPSS 7.5. (1997). SPSS Inc., Chicago.
Swan, J. E., and Combs, L. J. (1976). "Product performance and consumer satisfaction: A new concept." *J. of Marketing*, 40(April), 25–33.
"Top rank Florida residential home builders." (1996). *Florida Trend*, March, 84–85.
Torbica, Z. M. (1997). "Total quality management (TQM) and customer satisfaction in home building," PhD dissertation, University of Florida, Gainesville, Fla.
"TQM is underutilized, according to poll." (1995). *Engrg. News Rec.*, February 1, 14.
Tucker, R. L. (1990). "The big 'Q'." *Constr. Specifier*, May, 151–152.
Wiggins, J. H. (1988). "Construction's critical condition." *Civ. Engrg.*, 58(10), 72–73.
Wilkinson, A., Redman, T., and Snape, E. (1995). "New patterns of quality management in the United Kingdom." *Quality Mgmt. J.*, 2(2), 37–51.

國立雲林科技大學
九十二學年度研究所博士班招生考試試題

所別：工程科技研究所
科目：工程數學（丁）

1. (10%) Solve $xy' = x + y \qquad y(1) = 1$

2. (10%) Solve $(12y - 5x - 8)dy - (5y - 2x - 3)dx = 0$

3. (20%) Use Laplace transform to solve $\frac{1}{3}y'' + y' + \frac{2}{3}y = 0, \quad y(0) = 1, y'(0) = 0$

4. (15%)Solve the initial value problem：

   y' + y tan x = sin 2x y(0) = 1

5. (15%)Find the transient motions of the vibrating systems governed by the following equation：

   y'' + 2y' + 2y = cos t

6. (10%) A 95% confidence interval for a population mean is reported to be 220 to 228. If the sample mean is 224 and the sample standard deviation is 20, what sample size was used in this study?

7. (20%)某電子公司收到一批 2500 電子零件，從中抽驗 100 個，公司決定如果這 100 個最多有一個不良品時就全部接受此批貨，假設這批貨中有 5% 是不良品，試問公司接受此批貨的機率是多少？

國立雲林科技大學
九十二學年度研究所博士班招生考試試題

所別：工程科技研究所
科目：工程數學 (丁)

表 1.常態分配表

$$\Phi(z) = P(Z \le z) = \int_{-\infty}^{z} \frac{1}{\sqrt{2\pi}} e^{-\frac{t^2}{2}} dt \quad \Phi(z) = P(Z \le z) = \int_{-\infty}^{z} \frac{1}{\sqrt{2}}$$

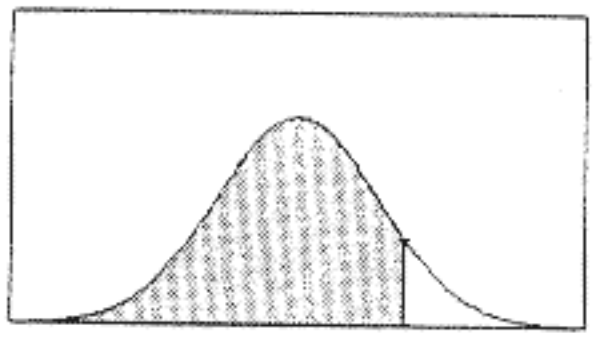

z

z	z 的小數點第二位									
	0.00	0.01	0.02	0.03	0.04	0.05	0.06	0.07	0.08	0.09
0.0	0.5000	0.5040	0.5080	0.5120	0.5160	0.5199	0.5239	0.5279	0.5319	0.5359
0.1	0.5398	0.5438	0.5478	0.5517	0.5557	0.5596	0.5636	0.5675	0.5714	0.5753
0.2	0.5793	0.5832	0.5871	0.5910	0.5948	0.5987	0.6026	0.6064	0.6103	0.6141
0.3	0.6179	0.6217	0.6255	0.6293	0.6331	0.6368	0.6406	0.6443	0.6480	0.6517
0.4	0.6554	0.6591	0.6628	0.6664	0.6700	0.6736	0.6772	0.6808	0.6844	0.6879
0.5	0.6915	0.6950	0.6985	0.7019	0.7054	0.7088	0.7123	0.7157	0.7190	0.7224
0.6	0.7257	0.7291	0.7324	0.7357	0.7389	0.7422	0.7454	0.7486	0.7517	0.7549
0.7	0.7580	0.7611	0.7642	0.7673	0.7704	0.7734	0.7764	0.7794	0.7823	0.7852
0.8	0.7881	0.7910	0.7939	0.7967	0.7995	0.8023	0.8051	0.8078	0.8106	0.8133
0.9	0.8159	0.8186	0.8212	0.8238	0.8264	0.8289	0.8315	0.8340	0.8365	0.8389
1.0	0.8413	0.8438	0.8461	0.8485	0.8508	0.8531	0.8554	0.8577	0.8599	0.8621
1.1	0.8643	0.8665	0.8686	0.8708	0.8729	0.8749	0.8770	0.8790	0.8810	0.8830
1.2	0.8849	0.8869	0.8888	0.8907	0.8925	0.8944	0.8962	0.8980	0.8997	0.9015
1.3	0.9032	0.9049	0.9066	0.9082	0.9099	0.9115	0.9131	0.9147	0.9162	0.9177
1.4	0.9192	0.9207	0.9222	0.9236	0.9251	0.9265	0.9279	0.9292	0.9306	0.9319
1.5	0.9332	0.9345	0.9357	0.9370	0.9382	0.9394	0.9406	0.9418	0.9429	0.9441
1.6	0.9452	0.9463	0.9474	0.9484	0.9495	0.9505	0.9515	0.9525	0.9535	0.9545
1.7	0.9554	0.9564	0.9573	0.9582	0.9591	0.9599	0.9608	0.9616	0.9625	0.9633
1.8	0.9641	0.9649	0.9656	0.9664	0.9671	0.9678	0.9686	0.9693	0.9699	0.9706
1.9	0.9713	0.9719	0.9726	0.9732	0.9738	0.9744	0.9750	0.9756	0.9761	0.9767
2.0	0.9772	0.9778	0.9783	0.9788	0.9793	0.9798	0.9803	0.9808	0.9812	0.9817
2.1	0.9821	0.9826	0.9830	0.9834	0.9838	0.9842	0.9846	0.9850	0.9854	0.9857
2.2	0.9861	0.9864	0.9868	0.9871	0.9875	0.9878	0.9881	0.9884	0.9887	0.9890
2.3	0.9893	0.9896	0.9898	0.9901	0.9904	0.9906	0.9909	0.9911	0.9913	0.9916
2.4	0.9918	0.9920	0.9922	0.9925	0.9927	0.9929	0.9931	0.9932	0.9934	0.9936
2.5	0.9938	0.9940	0.9941	0.9943	0.9945	0.9946	0.9948	0.9949	0.9951	0.9952
2.6	0.9953	0.9955	0.9956	0.9957	0.9959	0.9960	0.9961	0.9962	0.9963	0.9964
2.7	0.9965	0.9966	0.9967	0.9968	0.9969	0.9970	0.9971	0.9972	0.9973	0.9974
2.8	0.9974	0.9975	0.9976	0.9977	0.9977	0.9978	0.9979	0.9979	0.9980	0.9981
2.9	0.9981	0.9982	0.9982	0.9983	0.9984	0.9984	0.9985	0.9985	0.9986	0.9986
3.0	0.9987	0.9987	0.9987	0.9988	0.9988	0.9989	0.9989	0.9989	0.9990	0.9990
3.1	0.9990	0.9991	0.9991	0.9991	0.9992	0.9992	0.9992	0.9992	0.9993	0.9993
3.2	0.9993	0.9993	0.9994	0.9994	0.9994	0.9994	0.9994	0.9995	0.9995	0.9995
3.3	0.9995	0.9995	0.9995	0.9996	0.9996	0.9996	0.9996	0.9996	0.9996	0.9997
3.4	0.9997	0.9997	0.9997	0.9997	0.9997	0.9997	0.9997	0.9997	0.9997	0.9998
3.5	0.9998	0.9998	0.9998	0.9998	0.9998	0.9998	0.9998	0.9998	0.9998	0.9998
3.6	0.9998	0.9998	0.9999	0.9999	0.9999	0.9999	0.9999	0.9999	0.9999	0.9999
3.7	0.9999	0.9999	0.9999	0.9999	0.9999	0.9999	0.9999	0.9999	0.9999	0.9999
3.8	0.9999	0.9999	0.9999	0.9999	0.9999	0.9999	0.9999	0.9999	0.9999	0.9999
3.9	1.0000	1.0000	1.0000	1.0000	1.0000	1.0000	1.0000	1.0000	1.0000	1.0000
4.0	1.0000	1.0000	1.0000	1.0000	1.0000	1.0000	1.0000	1.0000	1.0000	1.0000

國立雲林科技大學
九十二學年度研究所博士班招生考試試題

所別：工程科技研究所
科目：工程數學 (丁)

表2.卡方分配表

$$p\left(\chi_k^2 \geq \chi_{k,\alpha}^2\right) = \alpha$$

$\chi_{k,\alpha}^2$

自由度	單尾顯著水準							
	0.99	0.975	0.95	0.9	0.1	0.05	0.025	0.01
1	0.0002	0.0010	0.0039	0.0158	2.7055	3.8415	5.0239	6.6349
2	0.0201	0.0506	0.1026	0.2107	4.6052	5.9915	7.3778	9.2103
3	0.1148	0.2158	0.3518	0.5844	6.2514	7.8147	9.3484	11.3449
4	0.2971	0.4844	0.7107	1.0636	7.7794	9.4877	11.1433	13.2767
5	0.5543	0.8312	1.1455	1.6103	9.2364	11.0705	12.8325	15.0863
6	0.8721	1.2373	1.6354	2.2041	10.6446	12.5916	14.4494	16.8119
7	1.2390	1.6899	2.1674	2.8331	12.0170	14.0671	16.0128	18.4753
8	1.6465	2.1797	2.7326	3.4895	13.3616	15.5073	17.5346	20.0902
9	2.0879	2.7004	3.3251	4.1682	14.6837	16.9190	19.0228	21.6660
10	2.5582	3.2470	3.9403	4.8652	15.9872	18.3070	20.4831	23.2093
11	3.0535	3.8158	4.5748	5.5778	17.2750	19.6751	21.9200	24.7250
12	3.5706	4.4038	5.2260	6.3038	18.5494	21.0261	23.3367	26.2170
13	4.1069	5.0087	5.8919	7.0415	19.8119	22.3621	24.7356	27.6883
14	4.6604	5.6287	6.5706	7.7895	21.0642	23.6848	26.1190	29.1413
15	5.2294	6.2621	7.2609	8.5468	22.3072	24.9958	27.4884	30.5779
16	5.8122	6.9077	7.9616	9.3122	23.5418	26.2962	28.8454	31.9999
17	6.4078	7.5642	8.6718	10.0852	24.7690	27.5871	30.1910	33.4087
18	7.0149	8.2308	9.3905	10.8649	25.9894	28.8693	31.5264	34.8053
19	7.6327	8.9066	10.1170	11.6509	27.2036	30.1435	32.8523	36.1908
20	8.2604	9.5908	10.8508	12.4426	28.4120	31.4104	34.1696	37.5662
21	8.8972	10.2829	11.5913	13.2396	29.6151	32.6705	35.4789	38.9321
22	9.5425	10.9823	12.3380	14.0415	30.8133	33.9244	36.7807	40.2894
23	10.1957	11.6885	13.0905	14.8479	32.0069	35.1725	38.0757	41.6384
24	10.8564	12.4012	13.8484	15.6587	33.1963	36.4151	39.3641	42.9798
25	11.5240	13.1197	14.6114	16.4734	34.3816	37.6525	40.6465	44.3141
26	12.1981	13.8439	15.3791	17.2919	35.5631	38.8852	41.9232	45.6417
27	12.8786	14.5733	16.1513	18.1138	36.7412	40.1133	43.1944	46.9630
28	13.5648	15.3079	16.9279	18.9392	37.9159	41.3372	44.4607	48.2782
29	14.2565	16.0471	17.7083	19.7677	39.0875	42.5569	45.7222	49.5879
30	14.9535	16.7908	18.4926	20.5992	40.2560	43.7729	46.9792	50.8922
35	18.5089	20.5694	22.4650	24.7967	46.0588	49.8018	53.2033	57.3421
40	22.1643	24.4331	26.5093	29.0505	51.8050	55.7585	59.3417	63.6907
45	25.9013	28.3662	30.6123	33.3504	57.5053	61.6562	65.4102	69.9568
50	29.7067	32.3574	34.7642	37.6886	63.1671	67.5048	71.4202	76.1539
60	37.4849	40.4817	43.1879	46.4589	74.3970	79.0819	83.2976	88.3794
70	45.4418	48.7576	51.7393	55.3290	85.5271	90.5312	95.0231	100.4252
80	53.5400	57.1532	60.3915	64.2778	96.5782	101.8795	106.6286	112.3288
90	61.7541	65.6466	69.1260	73.2912	107.5650	113.1453	118.1359	124.1163
100	70.0648	74.2219	77.9295	82.3581	118.4980	124.3421	129.5612	135.8067
200	156.4320	162.7280	168.2786	174.8353	226.0210	233.9943	241.0579	249.4451
300	245.9725	253.9123	260.8781	269.0679	331.7885	341.3951	349.8745	359.9064
400	337.1553	346.4818	354.6410	364.2074	436.6490	447.6325	457.3055	468.7245
500	429.3875	439.9360	449.1468	459.9261	540.9303	553.1268	563.8515	576.4928

國立雲林科技大學
九十二學年度研究所博士班招生考試試題

所別：工程科技研究所

科目：工程數學 (丁)

表3. t分配表

$$P(t_k \geq t_{k,\alpha}) = \alpha$$

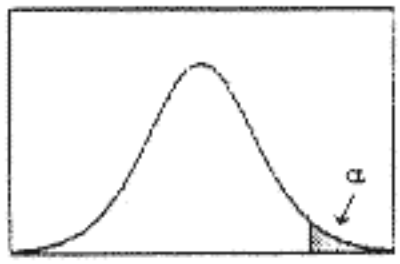

$t_{k,\alpha}$

自由度	單尾顯著水準						
	0.1	0.05	0.025	0.01	0.005	0.0025	0.001
1	3.0777	6.3138	12.7062	31.8205	63.6567	127.3213	318.3088
2	1.8856	2.9200	4.3027	6.9646	9.9248	14.0890	22.3271
3	1.6377	2.3534	3.1824	4.5407	5.8409	7.4533	10.2145
4	1.5332	2.1318	2.7764	3.7469	4.6041	5.5976	7.1732
5	1.4759	2.0150	2.5706	3.3649	4.0321	4.7733	5.8934
6	1.4398	1.9432	2.4469	3.1427	3.7074	4.3168	5.2076
7	1.4149	1.8946	2.3646	2.9980	3.4995	4.0293	4.7853
8	1.3968	1.8595	2.3060	2.8965	3.3554	3.8325	4.5008
9	1.3830	1.8331	2.2622	2.8214	3.2498	3.6897	4.2968
10	1.3722	1.8125	2.2281	2.7638	3.1693	3.5814	4.1437
11	1.3634	1.7959	2.2010	2.7181	3.1058	3.4966	4.0247
12	1.3562	1.7823	2.1788	2.6810	3.0545	3.4284	3.9296
13	1.3502	1.7709	2.1604	2.6503	3.0123	3.3725	3.8520
14	1.3450	1.7613	2.1448	2.6245	2.9768	3.3257	3.7874
15	1.3406	1.7531	2.1314	2.6025	2.9467	3.2860	3.7328
16	1.3368	1.7459	2.1199	2.5835	2.9208	3.2520	3.6862
17	1.3334	1.7396	2.1098	2.5669	2.8982	3.2224	3.6458
18	1.3304	1.7341	2.1009	2.5524	2.8784	3.1966	3.6105
19	1.3277	1.7291	2.0930	2.5395	2.8609	3.1737	3.5794
20	1.3253	1.7247	2.0860	2.5280	2.8453	3.1534	3.5518
21	1.3232	1.7207	2.0796	2.5176	2.8314	3.1352	3.5272
22	1.3212	1.7171	2.0739	2.5083	2.8188	3.1188	3.5050
23	1.3195	1.7139	2.0687	2.4999	2.8073	3.1040	3.4850
24	1.3178	1.7109	2.0639	2.4922	2.7969	3.0905	3.4668
25	1.3163	1.7081	2.0595	2.4851	2.7874	3.0782	3.4502
26	1.3150	1.7056	2.0555	2.4786	2.7787	3.0669	3.4350
27	1.3137	1.7033	2.0518	2.4727	2.7707	3.0565	3.4210
28	1.3125	1.7011	2.0484	2.4671	2.7633	3.0469	3.4082
29	1.3114	1.6991	2.0452	2.4620	2.7564	3.0380	3.3962
30	1.3104	1.6973	2.0423	2.4573	2.7500	3.0298	3.3852
35	1.3062	1.6896	2.0301	2.4377	2.7238	2.9960	3.3400
40	1.3031	1.6839	2.0211	2.4233	2.7045	2.9712	3.3069
45	1.3006	1.6794	2.0141	2.4121	2.6896	2.9521	3.2815
50	1.2987	1.6759	2.0086	2.4033	2.6778	2.9370	3.2614
60	1.2958	1.6706	2.0003	2.3901	2.6603	2.9146	3.2317
70	1.2938	1.6669	1.9944	2.3808	2.6479	2.8987	3.2108
80	1.2922	1.6641	1.9901	2.3739	2.6387	2.8870	3.1953
90	1.2910	1.6620	1.9867	2.3685	2.6316	2.8779	3.1833
100	1.2901	1.6602	1.9840	2.3642	2.6259	2.8707	3.1737
200	1.2858	1.6525	1.9719	2.3451	2.6006	2.8385	3.1315
300	1.2844	1.6499	1.9679	2.3388	2.5923	2.8279	3.1176
400	1.2837	1.6487	1.9659	2.3357	2.5882	2.8227	3.1107
500	1.2832	1.6479	1.9647	2.3338	2.5857	2.8195	3.1066
600	1.2830	1.6474	1.9639	2.3326	2.5840	2.8175	3.1039
700	1.2828	1.6470	1.9634	2.3317	2.5829	2.8160	3.1019
800	1.2826	1.6468	1.9629	2.3310	2.5820	2.8148	3.1005
900	1.2825	1.6465	1.9626	2.3305	2.5813	2.8140	3.0993
1000	1.2824	1.6464	1.9623	2.3301	2.5808	2.8133	3.0984